Phase and polarization modulations based on LCOS SLM

Jintao Hong

Department of Engineering

University of Cambridge

This dissertation is submitted for the degree of

Doctor of Philosophy

St. Catherine College 9.2021

I would like to dedicate this thesis to my loving families …

Declaration

I hereby declare that except where specific reference is made to the work of others, the contents of this dissertation are original and have not been submitted in whole or in part for consideration for any other degree or qualification in this, or any other University. This dissertation is the result of my own work and includes nothing which is the outcome of work done in collaboration, except where specifically indicated in the text. This dissertation contains less than 65,000 words including appendices, bibliography, footnotes, tables, and equations and has less than 150 figures.

Jintao Hong

9.2021

Abstract of the thesis

Phase and polarization modulations based on LCOS SLM

By

Jintao Hong

Liquid crystal on silicon (LCOS) technology has initially been developed for imaging and display applications. This technology combines the unique light-modulating properties of liquid crystal materials and the advantages of high-performance silicon complementary metal oxide semiconductor (CMOS) technology through dedicated LCOS assembly processes. Phase-only LCOS SLM are becoming an important tool for laser processing in a range of systems. A recent breakthrough in laser-induced self-assembled nanostructure in glass has made it possible to store data in fused silica. The technology of 5D optical data storage in transparent materials paves a promising way to almost unlimited lifetime data storage for future cloud. The phase-only SLM has already shown its potential for this application in tailoring ultrafast lasers writing beam for optical data storage. In data writing process, a light filed of target data pattern (multi-beam arrays) with target linear polarization state is required to encode information onto the nanograting structure created by laser pulses. In data writing beam generation, phase-only LCOS SLM can generate arbitrary data pattern by using diffractive holographic imaging. However, the polarization control of output image is still achieved by using an external polarization modulator. This leads to the complication, bulkiness, and large delay in current methods. Therefore, this research aims to develop a

phase and polarization modulation method based on phase-only LCOS SLMs to simultaneously control both the holographic image and its polarization state.

Phase-only modulation of light can tailor the output image by using computer-generated holograms onto LCOS SLMs. This is very useful for generate arbitrary multi-beam data writing light field. To fully control the polarization state of the data writing light field, the amplitude and relative phase of two orthogonal polarization components needs to be independently modulated. However, the phase-only modulation cannot directly affect the polarization of light. Therefore, three methods are proposed to achieve the phase and polarization control using LCOS SLMs. Also, two customized LCOS SLMs were designed and fabricated by using in-house-developed die-level assembly technique. They are used in all experiments of this research.

First method is parallel coding and two-beam combining. Two orthogonal input beams are parallelly and independently encoded with the same target image information but with the different amplitude information by using two phase holograms on two LCOS SLMs. Then, two modulated beams are now considered as two polarization components and be spatially superposed to form target polarization state. The first-order diffraction efficiency change controlled by using phase modulation depth on hologram is used to design a technique to encode amplitude information onto the hologram. This technique is used in all three methods for amplitude modulation of polarization components. This method requires high precision alignment process in beam combining.

In the second method, to avoid beam combining in polarization control, instead of modulating two beams, the object of modulation is changed to two polarization components of a single input beam. By using the characteristic of polarization sensitivity of phase-only LCOS SLM, two polarization components of single beam are sequentially and independently coded with information target image and amplitude using two LCOS SLMs. Because the spatial status to components of single beam remain unchanged in the modulation, the phase and polarization control is achieved automatically.

The third method is a compact system using only single LCOS SLM device. The principle of this method is two polarization components coding like in the second method, but the fundamental difference is in a polarization components rotation technique in compact system. Using this polarization rotation technique, two light components can be independently coded

by separately using two holograms on the two halves of LCOS SLM. The prototype of the compact system is developed and fabricated, and the effectiveness of the system has been experimentally verified.

To sum up, the phase and polarization modulation methods based on LCOS SLM has been explored and developed. They can provide dynamical control of both polarization sate and image of light field using only LCOS. The proposed methods can provide a more promising way to largely increase the data writing speed in the 5D optical data storage technology.

Acknowledgements

I would like to appreciate deeply all the people who have helped me during this time, in any form of aid.

First, I would like to sincerely thank my supervisor, Prof. Daping Chu. He gave me this opportunity to come to the University of Cambridge and to research on this topic I really like. He also helped me to get involved with a project in which I can make contributions. Realizing the phase and polarization modulation based on LCOS SLMs for the future optical storage in glass is the frontier topic, and this PhD topic really made me feel excited. Besides, Prof. Chu guided me through this field with his rich experience and structured thinking. His advises inspired me to come up with many ideas which later successfully achieved significant progresses.

Secondly, I would like to acknowledge Microsoft projects, which are highly related to my PhD topic, for their financial support on my research and study in Cambridge. Also, I want to thank Microsoft for their financial support through its study-abroad scholarship. Meanwhile, I would like to appreciate the help from Microsoft research scientist, Dr. Andreas Georgiou and Dr James Clegg.

I would also like to thank to Dr. Jin Li, Dr. Yuantong and Dr. Kasia for various discussions and comments. My thanks also go to my other colleagues in Centre for Photonic Devices and Sensors (CPDS) group for their helps from time to time. A word of appreciation goes to Mike and Pawn, both of whom I started this PhD study with, and we have gone through a lot.

Besides, many good friends I met here in Cambridge enriched my thoughts and changed the way I think. Someone says that friends are family you chose. Yes, now I know whoever the person said, it is right. Some of them has become my family. They are treasures of my life.

Most of all, I would like to thank my family, my parents, my partner Alexis, and my new family in England for their encouragement and support. I wouldn’t have been able to complete this degree without them.

Contents

List of Publications

While completing this thesis, papers have been either published or waited for submissions, and listed as following. The [D] presented the method of phase and polarization modulation using a parallel coding of two-beam combining, which is the content of chapter 3. In [D], the setup' SLMs are from the content of chapter 2. The [E] demonstrated another new phase and polarization modulation approach using two polarization components of a single input beam, which is the content of chapter 4. The [A], [B], and [C] are the integrated phase and polarization modulation method, which forms the chapter 5.

[A] Hong, J., Li, J., & Chu, D. (2021, July). Dynamic Control of Light Polarization for Optical Data Storage Using Holograms on Phase-Only Liquid Crystal on Silicon Spatial Light Modulators (LCOS SLMs). In Digital Holography and Three-Dimensional Imaging (pp. DM6E-6). Optical Society of America.

[B] Hong, J., Li, J., & Chu, D. (2022). Efficient dynamic control method of light polarization using single phase-only liquid crystal on silicon spatial light modulators for optical data storage. Applied Optics, 61(5), B34-B42.

[C] Hong, J., Li, J., & Chu, D. (2021, April). LCOS SLM based compact system of polarization modulation for data storage in glass. In *Holography: Advances and Modern Trends VII* (Vol. 11774, p. 117740A). International Society for Optics and Photonics.

[D] Hong, J., Li, J., & Chu, D. Dynamic linearly-polarized holographic pattern generation using tuneable optical vector for optical storage in transparent materials, Waiting for submission, 2021.

[E] Hong, J., Li, J., & Chu, D. Dynamic generation of linear optical vector beams with time-delay integral holographic pattern for next-generation optical storage in glass, Waiting for submission, 2021.

List of Figures

List of Tables

Abbreviations

2/3/5D	Two/Three/Five Dimensional
HHD	Hard Disc Driver
NVM	Non-volatile Memory
PMR	Perpendicular Magnetic Recording
SMR	Shingled Magnetic Recording
HAMR	Heat-Assisted Magnetic Recording
MAMR	Microwave-Assisted Magnetic Recording
GB	Gigabyte
TB	Terabyte
CGH	Computer Generated Holography
DMD	Digital Micro-mirror Device
FFT	Fast Fourier Transformation
H/QWP	Half/Quarter Wave Plate
HPM	Half-wave Plate Matrix
LCOS	Liquid Crystal on Silicon
NA	Numerical Aperture

GS	Gerchberg-Saxton
CMOS	Complementary Metal-Oxide-Semiconductor
DM	Deformable Mirror
VAN	Vertical-Aligned Nematic
TN	Twisted Nematic
ECB	Electronically Controlled Birefringence
LUT	Look Up Table
SLM	Spatial Light Modulator
LC	Liquid Crystal
LP	Linear Polarizer
BS	Beam Splitter

Chapter 1

Introduction

1.1 Research background

1.1.1 Current storage technologies for future Cloud Storage

Since the past decade, the cloud has become the major storage place for much of the world's data. The demand of stable and long-term cloud storage has risen substantially, and it's predicted that multiple zettabytes of data would have been moved into the cloud by the 2020 [1]. To deal with the increasing storage demand, data centres utilize many storage technologies, such as hard disk drives (HDD), flash, non-volatile memory (NVM), magnetic tape, and optical discs. All of technologies mentioned above has huge difference in terms of cost, storage density, record/access speed, power consumption, and media lifetime. It is obvious that all these storage technologies were designed when the cloud had not come into being, and there is no one storage technology that dominates the current cloud storage market.

The first example is flash storage. It can be a strong candidate of cloud storage technology, as it offers high throughput and low latency with acceptable lifetime. However, the cost of flash makes it only suitable for the hot data, the data requires high frequency of accessing and rewriting. The second example is hard disk drive (HDD). Most of cloud providers are using HDD as it offers very low cost (£/GB) compared with NVM and flash [2]. However, it has widely acknowledged problems of low energy efficiency (0.04W/GB) [3] and short lifetime of the hardware. HDD will not be a satisfactory candidate for long-term storage in cloud as it requires transferring data every few years to avoid any loss [4]. Therefore, the data storage technologies for future cloud storage needs a very good balance between performance and cost. There are currently four media that can be the candidates of cloud storage.

1. **Hard Disk Drive**

As a traditional storage technology, the increase of areal density made HDD a possible solution for today's data storage demand. PMR HDDs has reached its areal density limits [5]. Lately, the increase of the number of platters leads to the biggest capacity rise of HDDs, but it is not sustainable due to physical constraints of the 3.5'' HDDs casing [5,6,7]. SMR provided marginal increases but at the cost of removing random writing [8]. And HAMR and MAMR [9,10,11,12] has not been commercially available. The latest possible improvement is the increase in the number of heads per drive, however, it will only scale performance to the number of platters, which means an 8-fold performance improvement [13].

2. **Magnetic tape**

Magnetic tape has much lower cost per GB comparing with HDDs, however, it only suitable for the cold archival data storage due to its high access latency. The physical storage of magnetic tape requires frequent maintenance, and the tape drives and robots also need extra management. That means a careful environment control and a complex system service will become a low-cost sources for long term data storage. The media can degrade when the environment is not right.

3. Optical storage

Blu-ray has become today's major optical disc technology. Its data record and read processes are based on the change of a thin layer of organic or inorganic materials. Laser beams are used to encode the data by generating alternating marks and spaces on the surface of the thin film materials [5]. High-capacity optical discs are achieved by gluing layers of polycarbonate and thin films together. That is where its limit on density comes from as each layer requires enough transmittance to allow the write and read process to be conducted in the deeper layers. Today's single disc is composed of 4 to 8 layers, and this means the maximum capacity is limited to 1 TB according to its density. Also, Blu-ray disc has long lifetime, but it still requires a refresh cycle.

4. Holographic Data Storage

Like the formation of hologram in a block of photorefractive material, in holographic storage, the writing process requires interfering two laser beams (address reference beam and data encoding beam). Laser energy excites electrons to higher energy level and make them transit between different kinds of atoms in the compound, producing a stable change in the refractive properties of the material. And the change is reversible as well. This ensures that the data erasing, and overwriting is possible. Reading only needs the incidence of address reference beam to the media, and it can provide multi-megabyte reading. The biggest challenge of this technology is its cost compared with other storage technologies [14], and therefore it has not been used in commercial application.

These characteristics of current media and limitations of storage systems motivate us to search for the best storage technology for high-capacity and long term cool to cold data. The possible answer to this question is magnetic tapes as magnetic tape is the cheapest option today. However, a tape library has an average-case response time on the order of minutes to hours even under low load [15]. A new storage technology that can offer high capacity, long lifetime, and better access latency and even lower cost than magnetic tapes is needed for mass archival data storage in future cloud. The media that this storage technology will use is glass.

1.1.2 The principle and advantages of data storage using glass

This section introduces the fundamental principle and concepts of optical data storage using glass. 'Voxel' is the name of 3D nanograting in glass that stores the data. The principle and methods of voxel writing, and reading is explained for the understanding of the role of polarization control in this data storage technology.

1. Storing data in 'Voxel'

A recent breakthrough at University of Southampton has turned the concept of storing data in glass into reality [16,17,18]. When a series of ultrashort pulse laser beams on the femtosecond time scale is focused into a block of fused silica (i.e., quartz glass), a permanent self-assembled nanostructure forms in the silica. The induced 3D nanostructure is called voxel. As shown in the Figure 1.1, the voxel has a circular grating structure (nano-grating) with a diameter about the wavelength of the laser beams used. Each voxel in the fused silica has three significant properties: form birefringence, long lifetime and Re-writability.

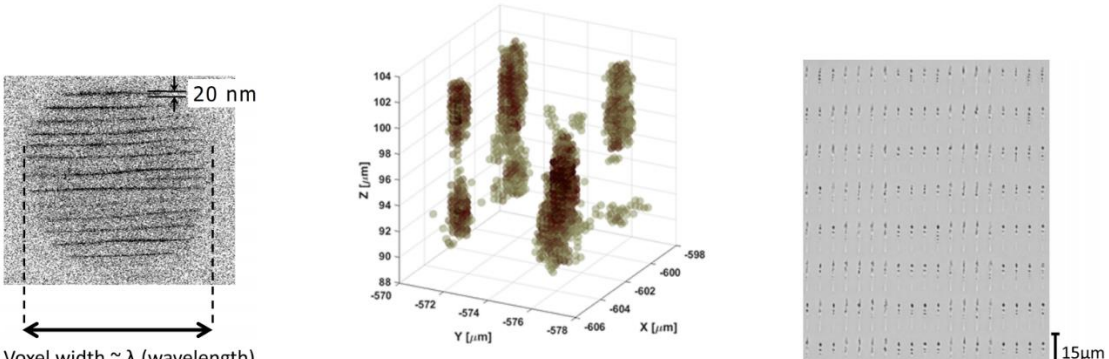

(a) Single voxel (top view)

(b) 3D reconstruction of four measured voxels

(c) Side view (8 layers)

Figure 1.1 The voxel in glass [5]

i. Form birefringence

The periodic nanostructure created by femtosecond laser has different physical properties than its surrounding silica material. First, the self-assembled nanograting has the direction

perpendicular to the light polarization of the laser. Second, the voxel shows a different refractive index for light with a different polarization. That means when a polarized light is incident on the voxel, a shift of phase of light's electric field is created. And the quantity of the phase shift is known as the 'retardence' of the voxel. Figure 1.2 shows the schematic of the voxel. The combination of the different direction of nanograting and its retardance can be defined as bits, which means multiple bits can be encoded on one voxel. In voxel writing, controlling the polarization of the laser beam and the number of pulses can actively affect those two properties of the created voxel. Reading the data bits is achieved by measuring these two properties of the voxels.

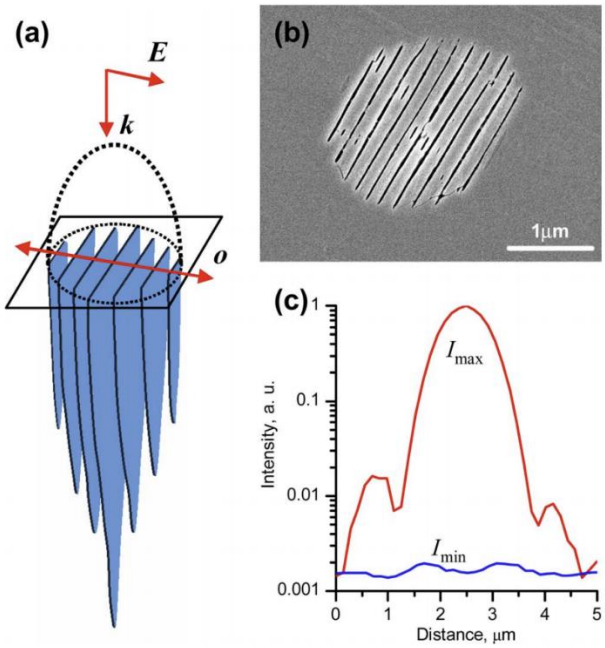

Figure 1.2 the schematic of a voxel [19]. The growth of nanograting retardance can fit in the integrated Gaussian function. The k is the propagation direction of write femtosecond laser beam, o is the optical axis of voxel, and E is the orientation of the electric field (angel of a linear polarization state) of write laser beam.

ii. Long lifetime

Once a voxel is created, it remains stable, and its properties of birefringence has a lifetime of the fused silica. When the media temperature elevates to 200 C degrees, the extrapolated

decay time is comparable with the age of the Universe – 13.8 billion years according to the Arrhenius plot [4]. Even at temperature of 1000 C degree, the voxel in the glass remains readable. Therefore, quartz glass provides very different properties compared with existing storage media. For example, apart from thermostability, glass is an electromagnetic field proof media. With long lifetime glass storage, errors occur during the data transferring into new media can be eliminated process [5].

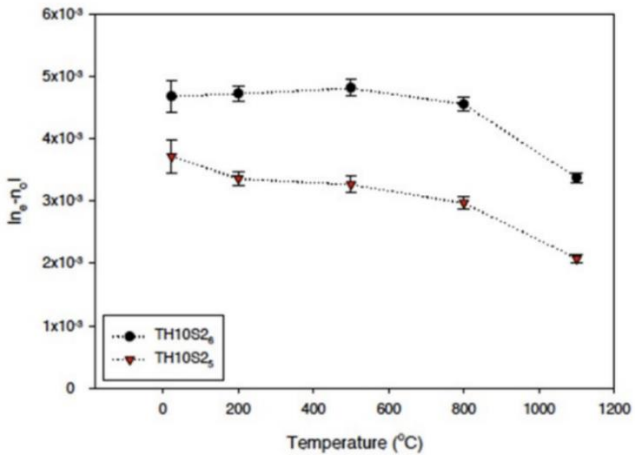

Figure 1.3 Intensity of femtosecond laser induced voxel's birefringence as a function of annealing temperature [4]. The pulses energy of the results of circle (black) is 1.60 μJ, and that of the results of triangle(red) is 2.14 μJ.

Apart from the outstanding properties of voxel, when we consider the storing data using voxel in glass as a potential optical data storage technology, it has further three major advantages: high storage density, re-writability, and flexible workloads.

iii. Re-writability

The two birefringent properties of voxel make storing data in glass possible. And the write and read processes of each voxel make a storage system based on glass feasible using current technologies. Besides, the induced nanograting in glass can be erased and rewritten. An existing nanograting can be overwritten by beams with a new polarization angle [19]. The polarization angle of voxels is measured by a polarization optics microscope. The glass sample is placed between a pair of crossed polarizers, and it is illuminated by probe light with

the same propagating direction of the write laser beam. The intensity of probe light transmitted through voxels in glass will change and be detected by a camera after the second polarizer. The detected intensity will be minimum I_{min} when the angle between voxel's optical axis and the polarization of the probe light is 0° or 90° and will be maximum I_{max} when that angle is 45°. This means that the optical axial angel of voxels can be measured by calculation according to the rotation of the second polarizer when light intensity reach maximum.

As shown in Figure 1.4, the original nanograting is replaced by polarization-rotated laser beams with 3, 30, 300, and 4000 pulses. It is clear to observe that new nanograting begin to form before old gratings being completely removed.

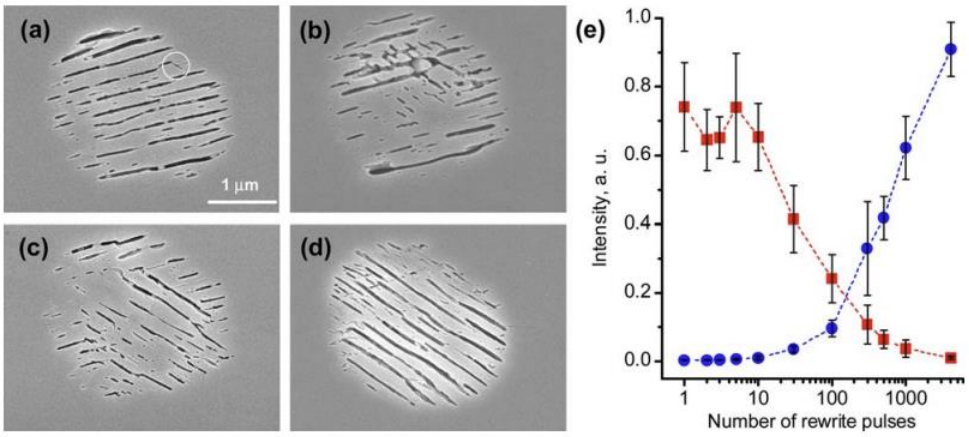

Figure 1.4 SEM images [19] of nanograting after (a) 3-pulses (the white circle indicates the initial location of new gratings growing) (b) 30-pulses (c) 300-pulses, and (d) 4000-pulses. (e) The evolution of nanograting polarization microscopic signal intensity as a function of number write laser pulses. Intensity of the birefringence signal of the original voxel (red) and that of new voxel (blue) are collected when input probe light polarization is at 45° to both voxels' optical axial.

It is obvious from the figure (Figure 1.5d) that the grating structure introduced by the previous writing is removed but the residual traces can be observed. As shown in Figure 1.6, the new voxel's signal I_{max} is significantly higher than I_{res} . The ratio of I_{max} /I_{res} is about 100 : 1. By comparing with the same ratio of I_{max} /I_{res} (500 : 1) from a newly written voxel

without any rewrite, there is an optical evidence of residual nanostructure [19]. However, even after 1000 times of rewrites with total pulses over 10^6times, the residual nanograting will only slightly decrease (I_{max} /I_{res}= 40 : 1) the optical detectability of new nanograting This ensure high readability of stored data in voxels.

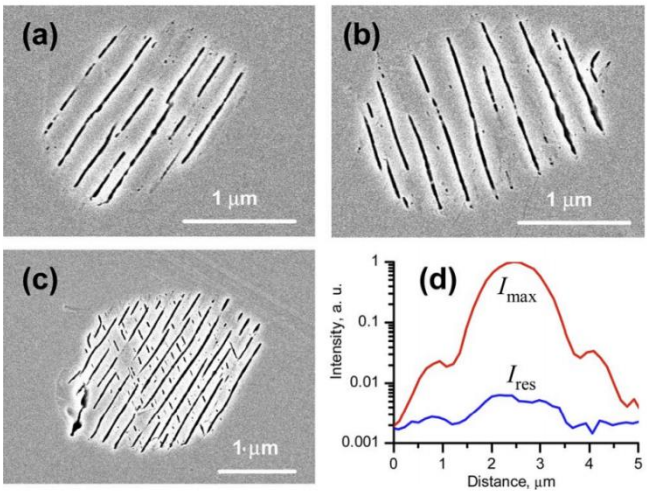

Figure 1.5 Rewriting results of voxels [19]. (a) A SEM image of a voxel created by 1500 laser pulses with pulses energy of 300nJ. (b) An optical axial rotated new voxel is made with same write beam parameter as first write. (c) Nanograting structure after 100 times write and rewrite. (d) The comparison of maximum birefringence signals from the final nanograting I_max and the residual nanograting I_res due to the imperfect erasure of previous voxel in (c).

iv. High density

Storing data in voxel can make high capacity possible. By focusing the laser beam at different position across a plane, a 2D voxel data arrays can be written. When the focal depth of laser beam is changed, many voxels' layers can be written across the depth of the glass block. This means a 3D structure of voxels is achieved. The volumetric storage in a three-dimensional media can bring not only high density (a volume equivalent to a DVD-disk can store about 1 TB. This technology can potentially get to 360 TB [4,18]) but also improvement in read performance. For example, the read process concurrently decodes many voxels in the same XY plane, therefore, increasing number of voxels means the volume of data in the field of

view when reading increased. Furthermore, the transmittance of fused silica is much larger than that of opaque thin films used in the current optical discs, which allowing light arrives deeper in the media for both accurate writing and reading many layers of voxels in glass (i.e., over 100).

v. Workload flexibility

Another outstanding advantage of optical data storage technology is its flexibility in storage workloads distribution. Workloads of a storage system can vary over time. For example, there can be write-dominated using patterns in the beginning, and over the longer term the workload can change to be read-dominated. In a storage system using glass, the read and write processes differ in three ways: (i) They use different technologies, (ii) the laser used for writing costs an order of magnitude more than that used in reading process, and (iii) the physical size of the hardware.

These three fundamental differences separate the read and write heads from the glass media, which means that only the resources that service the current system load needs are utilized. When only the volume of data writing increases, we can deploy new glass block without adding any extra reading hardware. It also provides an opportunity to get access to data in situ in the system, avoiding data transferring between tiers when access characteristics change. And this can make a huge change to cloud storage system as they currently use storage tiers backed by different storage media to reach the balance between acceptable performance and low cost.

2. Voxel reading

Recall the data is encoded on each voxel by modulating its two physical properties: orientation of optical axis and retardance, good news is that the techniques of quantifying birefringence in transparent materials are well-studied. As shown in Figure 1.6, the read hardware has two parts: illumination and imaging. On the illumination part, it creates a beam

of light with one polarized angle. As light beam passes through the voxels, its polarization state is changed by nanograting. And then the tuneable polarizer and the camera are used to detect the changes. The set of images of same field of view in one layer of voxels are taken to quantify the retardance and polarization angle.

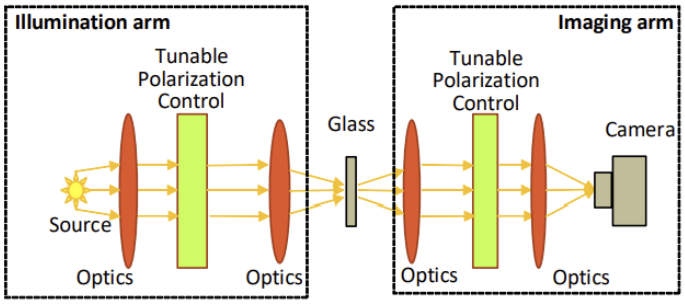

Figure 1.6 The schematic of the polarization optics microscope [5].

There is an example to illustrate the form of readout of the stored information in a layer of voxels. In the voxel reading experiments shown in Figure 1.7, a commercial quantitative birefringence measurement system integrated into an optical microscope is used for data readout. Light source was a halogen lamp giving circularly polarized light. The final birefringent signals of voxels were collected with an objective lens, and angles of polarization were measured with liquid crystal analyzer.

The typical retardance values measured in this experiment was 40nm. Longer writing laser pulse duration can increase the retardance values of each voxel, but it also results in higher stress and thermal accumulation of glass material, raising the possibility of material cracking [20]. Therefore, the retardance values in experiments are normally below 100nm [21]. The three voxel layers shown in Figure 1.8 (a)-(b) were separated by 20 μm across the depth and the distance between two adjacent spots was 3.7 μm. Figure 1.7 (c) showed the retardance distribution of the voxels on first layer, and Figure 1.7 (e) was the retardance values of each voxel of the enlarged 5 x 5 array characterized by birefringent microscopy. As can be seen in Figure 1.7 (e), the readout retardance values still have errors, and this mainly due to the retardance dependence on write-beam's polarization. This polarization dependence effect

could be related to the pulse front tilt of ultrashort laser pulses [16,22,23,24]. Therefore, additional calibration of retardance value was processed, and the final retardance readout was shown in Figure 1.7 (g) after error recurring. The information stored in voxels page was decoded into a binary code page by combining two sets of binary code represented by the pre-defined retardance values and the optical axis orientations.

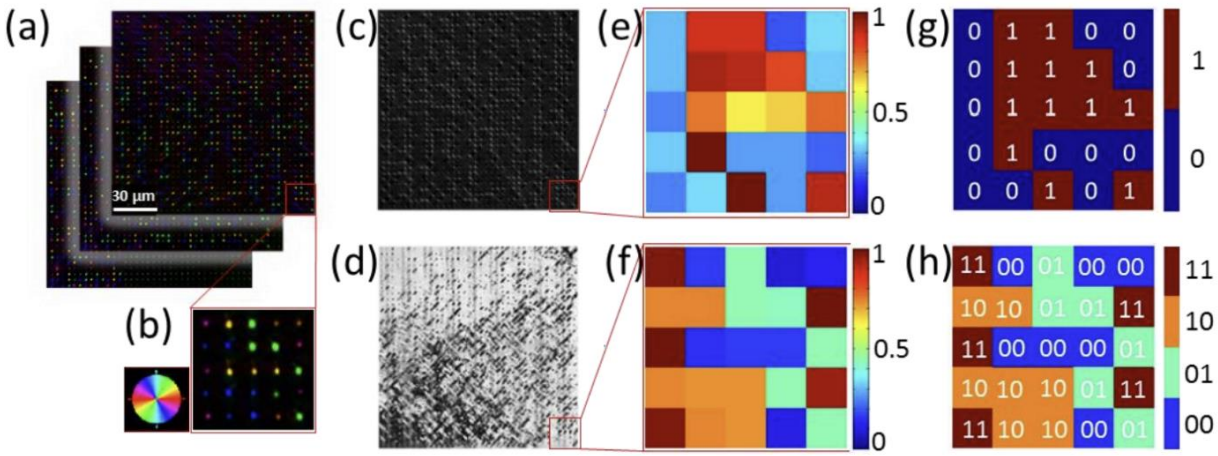

Figure 1.7 The Readout of the information stored on voxels [4]. (a) The multi-colored dots corresponding to different optical axis orientation of the form birefringence in three separate voxels layers. (b) A 5 x 5 voxels array enlarged from right-down corner of the whole voxels page. Pseudo color indicated the orientation of each voxel's optical axis. (c) Retardance distribution of all voxels retrieved from the top data page. (d) Optical axis distribution of all voxels retrieved from the top data page. (e) Direct measurement of retardance values of enlarged 5 x 5 voxels array. (f) Direct measurement of optical axis orientations of same area. (g) Binary code page retrieved after retardance values calibration procedures. (f) Binary code page retrieved after optical axis orientations calibration procedures.

A recent study in voxel readout conducted by Microsoft Research introduced a new end-to-end voxel reading approach. Traditional read approaches were originally designed for applications where the absolute magnitude of birefringence is directly tied to the desired measuring. However, in voxel reading, for each voxel, only the multi-bit value encoded in it needs to be determined. This means that increasing the accuracy of absolute magnitude of

birefringence measure will not be the method to improve reading accuracy. Therefore, a prototype of decoder for voxels reading in glass was developed according to that observation, using a deep learning approach [5,25,26].

The neural network studies the internal representation of voxels to maximize decoding accuracy, making no preconceived assumptions on importance of signal from different area in layer. The neutral network can learn the noise patterns in raw measurement. This means that background images are no longer required. This novel deep learning-based approach move the complexity of dealing with potential variabilities and noise from birefringence measurement into an offline problem. When a decoder for a given storage density and a certain glass material is trained, the total read processing time will be largely reduced. As seen in Figure 1.8, the current voxels decoder outperforms the traditional approach in accuracy.

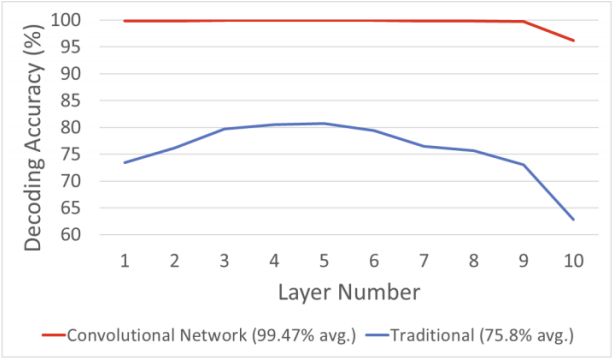

Figure 1.8 shows the decoding accuracy as a function of layer depth for voxels with 2 um lateral separation [5]. It compares the results for decoder using convolutional neural network and the traditional Four-Frame algorithm [27]. Fig G4. Decoding accuracy of new decoder (using neural network) and traditional measure. The prototype decoder achieves an accuracy of 99.47% across all 10 layers.

3. Voxel Writing

The voxel write process uses linear polarized light beams generated by a femtosecond pulse laser to create nanostructure in glass block. The femtosecond laser used for voxel writing is different from diode lasers used in Blu-ray drivers due to its power and cooling needs.

To make each voxel in glass carry large number of bits, a few possible combinations of different retardance and polarization angles are required to be written, because the number of combinations will define the number of bits one voxel can store. For example, if the writing beam can have four different linear polarization angles: 5°, 25°, 45°, 65°, and there are two different retardance levels, now we will have a total 8 combinations. Therefore, each voxel can store 3 bits of data in this case. The investigation on the growth of birefringence at varying repetition rate (time delay between each single laser pulses) and exposition (total number of pulses) at same pulse energy has been done. Figure 1.9 shows the evolution of retardance with different exposition time at same interpulse time, and with different pulse frequencies at same total number of pulses.

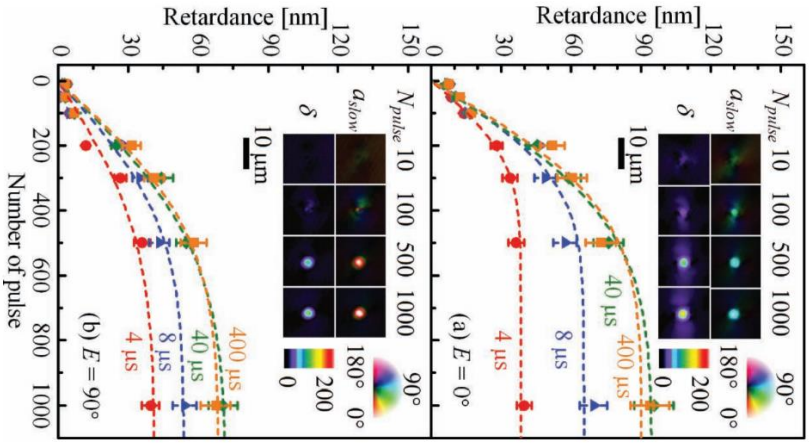

Figure 1.9 Growth of the voxel's retardance [28] under two orthogonal polarization writing beams with (a) the pulses at 0° linear polarization state and (b) at 90° linear polarization state. And four different interpulse time (4 µs, 8 µs, 40 µs, 400 µs) are used in write beams in both (a) and (b). (Insets) Polarization optics microscopy images taken with a polarizer indicating the orientation of voxel's optical axial (a_slow) and retardance's birefringent signal intensity (δ). The interpulse time of the write beam used this experiment is at 40 µs.

As shown in Figure 1.10, only stress birefringence caused by local heat accumulation was detected for sample under 100 total pulses exposure. Nanograting began to form and saturate after several hundreds of pulses due to total depletion of oxygen inside nanograting corrugations [28]. The optimal interpulse time of femtosecond laser pulses to create highest

retardance value is 40 μs, because the diffusion time was estimated to be at least 40 μs as the width of the oxygen defect regions in nanograting structure was ~ 20 nm [29].

These results in Figure 1.10 clearly indicate that the retardance value of voxel can be controlled by changing the interpulse time of its write beam. Furthermore, the different retardance value also depends on the polarization angle of write beams. And this effect is more obvious when the longer interpulse time beams are used because there is lower thermal accumulation. For example, using write beam with an interpulse time of 4 μs and pulse number below 100 pulses, the growth speed of voxel's retardance polarization angles at 0° and 90° is estimated to be 3.6×10^{-2} and 1.5×10^{-2} nm μs^{-1}, respectively [28].

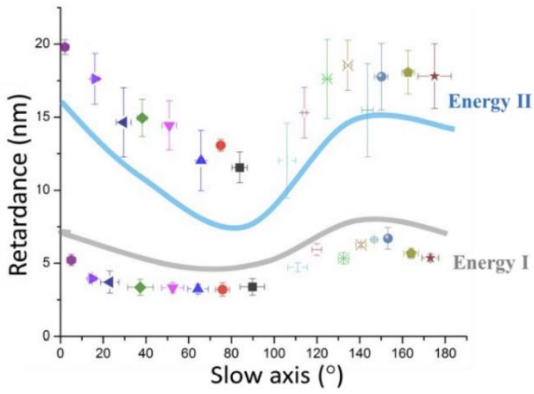

Figure 1.10 Retardance values as a function of 16 different optical axis of voxels that written by 400 pulses with 50 nJ (Energy I) and 75 nJ (Energy II) and interpulse is 5 μs [4].

To look deeper into the relationship between retardance value and polarization angle of write beam of voxels in glass, the results in Figure 1.10 provided more details. A series of voxels were written in glass by 400 laser pulses with 16 different polarization angles and two different energy levels. The two laser energies were 50 nJ and 75nJ. As can be seen in Figure 1.10, the retardance values created with different polarization angles fit in a sinusoidal dependence. The retardance values at voxels' slow axis at 0° and 90° are about 16.5 nm and 7.5nm respectively. Interestingly, the ratio of final retardance values (16.5 /7.5) with two orthogonal polarization directions almost matched with the results of growth rate ratio of retardance (36×10^{-2} /1.5×10^{-2}) with same polarization directions in [28]. The dependence

of voxel's retardance and optical axis under different write beam energy can be found and quantified. This can be utilized for the building of neural network reading engine as mentioned in the voxel reading section. This also means that to accurately read voxels with different optical axis orientations, additional calibration needs to be implemented for optimizing the voxel read process. For example, the pre-defined retardance intensity signal needs to be set and make a look-up table when analysing images taken by polarization optics microscope.

1.1.3 Fundamental challenges of data storage in glass

To make storing data in voxel feasible for practical application, there are two fundamental challenges:

(i) write as many bits as possible on each voxel
(ii) write as fast as possible on each layer

As for the first challenge, it is important to understand how data bits are calculated in a single voxel according to its two birefringence properties: retardance value and polarization directions. For example, if writing beam can have four different linear polarization angles: 0°, 45°, 90°, 135°, and there are two different retardance value available, then, the total number of the combinations of birefringence will be 8. Then, we can define each specific value as a 3-digits binary code (i.e., 000, 001, 010, …, 111). A long series of binary code can be encoded into a 2D array of voxels as a data page in a glass block. In this case, each voxel in glass can carry 3 bits of data.

As introduced in previous section, the retardance value of a voxel is determined by the laser beam, energy, and/or the number of pulses used. Apart from increasing number of available retardance values to store more bits in each voxel, the resolution of optical axis of nanograting can also play an important role in further improvement of data encoding density.

Since one voxel's optical axis orientation is directly determined by the polarization angle of its write laser pulses, more available optical axes of voxels means that the number of birefringence combinations increases. This will increase the bit density in voxel.

As for the second challenge, the recording speed of optical data storage in glass still needs a breakthrough to make this technology viable for future cloud. We could use the recording speed of current Blu-ray optical disc as a reference. A common X8 ~ X16 Blu-Ray writer can achieve data writing speed about 300Mbits/s. This means that when each voxel can carry 3 bits of data (3bits/voxel), 100 million voxels need to be written into glass in one second to reach the same writing speed of commercial Blu-ray writer. In voxel writing process, the time duration of femtosecond laser processing is very small comparing with the mechanical delay due to the glass movement. The current writing light field generation method introduced large glass movement during the data page writing process, and it shows limitations in further improving. Therefore, for next generation optical data storage technology in glass, a new method that can fundamentally increase the writing speed is needed.

1.2 Overview of current methods for phase and polarization control

This section introduces the importance of phase and polarization control of light in optical data storage technology using glass. The accurate phase and polarization control of light field is the key to data writing beam generation. The current methods for polarization control of light are also introduced and explained.

1.2.1 The use of light's phase and polarization control in optical data storage

As introduced in previous sections, each voxel in glass block has two optical parameters: linear polarization state and retardance. The increase of availability on either parameter of one voxel can lead to the increase the data storage capability. For example, a femtosecond laser writing system can generate a light field with four different linear polarization angles: 0°, 90°, 45°, -45°. The writing task requires two different patterns to encode the intensity of the light. Combining with the multi-level encoding of the polarization and intensity of light, we can obtain eight different coding-states for the data writing. This means that each coding state can be expressed by a 3 digits binary code with 23 = 8 states (i.e., 000,001,010,011, 100,101,110,111). The first bit represents the encoded intensity pattern and other two bits express the polarization states. This allows the laser direct writing to encode a long series of binary code into a 2D array of voxels on a data page in a glass sample. If a laser-direct-writing beam generation system can provide more linear polarization states, the data bits carried by one voxel will be correspondingly increases because the total number of combination coding-state of the intensity and polarization is increased. When writing voxels with different linear polarization states on one data page in glass, the location of each voxel varies on the data plane. Therefore, a dynamic control of image of output light filed is critical for the voxel writing in glass.

The phase modulation of light based on the use of computer-generated holograms on LCOS SLM is an effective way to generate image. Using different holograms to generate different beam pattern for voxel writing can make parallel writing possible and increase the total writing speed of data. Therefore, an efficient method capable of simultaneous multi-level encoding of polarization states and arbitrary image generation is very important for the laser direct writing beam generation in 5D optical storage in glass.

1.2.2 Current methods for polarization control

To date, multiple works of light polarization modulations have been reported. Here, we summarize them into two categories as follows.

(1) Polarization modulations for laser writing beam generations

Several works regarding polarization modulations for laser writing beam generations have been reported.

Allegre et al. utilized two phase-only SLM conjunction with a pair of waveplates to control the wavefront and polarization of a laser beam [30]-[31]. The modulation principle is shown in Figure 1.11 In this method, two SLMs are regarded as a "SLM convert". The first SLM is utilized to modulate the beam wavefront through a phase pattern. When light passing a half-wave-plate attached to the first SLMs, the horizontal polarization is tiled to +45°. The second SLM combined with a quarter-waveplate is utilized to convert incident linear polarization into a desired state of polarization. In this method, the modulation implementation is achieved by the second SLM and waveplate. However, the polarization state modulation is limited because two components of a vector beam cannot be arbitrarily accessible. *Allegre et al.* also developed another polarization beam generation method using a single SLM and a λ/4 wave-plate [32]. A phase-only liquid-crystal SLM was used to convert a linearly polarized femtosecond-pulse laser beam to radially or azimuthally polarized vortex beams.

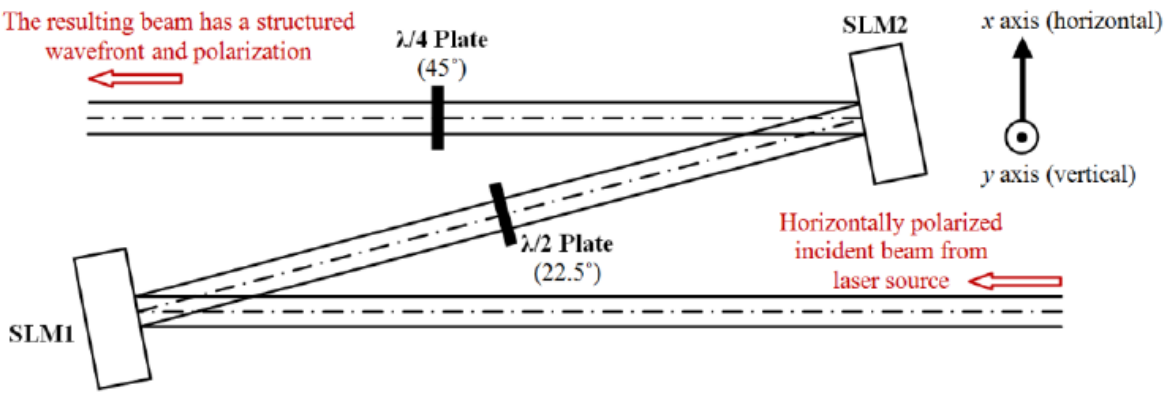

Figure 1.11 Schematic of polarization modulations using a SLM Converter, which consists of two SLMs and two zero-order waveplates [30].

Lam et al. developed a generation method of continuously rotating polarization by combining cross-polarizations [33]. The polarization modulation principle is shown in Figure 1.12. The beam modulator is composed a SLM and a quarter wave-plate. A transmissive SLM in conjunction with a quarter wave plate can produce orthogonal linear polarization on two sides of the laser beam. Although these methods can generate some polarization states on the two side of the laser beam in femtosecond laser beam writing process, the dynamic simultaneous generation of the arbitrary linear polarization states and holographic patterns still cannot be achieved.

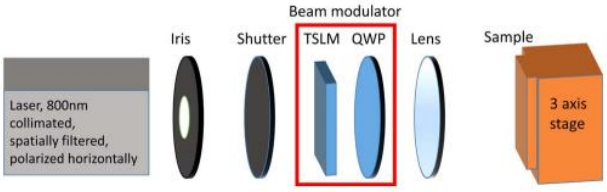

Figure 1.12 Schematic diagram of the experimental setup for the spatial variant polarization rotation and/or absolute phase modulation of the beam for surface structuring [33].

In [34], *Hasegawa et al.* utilized a pair of SLMs to create a holographic vector wave femtosecond laser processing system. The holographic vector wave generation principle is shown in Figure 1.13. The pulse was radiated onto the first SLM (SLM1), which displayed CGH1 for applying a pure phase delay to the p-component, that is, phase modulation. The HWP was arranged with an azimuthal angle of $\pi/8$ to rotate the linear polarization by $\pi/4$. The pulse was also radiated onto the second SLM (SLM2), which displayed CGH2 for applying a phase delay between the p- and s-components, that is, polarization modulation. SLM2 was located at the image plane of SLM1. The circular or elliptical polarization reflected from SLM2 was converted to linear polarization using a QWP set to an azimuthal angle of $\pi/4$.

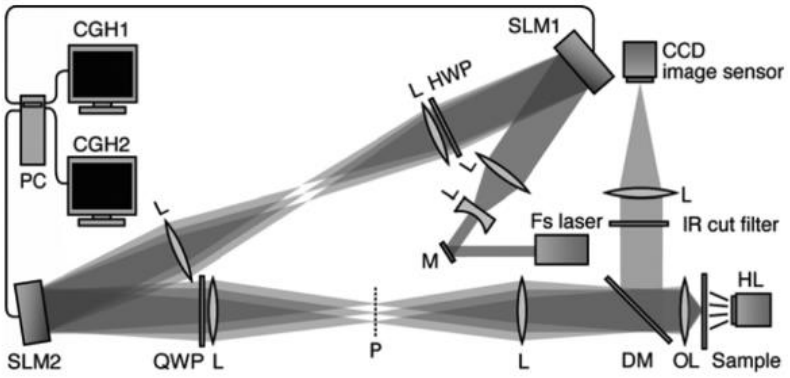

Figure 1.13 Holographic vector wave femtosecond laser processing system [34].

In [35], Ono et al. demonstrated a vector hologram beam generation method using two radially polarized beams that works as inhomogeneous polarized light. The experimental setup principle is shown in Figure 1.14. A two-wave mixing technique using radially or linearly polarized input light from two laser sources is adopted. The polarization distribution in the cross-section of the two writing beams was controlled by a SLM.

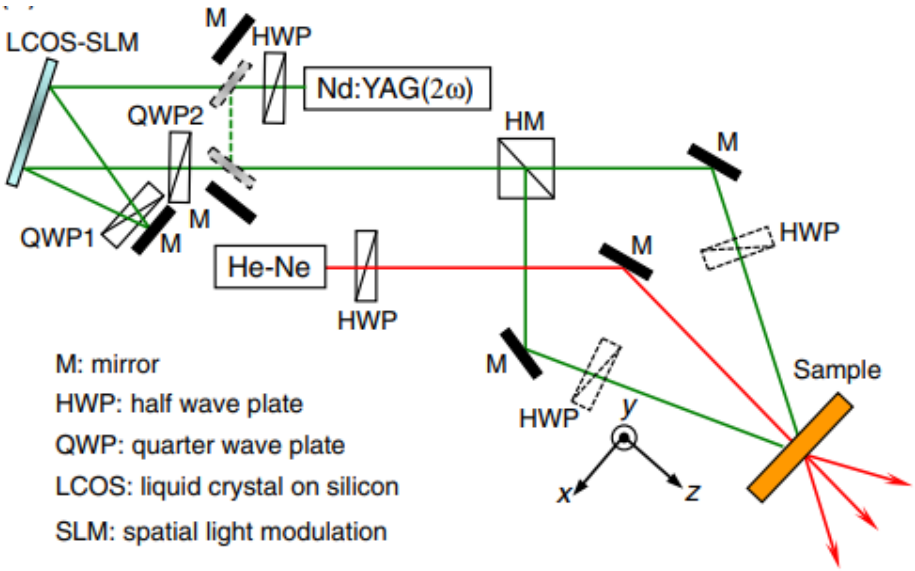

Figure 1.14 Experimental setup for intensity- and polarization-modulation holograms using inhomogeneous polarized light [35].

The University of Southampton developed an improved method using a rotation-free HWP to achieve polarization modulation with lower mechanical delay [4,17,36,37,38]. This method

used a LCOS SLM to implement data pattern generation and a half-wave plate matrix (HPM) to alter the writing beam's polarization state. The HPM consists of an array of half wave-plates that is used to produce the designed polarization states, which was fabricated by a laser to imprint a half-wave matrix consisting of four segments with predefined fast axis directions. A similar work is done where a waveplate array was fabricated with a femtosecond laser inside silica glass [39]. As shown in Figure 1.15, in this method, the fixed HMP can provide desired polarization states for data pattern when the glass sample is moved to the correct spatial position. The mechanical movement for polarization modulation is transferred from half-wave plate to the substrate of glass. This change brings the delay to hundreds ms range; however, the mechanical delay of glass block movement still prevents the recording speed of data reaching the current Blu-ray disc recording speed. The delay caused by glass movement is considerably large when we compare this to the refresh rate of data pattern generation and time duration of laser exposure.

Another limitation of this method is the number of available polarization state for writing. This method can only provide four fixed polarization states for the information encoding due to the design of HMP. This means significant limitation in storage density. Although the number half-wave plates on the HMP can be increased, it will lead to more spatial movement of glass substrate due to the working principle of this method.

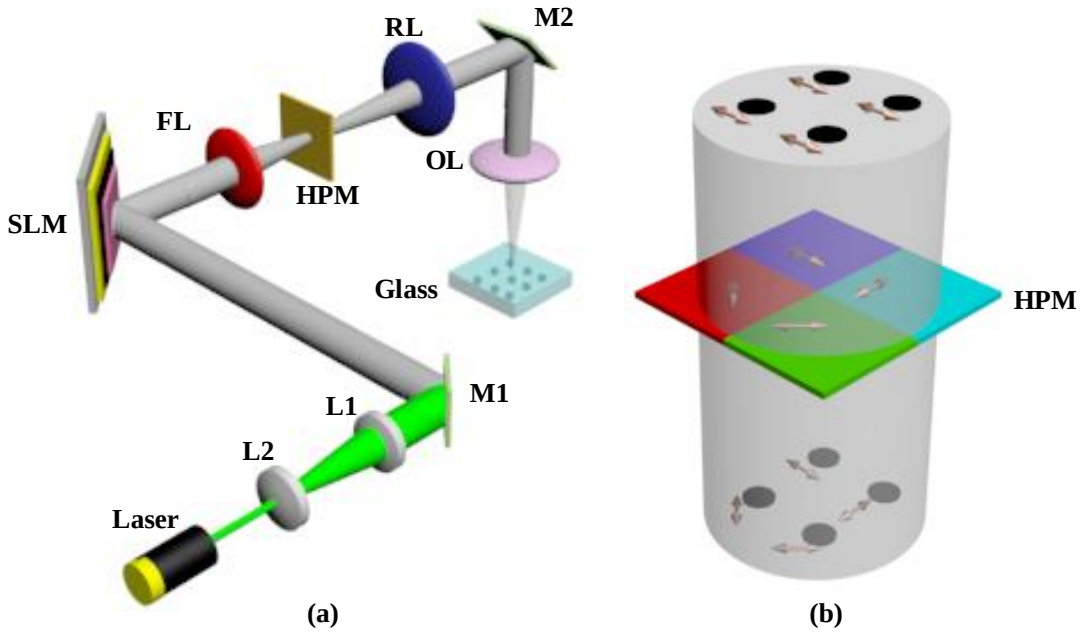

Figure 1.15 The schematic of current SLM-based holographic ultrafast direct writing system of optical storage: (a) the optical configuration of the whole system, (b) the polarization state changes through HPM, Fourier lens (FL), Relay lens (RL), objective lens (OL), Mirrors (M1-M2), lenses (L1-L2), Half-wave plate matrix (HPM). When linearly polarized beams modulated by holograms presented on the SLM pass through the HPM, the desired polarization state with encoded optical information is obtained.

In voxel writing, only linearly polarized light is used to generate the writing beam, thus, rotatable half-wave plate (HWP) is a direct way to change the angle of a linearly polarized light. However, utilizing a rotatable HWP in voxel writing beam generation has a challenging problem: the significant decrease in writing speed due to the rotation of HWP. In this method, the dot pattern for voxel writing with linear polarization state is generated using a SLM, the light field then passes through a HWP for polarization angle modulation. Every time a new linear polarization angle is to be written, the HWP needs to be rotated to a certain angle to change the incident beam polarization state. The mechanical rotation process will cause a delay (usually in the order of second) [28,40]. This delay is significantly large when it comes to a recording speed of a data storage technology. Moreover, the whole writing beam generation system will become complicated because of the difficulty in the synchronization of voxel pattern generation and the external rotatable HWP.

(2) Other polarization modulations work

Apart from the laser writing beam applications, some polarization light generation methods also have been reported. In [41], a polarization control method using a single SLM through three cascaded interactions is investigated to avoid the large light loss. In [42], a parallel aligned nematic SLM is utilized to generate complete arbitrary spatially variant polarization modulation. In [43], they utilized a single digital hologram presented on a SLM to implement the simultaneous generation of many vector beams. They demonstrated that the simultaneous generation of sixteen vector vortex beams with various polarization distributions and spatial shapes on a single SLM. In [44], a reflective twisted nematic SLM in combination with a beam splitter and a quarter-wave plate was utilized to implement a polarization rotator. Their experimental results indicated that a curve of the behavior of this polarization rotator proves a modulation up to 177°, possibly suitable for engineering of cylindrical vector fields. In [45], the system can be regarded as the combination of two variable retarders with tunable retardance, with a relative orientation of 45° among them.

Although the system introduces some important losses, mainly due to the four passages through the beam splitters, it has been experimentally validated to act as a polarization generator covering the complete Poincar´e sphere. In [46], a spatial polarization modulation method was reported through a phase-only SLM utilized in a configuration in between two quarter wave plates. These methods mainly focused the spatial polarization generation. In [47], a prism and grating free setup built around a single phase-only spatial-light-modulator was constructed to implement full control of spatial intensity, phase and polarization distributions. In [48], Chen et al. utilized a SLM and two half-waveplates or quarter-wave-plates to implement the amplitude, phase, and polarization control. This method mainly depends on a macro-pixel encoding method to achieve polarization control. In [49], *Pascuala et al.* presented a method of generation of arbitrary polarized vector beam modes by employing two SLMs. Each SLM displayed a different phase-only mask, each one encoding a different pattern onto two orthogonal linear polarization components of the input beam. Although current polarization modulation methods can control the polarization, they are not

suitable for the 5G optical storage application because most of them cannot still achieve arbitrary liner polarization state generation and phase coding at the same time.

Other polarization control works have been reported for the other applications. In [50], a polarization control method was reported for focus-shaping in high-NA microscopy. In a scattering imaging [51], a full polarization wavefront correction system is developed to shape the scattered light wavefront in two orthogonal polarizations with a single LC-SLM. In [52], a digital optical phase conjugation is used to achieve the polarization modulation for optical focusing scattering media. In the digital laser [53], a single intra-cavity SLM is utilized to implement a digital laser for on-demand modes with polarization control. This method can digitally control and switch basing modes with desired linear polarization at video rates. In [54], a polarization-dependent phase modulation using a single SLM is developed to implement the rotating point spread functions in the super-localisation.

However, those methods usually were developed for the generation of spatially verified polarization distribution, for example, vortex polarization light field for optical tweezers. However, in the application of optical data storage in glass, each voxel writing only requires one uniform linear polarization state of light. This means that the required writing light field could usually be a discrete dot array and each dot with its own linear polarization state instead of an integral beam in previous polarization modulation applications. Therefore, a novel linearly polarized light controlling method is needed for voxel writing.

From the existing methods, current polarization approaches still have limited modulation capability, specifically, in the simultaneous implementation of arbitrary linear polarization and phase patterns. Alternatively, in my thesis work, I would like to develop new polarization modulation approaches with the simultaneous generation of the arbitrary phase and polarization modulations for the future applications of laser beam generations

1.3 Aims of this research

- A simultaneous phase and polarization modulations method based on LCOS SLMs
- A prototype of compact LCOS SLM based phase-and-polarization modulation system

Phase modulation

To acquire a target image from a uniform input light beam using LCOS SLM, a diffractive pattern containing the target image information is loaded on the LCOS SLM. The diffractive pattern will shape the phase profile of input light beam, and then the target image can be reconstructed by the diffraction of light. The diffractive pattern is a hologram, and computational techniques such as the Gerchberg-Saxton algorithm (GS algorithm) are used to generate it [55,56,57]. The computer-generated hologram (CGH) on LCOS SLM provides us with a dynamic and fast way to spatially modulate the phase front of a light wave. Moreover, due to the pixelated structure of LCOS SLM, each pixel on LCOS SLM provides a specific phase value using the electronically-controlled birefringence of liquid crystal molecules to form a whole CGH, therefore, the phase modulation is reconfigurable and tuneable. In generating the writing beam of optical storage, the phase modulation based on LCOS SLM can split the beam to generate a required foci distribution for laser processing in glass. This can provide parallelisation so that the writing speed of voxel data page can be greatly increased.

The appropriate design of phase CGH enables a great level of variety and control in the form of the output light field. First, the target image can be arbitrarily designed and calculated. Second, by using suitable hologram design, the output target image can be assigned different target intensity values. This can give us chance to perform extra control of light, for example, its polarization.

Polarization modulation

Techniques have been developed for polarization control of a light field in many applications. In the application of optical data storage in glass, the polarization state of light we are interested in is linear polarization state. Each voxel writing requires only one direction of linearly polarized light, also, the number and location of voxels with the same polarization angle is random on a data page. For example, as for a voxel data page with four different linear polarization states, the data page consists of four different dot patterns and polarization state of foci dot on each pattern are identical. Therefore, this gives us a challenge: we need to generate a random distributed multi-beam pattern and control its linear polarization state at the same time. Because the dot pattern is generated by phase modulation in diffractive hologram, the polarization modulation in this research project means modulating the polarization state of holographic target image. A polarization modulation needs to be combined with the existing phase modulation using CGH on LCOS SLM.

To precisely acquire a certain polarization state of light, we need to be able to control the amplitude and phase shift of the two orthogonal polarization components. Meanwhile, we must ensure the target image information from phase modulation is not affected in the polarization modulation process. Thus, a simultaneous phase and polarization modulation method based on LCOS SLM is the major target of this research project.

Zero order elimination

When we use diffractive computer-generated hologram on LCOS SLM to produce target image, the generation of zero order diffraction noise is unavoidable. Due to the pixelated structure of electrode on LCOS SLM, the light that is incident on the gap area between pixels will not receive designed phase modulation. Therefore, this part of light will not join the forming of diffraction pattern in the replay field. Instead, the unmodulated light will keep the original propagation direction and fall on the location of zero diffraction order.

In Fourier hologram, the target image can be reconstructed by the diffraction of light at an infinite distance. To acquire the target image, a converging lens is used to perform the diffraction process at its focal plane. The unmodulated zero order light can form a high-intensity spot at the central focal position of the lens. This can be catastrophic for optical data storage in glass, as the zero-order spot intensity can be many times the intensity of the individual foci designed within the array. The unwanted zero-order spot can damage glass material and cause severe scattering of light inside the material.

Therefore, a technique for zero-order removal is required in this project. Due to the fundamental difference between modulated light and unmodulated zero-order light, the modulated light and zero-order light will show different behaviour under holographic lens on LCOS SLM..

1.4 Key contribution and novelty of this thesis

In this thesis, methods of simultaneously control the phase and polarization state of light field based on phase-only LCOS SLM have been studied and explored. The phase control of light field is accomplished by using CGHs on LCOS SLM. The polarization control is achieved by independently control of the amplitude of two orthogonal light components. This thesis explored and developed methods using CGHs to encode both information of phase and polarization modulations onto a light field. Two separate information are simultaneously encoded in the form of phase, and then translated into desired information of light field's image and polarization state. To ensure the high quality of LCOS devices, a die-level assembly techniques of LCOS SLM has been developed and improved. Motivated by the aim of improving the data writing beam generation for optical data storage using glass, a compact system of phase and polarization controls is developed and fabricated. With a single LCOS SLM device that can both, slit the beam and introduce polarization modulation, it is possible

to accelerate significantly the speed of data write, reduce the amount of energy required and reduce cost, for an ultimate high-density fast-access and low-cost data storage for the cloud.

1.5 Thesis Outline

In chapter 1, by comparing the existing candidate data storage technologies for future cloud storage, the advantages and principle of optical data storage in glass are introduced. I summarized the fundamental challenges of this data storage technologies and analysed the current method of generating data writing beam. Also, I explained the research targets of my project.

In chapter 2, as I chose LCOS devices as the spatial light modulator for my proposed system, I provided the introduction of LCOS SLM devices. And I summarized the process and experimental results of the in-house developed die-level fabrication technique of phase-only LCOS SLM. The two LCOS SLMs I fabricated in cleanroom are the experimental devices in my whole project.

In chapter 3, I introduce my proposed method of simultaneous phase and polarization modulation using parallel information coding on two separate beams and combining. This method is based on the use of two LCOS SLMs devices. The proposed method can generate target data pattern and control its polarization state simultaneously. The principle of the method is provided, and the effectiveness of this method is experimentally verified.

In chapter 4, I introduce the second proposed method of phase and polarization modulation using single beam coding. This method is still based on the use of 2 LCOS SLMs, but instead of using two beams, this method codes the two polarization components of input beam to realize the target control. The principle of the method is explained, and its effectiveness is also shown by experiments. Also, this newly proposed method and the one in chapter 3 are compared.

In chapter 5, to further improve the proposed method in chapter 4, I propose the third method for the modulation of phase and polarization of light. This method only uses one single LCOS SLM device, and it provide me with an opportunity to develop a compact system. Therefore, I designed and fabricated a compact optical system based on one LCOS SLM. This prototype device is verified in experiments. This compact system can be potential plug-in data writing technology for optical data storage in glass. Also, a zero-order noise elimination method is proposed because large zero-order noise will cause damage to the glass when LCOS SLM is used to generate diffraction holographic patten.

In chapter 6, the comparison of current method, method in chapter 3 and method in chapter 4 is provided and discussed. The result of the whole project is summarized. And the importance of the improvement achieved by my project in the whole optical data storage technology in glass will be discussed and concluded. Also, the possible future work of the project is discussed.

Chapter 2

Fabrication of high-quality phase-only LCOS-SLMs

2.1 Overview

A LCOS SLM can modulate the amplitude, polarization, or phase of the incident light beam with the use of electro-optical properties of liquid crystal molecules. Currently, there are two types of mature light modulation techniques which are amplitude modulation and phase modulation, respectively. As for the amplitude modulation of light, the LCOS device rotates the polarization direction of the input linear polarized light so that the amplitude of light can be altered when the light passes through a polarizer behind the liquid crystal. In terms of the phase modulation, the phase delay between the input light and output light is realized by the combination of birefringence property of liquid crystal and the electrically altering of the refractive index along the light path. In a phase-only LCOS SLM, the incident light can not be absorbed by polarizers or other light absorbing components, therefore, the optical system

could achieve very high light efficiency. After decades of intensive studying in LCOS, researchers have made enormous progress in the development of the phase modulation LCOS. [62] The improvement of CMOS technology also strongly supports the phase modulation LCOS to reach higher resolution, frame rate and wider greylevel. The Phase modulating LCOS devices have now become a key technology for a wide range of applications such as telecommunications, volume hologram data storage and holographic display. [63]

In this chapter, the current spatial light modulation devices have been firstly introduced in section 2.2. Also, the motivation of using phase-only LCOS SLM for the phase and polarization modulations has been explained. In section 2.3, the fundamental principle and concept from liquid crystal to electro-optical effect of phase-only LCOS has been reviewed. The choices of liquid crystal electro-optical structures have also been reviewed in this section, and the reason of using certain structure for LCOS device fabrication in this research is explained. In section 2.4, the die-level assembly techniques of fabricating the phase-only LCOS SLM used in this research has been summarized and explained.

2.2 Why LCOS SLM

In voxel writing beam generation, the data pattern (multi-beam array) and linear polarization of the data writing pulses need to be both controlled. As for data pattern generation, the high accuracy spatial light modulator (SLM) is needed to provide high resolution image in the focal plane. Moreover, the voxels carrying different information can be randomly distributed on a plane, therefore, a reconfigurable SLM device that enables dynamically control is needed. Also, a programmable spatial light modulator can play an important role in voxel writing when errors and focal aberrations in the voxel write system needs to be calibrated and compensated.

There exist several options of spatial light modulators (SLMs) that can effectively modulate the properties (phase, amplitude) of a beam across its profile. These SLM devices are

essential components of most adaptive optics systems. And in previous research in optical data storage in glass [4], they are utilized in writing system. There are three considered commonly available and feasible for use in this project.

1. **Digital mirror devices (DMDs)**

DMD technology is based on the MEMS platform and have been well developed for optical projector application. DMDs consist of a micro-mirror at each pixel that allows rapidly switching between two fixed angles, and this provides the ability of amplitude modulation of light by directing light into or out of the incident beam path. The micro mirror array can offer high-speed switching with rates up to 40kHz, and the control of mirror units is easy and low cost. Because of its high framerate, the grayscale amplitude modulation is achievable now. However, due to the binary nature of the direct amplitude modulation, the light modulating efficiency is lower than phase modulation that using diffraction. When ultra-short pulses from femtosecond laser is used as the light source, a main limitation of DMDs will make it difficult to be the right spatial light modulator. First one is light dispersion generated by the device: when all micro mirrors are in the ‘on’ position, the device forms a uniform blazed diffraction grating with a pixel pitch of approximately 5 μm, the angular dispersion will significantly affect pulses with durations less than approximately 1 ps[58]. Moreover, current DMDs have average power limitations about 25W because of the low thermal mass of the micro mirrors, and this will limit their potential in laser machining process.

2. **Deformable mirrors (DMs)**

DMs consist of a highly reflective surface whose profile can be controlled by forces from an array of actuators. The mirrors actuated by electrostatic, electromagnetic or piezoelectric means can provide a surface of continuous membrane or arrange it into segments. DMs have good reflectance over a wide range of wavelengths and insensitive to polarization. DMs can

provide large amount of phase modulation to the wavefront of light but the phase modulation resolution is low due to its low pixel resolution. Typically, DMs have tens to hundreds of actuators, which is much smaller than the normal number of pixels for a LCOS SLM or a DMD. Considering the application in creating write beam for data storage in glass, DMs are suitable for a secondary light modulation when the requirement of high light modulation accuracy is required.

3. Liquid crystal on silicon spatial light modulators (LCOS SLMs)

Liquid crystal based birefringent optics elements are most widely used in adaptive optic system due to their simplicity of utilization, flexibility in system integrating and ultra-high resolution. Some early models of liquid crystal based SLMs were designed as transmissive devices, however, the great majority now are operated in reflective mode with a liquid crystal layer on a silicon (LCOS) back plane. Most current LCOS SLMs are designed to provide phase-only modulation using nematic liquid crystal materials. When the case that only phase is modulated happens, the polarization state of incident laser beam needs to be parallel with the long axis of liquid crystal molecules.

Current Phase-only LCOS SLM devices operating in nematic phase provides multi-level phase modulation of the output laser beam. Current devices normally offer 256 phase levels within 2π range, and a recent study has shown that 1024 phase levels has been achieved with low phase flickers [59,60]. The nematic LCOS SLMs generally have limited switching rates in the tens of hertz, and this number become even slower when longer wavelengths of light in use, because a necessary increase in the device thickness is needed to ensure 2π modulation range. However, it has been shown that, using overdrive techniques, it is possible to approach modulation rates of 1 kHz while liquid crystal material is still in the nematic phase with greyscale modulation capability [61].

The LCOS SLM can have outstanding advantage in ultra-high resolution of holographic image generation. This ensures the high resolution of dot array pattern in data writing. Also,

due to the use of computer-generated hologram (CGH) in LCOS SLMs, the pre-determined data pattern can be easily calculated in holograms, and they are directly loaded on LCOS devices. More importantly, the phase-only LCOS SLMs show the potential that they can be used to control the polarization and/or phase of the output beam after a proper design of modulation scheme. Therefore, the LCOS SLM device is considered as the most suitable choices over three kinds of SLMs discussed above.

2.3 The principle of phase-only LCOS SLM

2.3.1 Liquid Crystal

Liquid Crystals are unique compounds with the properties of both liquids and crystals. Liquid crystal exists in mesophases, which have diffused molecular order and orientation. The nematic phase, smectic phase is discussed here because these two liquid crystal mesophase are widely used in LCOS SLM devices [64].

The liquid crystal phases are distinguished by the difference in the ordering of liquid crystal molecules which also means its liquid properties and viscosity [64].

The arrangement of the centres of gravity of the molecules in space is the positional order. The liquid crystal materials are temperature-sensitive materials; thus, the molecular arrangement is initiated by temperature. At high temperatures, the liquid crystal materials are isotropic, which means that they act as a liquid with no positional or orientational order. At lower temperatures the liquid crystal will be in highly ordered mesophase [65,66].

Nematic liquid crystal is the most studied and used liquid crystal material. This is the least ordered mesophase before the isotropic. Thus, the nematic liquid crystal molecules retain a relatively low viscosity and are prone to flow. [67] The anisotropy in the shape of nematic molecules leads to the dielectric anisotropy, which means that a nematic molecule can be

reoriented in any direction with the use of an electric field. It is notable that the direction of nematic liquid crystal molecules is based on the average direction across billions of individual molecules as shown in the Figure 2.1. Moreover, the 'rod-shaped' molecules result in the optical anisotropy which leads to the birefringence property.

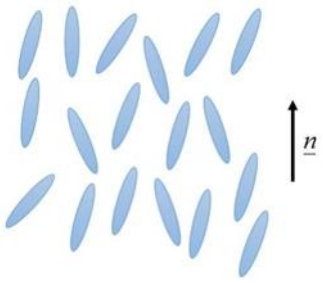

Figure 2.1 The molecular arrangement of Nematic liquid crystal phase. The vector n shows the direction of molecular ordering.

2.3.2 Refractive Index of Liquid Crystal

When we combine the flowing property of liquid which allows the molecules to move when an electric field is applied across and the optical anisotropy of molecules, the axes of the indicatrix can be effectively rotated as the molecules move, which can create a moveable wave plate or optical retarder for the incident light. This is the basis of most liquid crystal intensity and phase modulation characteristics when it combined with the polarisation of light. In the uniaxial optical indicatrix of molecule, the two axes of the molecule appearing as the refractive index. [68] The refractive index for the light with electric field polarisation perpendicular to the director is referred to as the ordinary n_o ,as shown in Figure 2.2, and the extraordinary refractive index n_e is for the light with electric field polarisation parallel to the director.

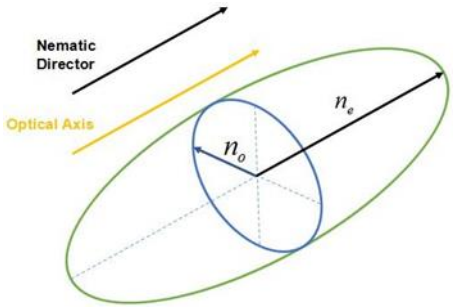

Figure 2.2 A schematic of optical indicatrix of refractive index of nematic liquid crystal.

The difference between the two refractive indices is defined as the birefringence:

$$\Delta n = n_e - n_o \tag{2.1}$$

For most liquid crystal materials, the birefringence is positive, ranging from 0.05 to 0.45, and the ordinary refractive index is around 1.5. With the voltage-driving movement of director and optical indicatrix reorientation, effective refractive index seen by the incident light decreases. The intermediate state of effective refractive index is related to the magnitude of n_e and n_o and the angle of orientation of the director.

For a monochromatic, polarized light wave, the effect of liquid crystal molecules can be described by a Jones matrix., the polarized light is a fully polarized state in the sense that the Stokes parameters [69] add up to 1 [70]. For parallel aligned liquid crystal cells, the Jones matrix [71] is given by

$$W = e^{i\phi}\begin{pmatrix} e^{(-i\beta)} & 0 \\ 0 & e^{(i\beta)} \end{pmatrix} \tag{2.2}$$

where the birefringence β and the phase offset φ are given by

$$\begin{aligned} \beta &= (n_e - n_o)\frac{\pi d}{\lambda} \\ \phi &= (n_e + n_o)\frac{\pi d}{\lambda} \end{aligned} \tag{2.3}$$

Where the n_e and n_o are the ordinary and extraordinary indices of refraction of the LC material, respectively, d is the thickness of the cell, and λ is the wavelength of the light wave. The possibility of changing the birefringence β as a function of the voltage applied to the liquid crystal molecules makes the liquid crystal cell a switchable waveplate. [71]

2.3.3 Electro-Optic Effect for LCOS SLM

In LCOS SLM devices, the liquid crystal molecules can be arranged in different structures by alignment process. Thus, the incident light will be modulated in different ways depending on the electro-optic effect in different structures when the voltage is applied to the liquid crystal layer. Diverse types of electro-optic structures for liquid crystal have been studied and used in LCOS devices for many years, such as vertically aligned nematic (VAN) [72], twisted nematic (TN) [73], electrically controlled birefringence (ECB) [74][75][76] etc. Many of them are initially designed for phase-only LCOS SLM devices, and some structures work for amplitude modulation. The arrangement of liquid crystal can directly determine the operation mode of the light modulation; therefore, this is very important for the design of LCOS device. In this section, three different device structures will be explained, TN and VAN are for amplitude modulation and ECB is mainly used for phase-only modulation mode.

1. **Twist nematic**

The twisted nematic mode was first introduced by Ferguson et al. in 1986 [77][78], and it has been developed and used in display application for many years. In the TN mode, the direction of liquid molecules twists from one substrate surface to the other in the thin layer. Thus, the alignment directions on the two surfaces are perpendicular to each other, which can achieve the 90-degree twist across the liquid crystal cell. The nematic liquid crystal molecules are less ordered and free to rotate in any position, therefore, it is possible to make more complex

structures. As shown in Figure 2.3, the helical path of molecules can be extended by adding suitable chiral dopants to create the structures with twists of the order of 270°.

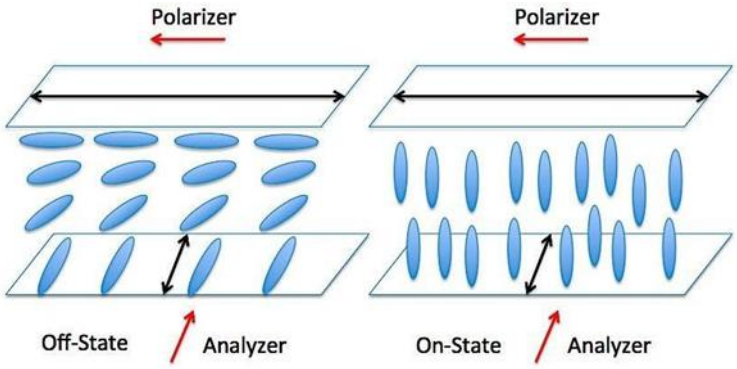

Figure 2.3 A schematic of the twisted nematic arrangement. The two black arrows indicate the two alignment directions. [79]

When there is no electric field applied across the liquid crystal cell, the liquid crystal molecules remain the twist structure in the off state. The incident polarised light that passes through the liquid crystal layer will experience a polarisation transformation. This transformation can result in the emerging light with an elliptic polarisation. In the on state, the liquid crystal molecules are realigned along the electric field, which decreases the rotation of the polarisation passing light, until the light polarisation cannot be rotated anymore so that the light is blocked by a polarizer. The orientation of the polarisation of light can be altered by the change of the applied voltage, thus, the amplitude modulation of the light can be achieved by the polarizer. In phase-only modulation, the analyser must be removed, because this can result in the modulation of both the phase and the polarisation. This means that the certain modulation of phase is bonded with a fixed polarisation, therefore, the arbitrary complex field of light cannot be modulated on each pixel.

2. Vertically Aligned Nematic (VAN)

In the VAN structure shown in Figure 2.4, the liquid crystal material with negative dielectric anisotropy is required, and this mode is used for amplitude modulation. The linear polariser is set at 45° with respect to the orientation of the LC alignment and at 90° with respect to the analyser. Like the TN mode, the liquid crystal molecules rotate the plane of polarisation of the light due to the applied electric field, and the analyser converts the rotation of polarisation into amplitude difference.

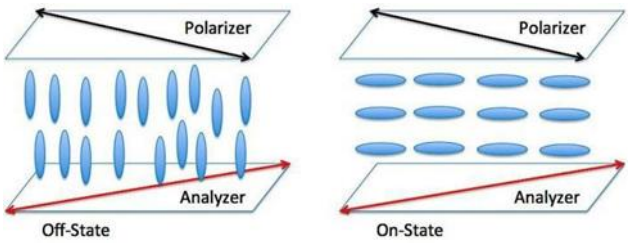

Figure 2.4 A schematic of the liquid crystal vertical alignment mode. The two-directional arrows indicate the directions of polariser and analyser. [79]

In the off state, the homeotropic orientation of liquid crystal is perpendicular to the surface of the alignment layer, which results in no rotation of the polarisation of incident light. The crossed polarisers ensure that the light is completely blocked, resulting in high contrast ratio. Therefore, the VAN structure is widely used in amplitude modulation displays LCOS devices. However, for phase-only LCOS devices, the VAN mode has not that advantage in amplitude modulation, and the limitation in the use of liquid crystal materials make it not applicable to phase-only operation. Due to the requirement of liquid crystal materials, the absolute value of dielectric anisotropy of negative dielectric anisotropy materials is normally less than that of positive ones. This can result in the longer response time of liquid crystal molecules.

3. Zero-Twisted Electrically Controlled Birefringence (ECB)

The ECB structure uses nematic liquid crystal with a positive dielectric anisotropy, therefore, the director of molecules switches from almost planar to homeotropic when a voltage is applied across the cell. [80] The polarisation direction of the incident light is aligned with the initial liquid crystal director, the refractive indexes that the light experiences can be the complete range from n_e to n_o continuously with the analogue increase of voltage level. Therefore, the ECB mode is highly suitably for the phase- only modulation.

The ECB structure is formed by the anti-parallel planar alignment on the two surfaces with small tilt angle. The small tilt angle is necessary to prevent reverse tilt switching [81], however, to maximise the depth of phase modulation, the small tilt angle must be minimised. In the fabrication of nematic LCOS SLM device, the rubbing alignment can provide a 2 degrees tilt angle from the surfaces of glass and silicon backplane substrates [82].

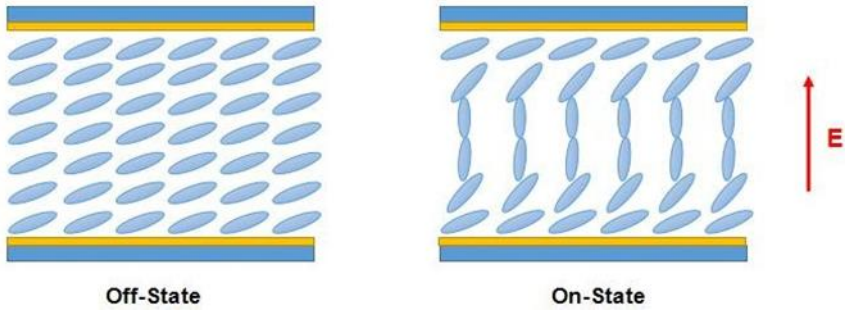

Figure 2.5 A schematic of the initial Von and Voff state of ECB mode with small tilt angle. There is zero-twisted configuration in ECB.

The ECB has a molecular switching feature which is considered as its main drawback. When applied driving voltage is switched off, the molecules would rotate back to their initial state. The molecules in the middle of the ECB layer will experience a torque- like force causing a backflow of the liquid crystal, therefore, the molecules must rotate through a large angle to

relax [83] This torque-like force in the mid-layer is asymmetric due to the anti-parallel alignment. (Figure 2.5) As a result, the relaxation of the molecules will be delayed, leading to slow response in the operation. The ECB mode currently remains the first choice for liquid crystal structure in phase-only devices as it has a relatively high controllable movement of liquid crystal molecules.

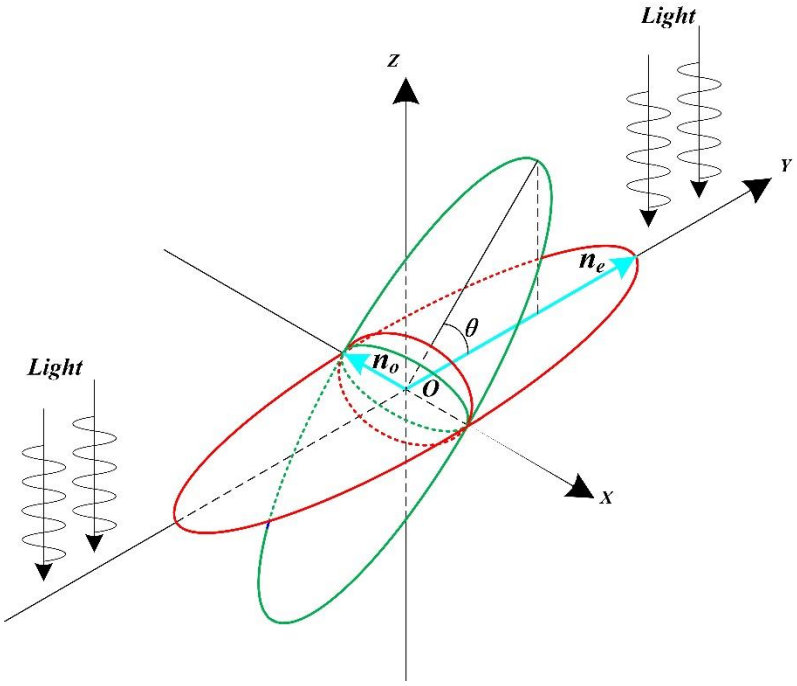

Figure 2.6 A schematic of liquid crystal molecules rotation in ECB for phase-only modulation.

When the input light is passing through the ECB structure, the linearly polarized light parallel to the extraordinary axis of the liquid crystal materials can be seen as a function of the voltage-controlled birefringence. [71,84] As shown in Fig 2.6, when the input light is a linearly polarized light with oscillation plane at Z-Y plane, the light wave will experience the refractive index n_e of liquid crystal molecule that is aligned to the Y axis (the red liquid crystal molecule). Thus, a phase retardance can be introduced to the input light.

The silicon backplane in the architecture of the LCOS devices consists of the driving circuitry which is covered by the pixel arrays layer. The pixels on the surface of silicon backplane are aluminium mirrors that can reflect the incident light back for the modulation in the liquid crystal and exit. In the phase-only modulation in ECB structure, both electrodes sandwiching the liquid crystal molecules at X-Y plane, liquid crystal molecules can be rotated along the X axis by using electric field. The voltage on each pixel can be precisely controlled the electrical driving circuitry, therefore, the angle between the long axis of liquid crystal molecules and Y axis can be precisely controlled. By applying the optimized voltage pulses arrangement, the position of the liquid crystal molecules can keep stable for certain phase retardance. As shown in green molecules of Fig 2.6, when the liquid crystal molecule is rotated to an angle θ, the projection of refractive index n_e towards Y axis will be altered. Therefore, the new phase retardance induced on the linearly polarized light can be controlled by the angle θ and value of n_e. The phase value introduced to input light is given by

$$\delta = \frac{2\pi\Delta n_{effective} d}{\lambda} \tag{2.4}$$

where λ is the wavelength of the input light, d is the thickness of liquid crystal cell, and $\Delta n_{effective}$ represents the effective birefringence controlled by liquid crystal molecule rotation. And in a reflective mode phase-only LCOS SLM, the total phase value would be

$$\delta = 2 \cdot \frac{2\pi\Delta n_{effective} d}{\lambda} \tag{2.5}$$

In phase-only LCOS SLM, the stability and accuracy of phase value on each pixel is determined by the ability to hold the liquid crystal molecules' angle steadily. And the number of different angles of molecules that can be achieved from planar to homeotropic (0° to 90°) would define the resolution of the phase-only modulation.

2.4 Die-Level assembly technique of phase-only LCOS SLM

In this section, the in-house developed fabrication techniques of the phase-only LCOS SLM has been summarized and explained. Phase-only LCOS SLM is key component for implementing the phase and polarization modulations of light. The performance of a LCOS SLM is directly determined the quality of fabrication. Therefore, the die-level assembly techniques have been tested and developed for building high-quality custom phase-only LCOS SLM.

2.4.1 Related technologies

In general, the assembly process of LCOS devices is divided into two methods, wafer level assembly and die-level assembly. [79] The wafer-level assembly has been widely used in commercial amplitude modulating LCOS devices. [85][86] The wafer-level assembly technique origins from the high-volume production lines. The LCOS devices are fabricated on the large size glass and silicon wafers, and then they are diced into separate LCOS modules. [85] This method requires production equipment with programmed processes. For the research purposes of LCOS devices, the wafer-level assembly technique is not suitable due to the high cost of introducing the commercial production line. Therefore, the die-level assembly methods will be the better choices not only because of its low cost but also for the reasons below [87][88]:

For a research prototype device, the design of LCOS SLM structures must be tested, thus, the die-level assembly technique allows us to fabricate the individual devices with different assembly processes. The die-level fabrication process can be optimized by the individual investigation of each process stage. The optimization of assembly process can further improve the performance of the LCOS devices. In conclusion, the die-level assembly is more appropriate to custom devices and pre- production prototypes due to its flexibility and efficiency. More importantly, the quality of assembly provided by the die-level process is comparable to the wafer-level assembly process [89].

2.4.2 Die-Level Assembly Process

In this part, the process of the die-level assembly method used to fabricate the two LCOS SLMs used in this research is summarized.

The die-level assembly of LCOS cells was carried out in Class 1000 and Class 100 clean rooms in the Cambridge University Department of Engineering. To improve the fabrication performance, the programme-controlled and semi-manual systems for the die-level assembly process has been applied. This assembly method allows the precise control of the glue dispensing process and packaging of LC cell so that high quality phase-only LCOS devices can be made in reproducible fashion. Figure 2.7 shows the flow of in-house developed assembly techniques. The cleaning process for glass substrates and backplanes are conducted in the wet bench at class 1000 cleanroom, while the rest of processes are finished in class 100 cleanroom.

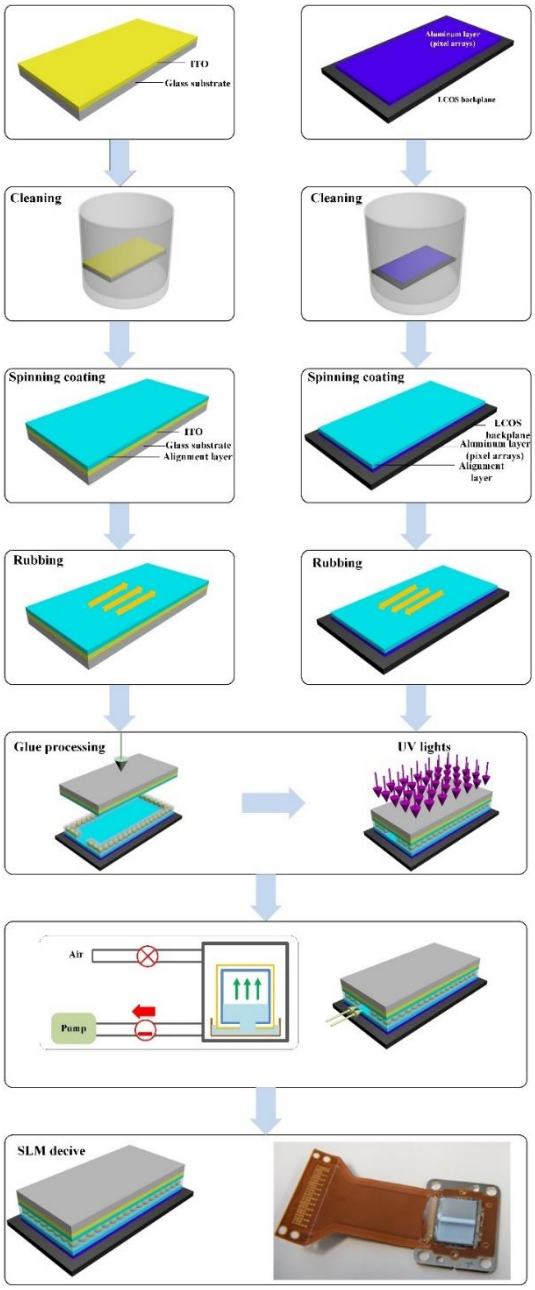

Figure 2.7 The fabrication procedure of our LCOS SLM.

As shown in Fig 2.7, the main fabrication procedures of LCOS SLM device are followed as: Cleaning, alignment material coating, alignment layer rubbing, glue line writing and assembly, and liquid crystal material filling. The principles, purposes and process of each step are explained below.

1. Alignment material coating

The alignment of liquid crystal is the essential for the performance of LCOS SLM devices. The selection of alignment method will depend on the liquid crystal materials and the specific requirements for different applications, and the alignment deposition require stability and suitable electrical properties. There are three types of polyimide-based alignment treatments in use which are planar, pre-tilted planar and homeotropic. In the example of current phase-only LCOS SLM devices which are based on nematic liquid crystal material, the slightly pre-tilted planar alignment is normally in use as it could avoid the reverse tilt disclination occurring during the movement of the liquid crystal molecules. Figure 2.8 shows the principle of alignment material spin coating.

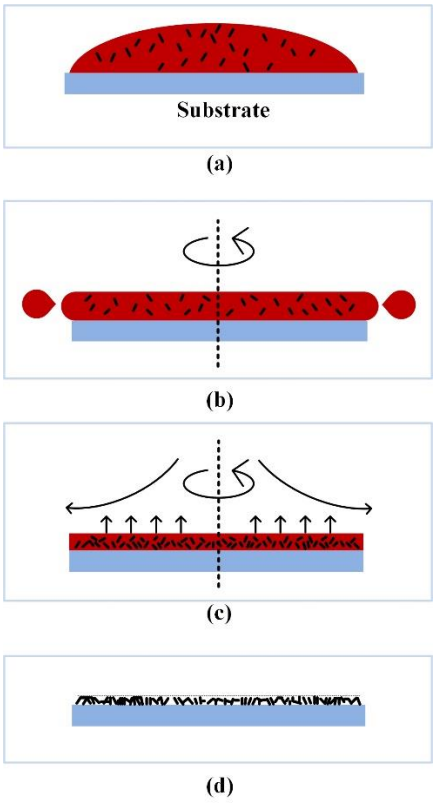

Figure 2.8 The schematic of spin coating process of alignment layer material. The process begins with dropping the material solution onto the substrate (a). Then, the spin coating rotator accelerates to the target speed. The

shape of material solution changes into a film due to centrifugal force (b). Meanwhile, the air flow above material can cause the evaporation of solvent (c). The material forms a uniform film on the substrate surface.

The alignment material coating process starts with spin coating of the polyimide material solvent, and it is followed by baking. The aim of baking process is to evaporate the solvent in alignment polyimide and solidify the alignment material after the spin coating process.

2. Alignment layer rubbing

The orientation of the liquid crystal molecules at the surface can be achieved by rubbing the polyimide films on both glass and silicon-backplane in a specified direction. The grooves are created on the surface by the rubbing process, and it will align the molecules on the substrate surface. In general, the rubbing with textured cloth is the most widely used method to form the alignment. [90] In the fabrication of phase-only LCOS SLM device, velvet was selected as the rubbing media due to its dense surface which provides a relatively gentle contact to the substrate. Moreover, the velvet rubbing not only cause less damage to the polyimide thin film, but also could create uniform grooves on the surface.

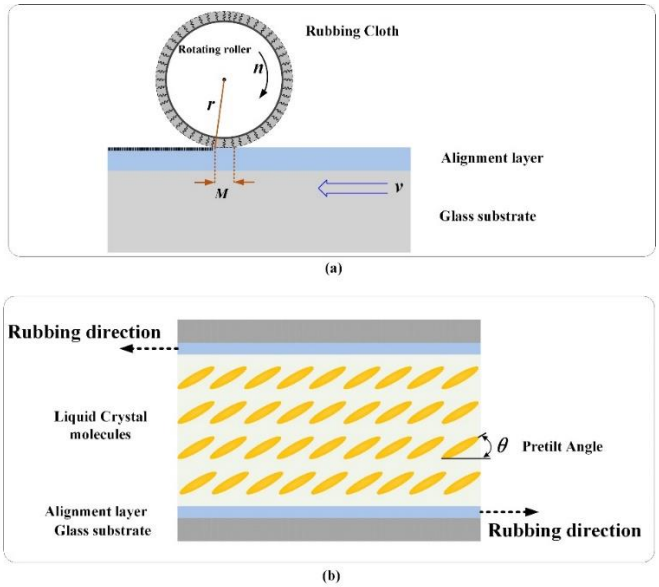

Figure 2.9 The rubbing principle for the SLM assembly

The alignment arrangement is defined by the molecular alignment angles with respect to the glass substrate. The tilted alignment produces an acute angle between the long axes of the molecules and the glass substrate. [79] For the phase-only LCOS SLM device in this project, as shown in Figure 2.9, the alignment method adopted is anti-parallel with tilted alignment. The nematic liquid crystal material with high birefringence is normally used in these types of device structure.

3. Glue line writing and assembly

The glue line serves for two purposes: the sealing of the LCOS cell, and the spacers in the glue could provide uniformity across the whole cell in a certain thickness. Moreover, the length of the cell gap determines the optical properties of LCOS SLM devices. the glue line writing and device assembly are performed consecutively by semi-automated robotic equipment. As shown in Figure 2.10, the glue line dispensing currently is achieved by a digital glue writing system Kadett which is modified for the phase-only LCOS device. The dispenser control is connected to the syringe barrel with the dispenser needle. The system can distribute the glue on the silicon substrate automatically after the designed glue line map loaded into the system.

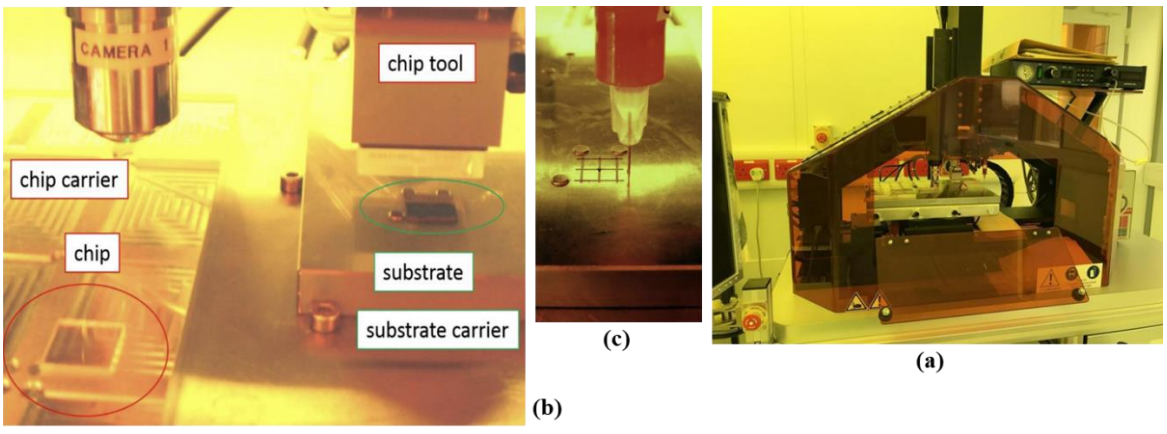

Figure 2.10 The glue line writing and die-level assembly system Kadett in class 100 clean room (a) and (b). The glue line dispenser syringe and needle (c).

In the assembly process, the glass substrate is picked by the bonding head, then it is moved with a vacuum head to the desired position above the silicon backplane substrate. After the dispensing of glue line, the bonding head with glass substrate attached is precisely positioned on the silicon substrate with the certain applied force. The final step of assembly of the LCOS cell is the curing of the glue. The assembled cell will be exposed to the ultra-velvet light to fully cure the glue.

4. Liquid crystal material filling

The liquid crystal material needs be filled after the assembly of cell. The filling process is achieved by using air pressure to push the liquid crystal material into the cell. During the filling process, the liquid crystal material needs to be heated up to transform the phase of liquid crystal from nematic phase into isotropic. Figure 2.11 shows the procedures of liquid crystal material filling.

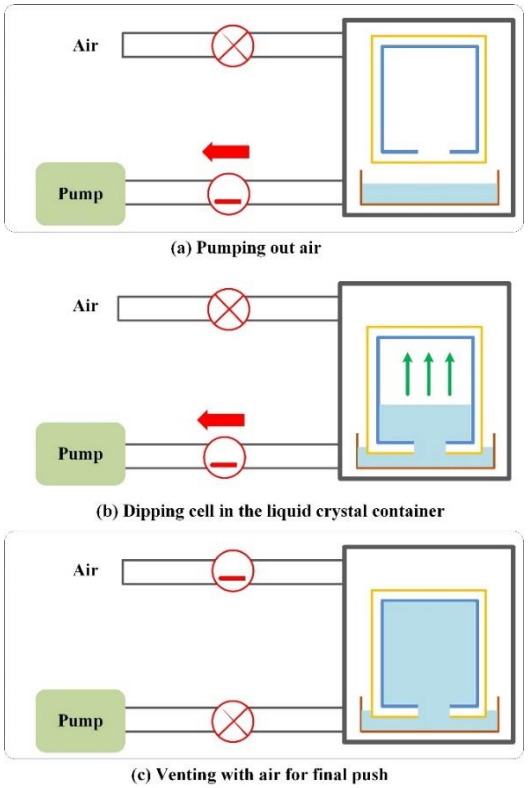

Figure 2.11 the principle of the LC material filling

When the air pressure of the chamber reaches a stable point after air pumped out, the heater panel will be lifted down so that the filling holes of cells could completely immersed in the liquid crystal. The liquid crystal can be pushed into the cell due to pressure difference between the filling rig (High) and the liquid crystal cell (Low) when the vacuum value is opened. The final process is the sealing of the liquid crystal filling hole using the same glue as the glue lines. This glue sealing process is finished by handcrafting with the use of the syringe which connected with a glue dispenser.

2.5 Conclusion

In this chapter, the principle of LCOS SLM has been introduced. As a technology of spatial light modulation, LCOS SLMs, combines the unique light-modulating property of liquid crystal materials and the developed technology--silicon complementary metal oxide semiconductor (CMOS). [62,91]

A Phase-only LCOS SLM based on ECB structure has been designed and developed according to the purpose of phase and polarization modulation in the later research. Then, two phase-only LCOS devices has been fabricated in the clean room by using dye-level assembly techniques. The processes of fabrication techniques are also summarized and explained. These two LCOS SLMs are key devices for the experiments in this research project.

Chapter 3

Phase and polarization modulation using two-beam parallel coding

3.1 Overview

In this chapter, a both phase and polarization modulation method is proposed for simultaneously modulating the phase and polarization state of light field.

In this method, the phase modulation means the holographic pattern information encoding of input light field. This modulation is achieved by using Computer Generated Hologram (CGH) on phase-only LCOS SLM. The polarization modulation here means the control of the polarization state of output holographic pattern. An importance of this method is that the two targets ‘desired holographic pattern and desired polarization state’ can be achieved at same time. Both phase and polarization modulations are simultaneously completed by using LCOS SLMs, and there is not any external special devices needed.

When we consider the modulation of the linear polarization state of a beam, if we can independently control the amplitude ratio and phase shift between the vertical and horizontal polarization components of the light, we can achieve any polarization state that we need. As shown in Figure 3.1, two orthogonally polarized beams are independently encoded with holographic pattern and amplitude information by using two LCOS SLMs, then, the two modulated beams are combined into one output light field.

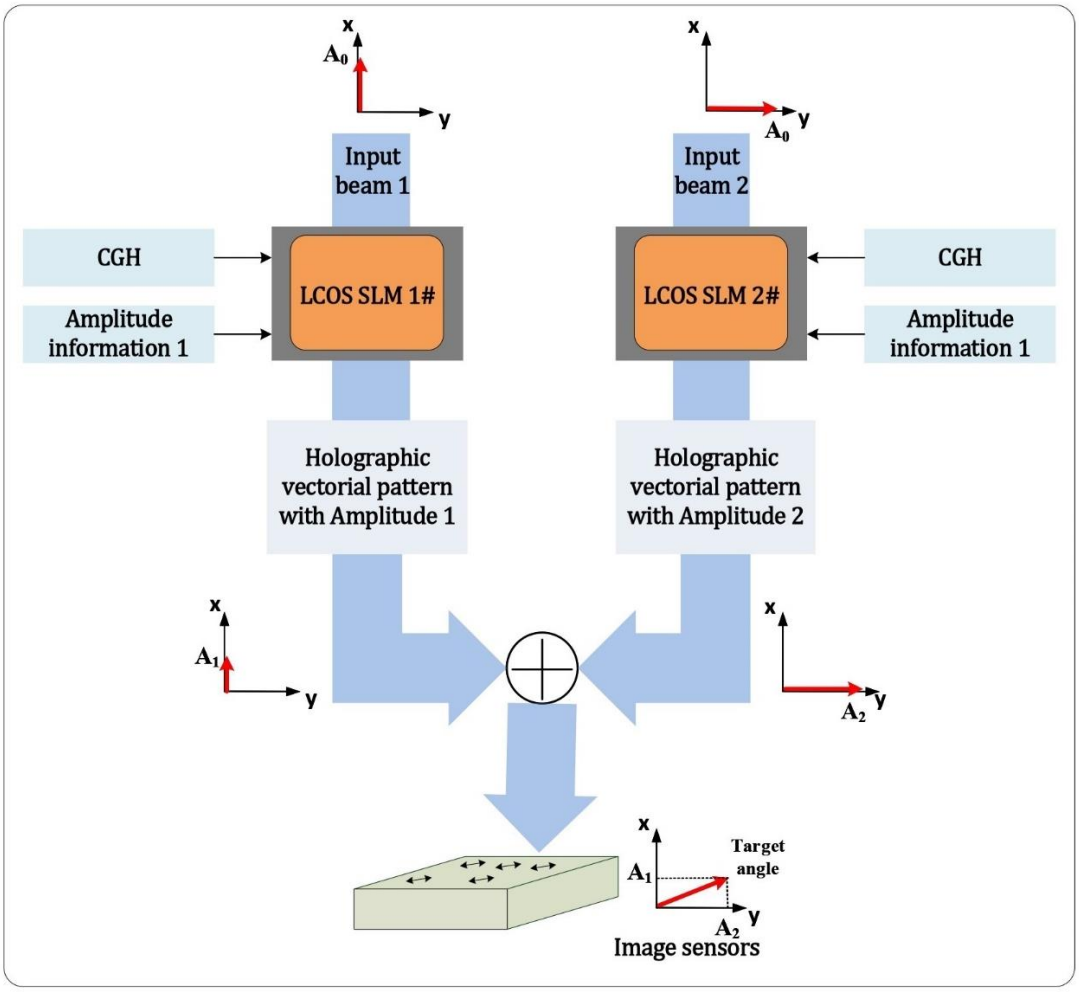

Figure 3.1 The schematic of proposed method using two beam parallel coding and combining. The information of target image and amplitude are independently encoded onto the input beams to form the target polarization state.

The CGH on LCOS SLM can carry both holographic image and amplitude information. The amplitude of holographic vectorial light field is modulated by changing the phase depth of CGH. By controlling the amplitude ratio of two basis beams, the polarization direction of combined beam can be altered.

The principle of the method is introduced in section 3.2. To acquire the output holographic vectorial pattern, the combining of two modulated beams plays an important role in this method. The principle and combining method also explored and covered in section 3.3. The arbitrary holographic vectorial patterns are experimentally generated to verify the effectiveness of the method. Also, in section 3.4, the comparison of the proposed method and existing method for generating data writing light field is discussed.

3.2 The proposed method

3.2.1 The principle of the proposed method

Figure 3.2 shows the principle of the proposed phase and polarization modulation method. First, two coherent laser beams are input into two separate optical vector channels (horizontal and vertical channels). The two independent channels are used to produce two basis holographic vector components with orthogonal polarization direction for their later combining. As mentioned in chapter 2, the phase-only LCOS SLMs are sensitive to the polarization state of the input light due to the operating principle of liquid crystal modules [71,92,93,94,95]. This means that the polarization state of input light needs be parallel to the alignment direction of liquid crystal molecules for the phase-only modulation. In this method, we utilize phase modulation to encode holographic image information on the beams. Therefore, the polarization state of input beams in two optical channels are first changed into parallel with liquid crystal working direction to ensure the high-quality holographic information is encoded on two channels. In the practical design, two LCOS SLMs are

parallelly placed for the symmetrical of optical path, thus, both optical channels provide phase modulation at a horizontal polarization state.

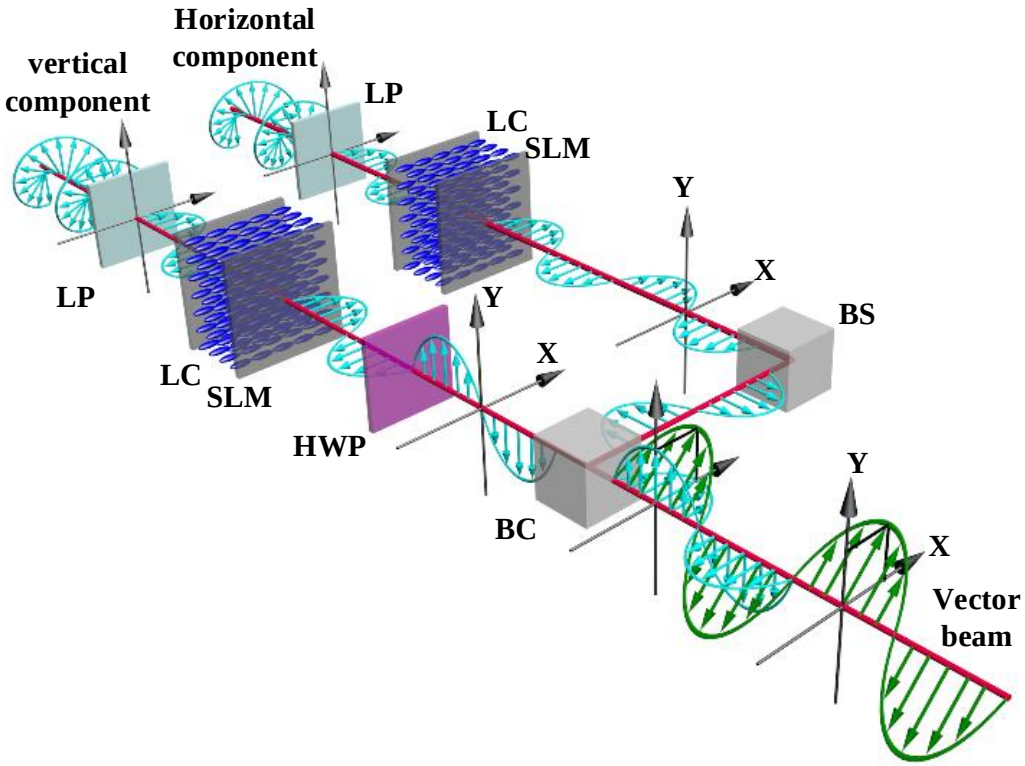

Figure 3.2 the principle of the proposed method using tuneable optical vector, where LP is a linear polarizer, LC is liquid crystals, HWP is a half wave-plate, BS is a beam splitter, and BC is a beam combiner.

After two vector beams are modulated horizontally, there needs a process to convert one of them into a vertically polarized beam for polarization modulation. In the horizontal channel, the hologram on the LCOS SLM directly encodes the horizontal polarization input beam to produce the horizontal basis vector. In the vertical channel, the vertical vector beam is generated by using a half-wave plate (HWP) after passing LCOS SLM. The modulated horizontal vector beam pass through an HWP at 45°. Then, the HWP is used to rotate the horizontal polarization state into the vertical state. Now, the horizontal and vertical vector components with given holographic image and amplitude information are formed. Finally,

two orthogonal vector beams are combined into one beam with a single linear polarization state using a beam combiner.

By applying this proposed method, we can independently modulate the phase and polarization information of the light field. This can fundamentally increase the whole data page writing speed because the glass sample movement is avoided. Moreover, changing of data pattern and polarization direction can be simply done by changing the CGH on LCOS SLM.

Here is the theory of this proposed based on Jones matrix. Let two computer-generated holograms, denoted by $G_V(x,y) = e^{i\varphi_V(x,y)}$ and $G_H(x,y) = e^{i\varphi_H(x,y)}$, be presented on two SLMs in the vertical and horizontal vector channel, respectively. To consider a simple case, we just analyze the zero and first order of the output light field after modulation. When the incident light in the vertical channel is modulated by LCOS SLM and its vector direction is rotated by 90° after the HWP, the Jones vector of the observed light field here can be expressed as:

$$\mathrm{E_V} = \begin{bmatrix}1\\0\end{bmatrix} \mathrm{A_1^V} \cdot \mathrm{e^{i\varphi_V(x,y)}} \tag{3.1}$$

where $\mathrm{A_1^V}$ is the first-order intensity of the diffraction light at vertical optical channel. At the same time, the horizontal channel is modulated by another LCOS SLM. The Jones vector of the observed light field here can be expressed as:

$$\mathrm{E_H} = \begin{bmatrix}0\\1\end{bmatrix} \mathrm{A_2^H} \cdot \mathrm{e^{i\varphi_H(x,y)}} \tag{3.2}$$

The information of amplitude and holographic target image have been stored in the form of phase in the beam after two independent phase modulations. To acquire two reconstructed light field with target intensity and image for further combining, two converging lenses are used to move the diffraction of light from infinite far field to the focal plane of lens.

When the two optical vector channels are provided with a same target image information, i.e., $e^{i\varphi_V(x,y)} = e^{i\varphi_H(x,y)} = e^{i\varphi(x,y)}$, two orthogonal linearly polarized light fields can be superposed into one beam with a final linear polarization state. By combining the two orthogonal polarization components, we can obtain the final light field with target image and specific polarization angle programmed by CGHs on LCOS SLM. A beam combiner is used to complete the spatial superposition of two orthogonal polarization beams. The two base vectors are combined into an optical vector as:

$$E = E_H + E_V = \begin{bmatrix}1\\0\end{bmatrix} A_1^V \cdot e^{i\varphi_V(x,y)} + \begin{bmatrix}0\\1\end{bmatrix} A_2^H \cdot e^{i\varphi_H(x,y)} \tag{3.3}$$

$$E = \begin{bmatrix}A_1^V\\A_2^H\end{bmatrix} \cdot e^{i\varphi(x,y)} \tag{3.4}$$

The first-order intensity of diffraction has a relationship and can be controlled by the phase depth of the hologram. Based on Eq3.3, the polarization angle of the final optical vector of first-order light depends on the amplitude ratio of the vertical and horizontal polarization components of first-order light. We can effectively control the amplitude distribution ($A^V{}_1$, $A^H{}_1$) of two orthogonal polarization components of light to generate an arbitrary linear polarization state. Based on Eq3.3 and Eq3.4, the simultaneous implementation of the polarization modulation and holographic image can be achieved. Therefore, the proposed method can provide the simultaneous phase and polarization modulation of light, and in the application of writing beam generation in optical data storage, this method can dynamically generate a target foci array with the wanted linear polarization state.

3.2.2 The control of polarization angle of output beam

To control the polarization angle of output vector beam, we need to first understand the parameter that determines the polarization state of light. When we split a polarization state into two orthogonal polarization components in a coordinate, there are two parameters that

can be used to precisely define a specific polarization state of light: the amplitude ratio and phase shift between two polarization components.

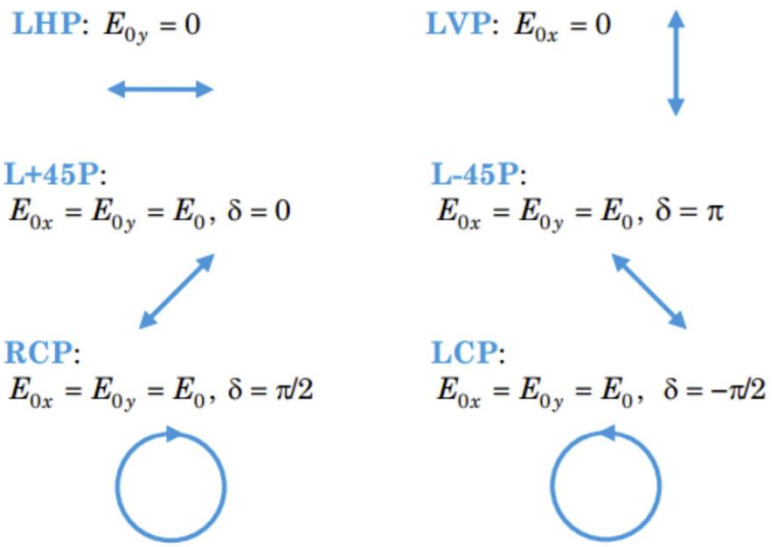

Figure 3.3 The example of different polarization state is determined by the amplitude ratio and phase shift between two polarization components.

As shown in examples in Figure 3.3, when both polarization components has the same amplitude, the phase shift can determine the final polarization state. When the phase shift is 0, the amplitude ratio can determine the angle of linear polarization. The extreme case is when one of the polarization components is 0, the final polarization state is either linear vertical or horizontal polarization. Therefore, we can effectively manipulate the output linear polarization angle by altering the amplitude ratio and maintaining the phase shift at 0 at the same time.

As shown in the Eq3.4, we acquire the Jones vector of output vector beam. To examine the polarization state of the output beam, we can rewrite the Jones vector as

$$\mathrm{E} = \begin{bmatrix} \mathrm{A}_1^{\mathrm{V}} \cdot \mathrm{e}^{\mathrm{i}\varphi(\mathrm{x},\mathrm{y})} \\ \mathrm{A}_2^{\mathrm{H}} \cdot \mathrm{e}^{\mathrm{i}\varphi(\mathrm{x},\mathrm{y})} \end{bmatrix} \tag{3.5}$$

We can see that due to the use of same holographic target image information on both horizontal and vertical polarization components, the phase distribution encoded on both polarization components are identical. The phase distribution encoded by CGH leads to the identical target image reconstruction process (diffraction of light) in far field. Therefore, in the proposed method, the phase shift between two components remains zero after the combination of two basis beams. This fact provides us with one of the conditions for linear polarization state: the phase shift between two polarization components remains at zero.

To control the angle of linear polarization state, now, we need to control the amplitude of two basis beam A^{V}_{1} and A^{H}_{1}. The holographic imaging is based on the diffraction of light in far field or at the focal plane of lens. This means that the property of two basis beams follows the characteristics of the diffraction of light. Therefore, in the proposed method, the accurate control of diffraction efficiency of computer-generated hologram is the key to the intensity control of the two basis vector beams.

The diffraction efficiency is the key parameter for the successful use of LCOS SLMs. Diffraction efficiency can be altered by different sources in the optical system. First, the pixelated structure of LCOS SLM can reduce the diffraction efficiency on each order [96]. However, due to the recent improvement of the fill factor of pixel electrode (ratio between pixel area size and pixel pitch), the diffraction efficiency reduction caused by the LCOS devices has become less [62,97]. When pixel size is further reduced, other sources of diffraction efficiency decrease in LCOS SLMs are caused by the driving of liquid crystal molecules. For example, fringing-field effect of electrical field and phase flicker that causes a phase fluctuation effect [98] [99]. Another source of diffraction efficiency altering is the complex modulation of LCOS SLM. Any deviation from a complete phase-only modulation with 2π modulation depth can result in the diffraction efficiency degradation [100]. Thus, the controllable efficiency reduction caused by a limited phase modulation depth can be used to develop a technique to encode amplitude information onto a phase grating (computer-generated hologram) on LCOS SLM.

In a computer-generated hologram on LCOS SLM, the different phase depth used in hologram generation can lead to the different diffraction efficiency on each diffraction order. The phase depth of a hologram means the maximum greylevel the hologram uses. As shown in Figure 3.4, it is a part of CGH phase profile of a target image generated under three different phase depths.

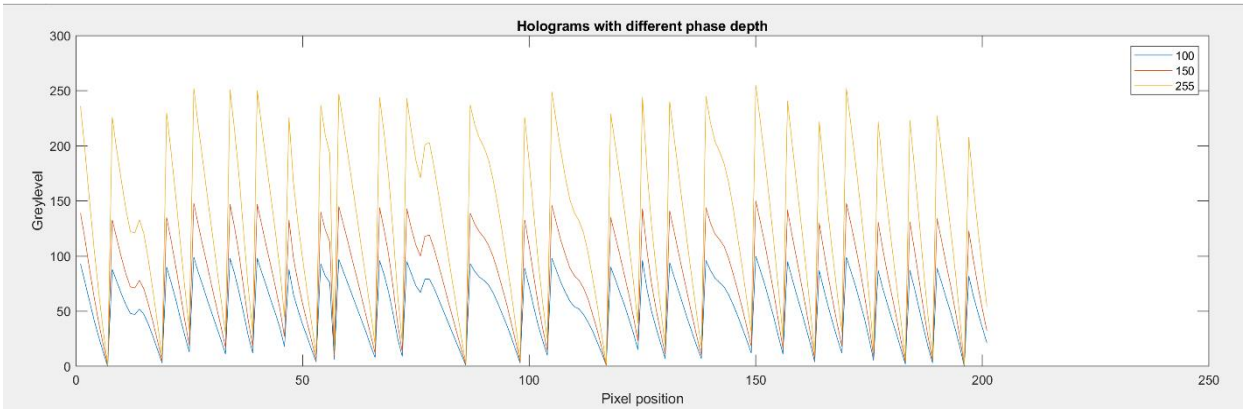

Figure 3.4 The partial phase profile of one hologram under three different phase depth.

We can see that for three holograms of the same target image, the blazed-gratings like phase profile has the same period pattern under three different phase depths. The difference of holograms is the maximum greylevel and the related phase gradient at each periodic pattern.

Because the amplitude of first-order diffraction can be controlled by using phase depth, we can apply this technique on both horizontal and vertical optical channels to independently control their intensity. Now, the polarization angle of final output beam can be actively controlled by combining two intensity-modulated basis beams.

To make the proposed feasible in practice, we first need to find out the relationship between first-order intensity and its corresponding phase depth of a computer-generated hologram. We can start from simulating the diffraction behaviour of a blazed grating. Figure 3.5 shows an example CGH of a target image. As can be seen in the figure, the phase profile of the CGH can be seen as a combination of many blazed gratings across the whole hologram plane.

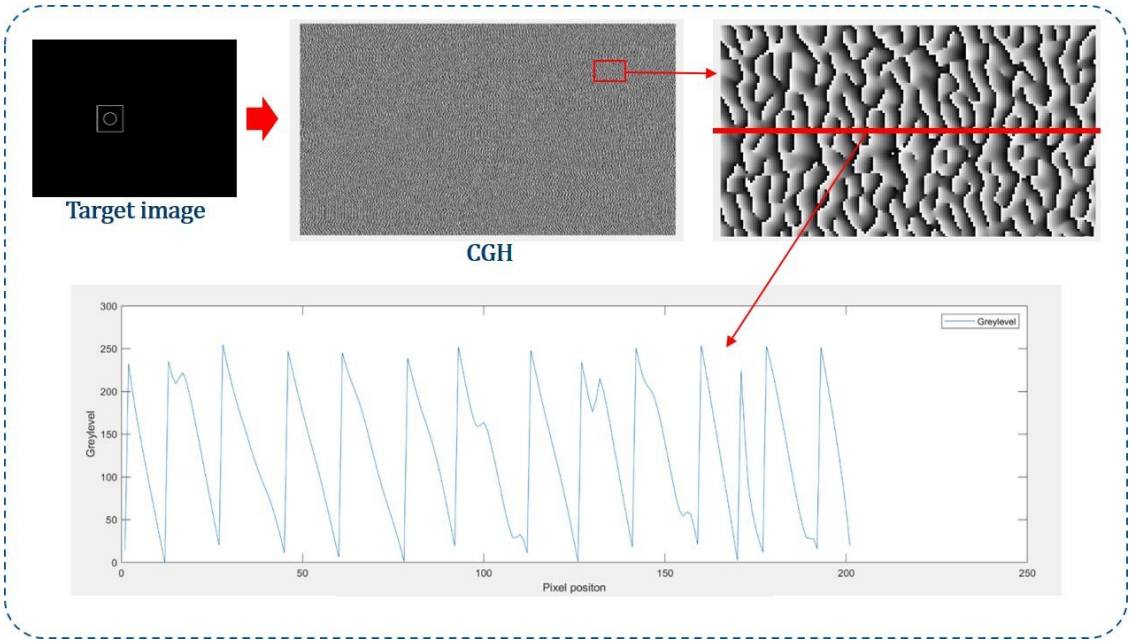

Figure 3.5 The partial phase profile of hologram with three different greylevel displayed on the active area of a LCOS SLM.

To study the diffraction efficiency of the blazed gratings, the phase profile of a blazed grating needs to be determined. Due to finite pixel resolution of the LCOS SLM, a blazed grating on LCOS devices is a stepped grating as shown in Figure 3.6. As can be seen in the phase profile, M ($0<M<1$) indicates the maximum of the phase value of a grating, and the maximum phase depth is 2π according to the default configuration of most phase-only LCOS SLMs.

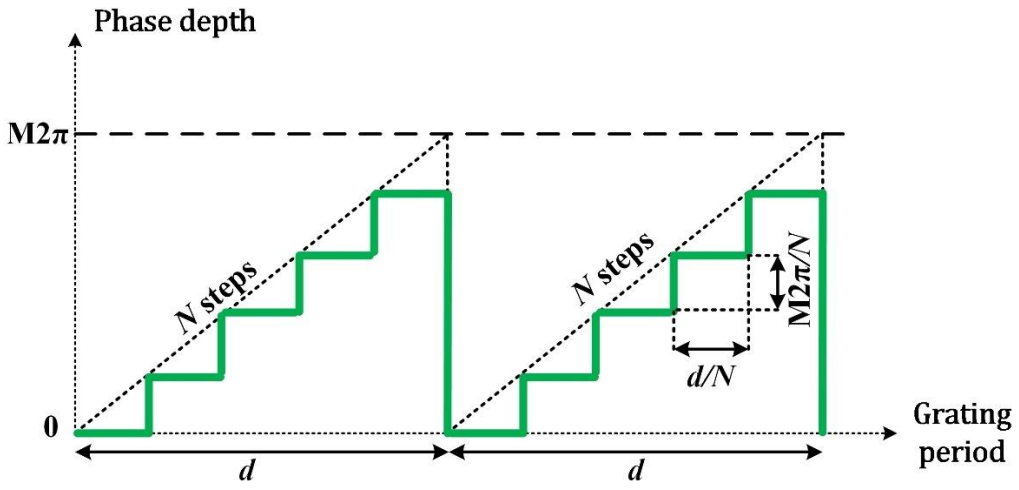

Figure 3.6 Phase profile of a blazed phase stepped grating on LCOS SLM with period d, maximum phase depth M2π and N steps

The intensity of each diffraction order can be calculated from the Fourier series coefficients of the phase grating. It is a straightforward calculation to derive the Fourier coefficients of the stepped phase grating [101].

$$C_\mu = e^{i\frac{\pi\mu}{N}} \frac{e^{-i\pi(M-\mu)}}{e^{-i\frac{\pi}{N}(M-\mu)}} \cdot \frac{sin(\frac{\pi\mu}{N})}{\pi\mu} \cdot \frac{sin\ (\pi(\mathrm{M}-\mu))}{sin\ (\frac{\pi}{N}(M-\mu))} \tag{3.6}$$

where μ is the diffraction order number.

Therefore, by analysing the Fourier coefficients of the grating, the relative efficiency of each diffraction order can be expressed as:

$$\alpha_{\mu(M,N)} = \left|C_\mu\right|^2 = \left[\frac{sin(\frac{\pi\mu}{N})}{\pi\mu}\right]^2 \cdot \left[\frac{sin\ (\pi(\mathrm{M}-\mu))}{sin\ (\frac{\pi}{N}(M-\mu))}\right]^2 \tag{3.7}$$

When we consider a case for a continuous phase grating where the step number is infinite, the resulting diffraction efficiency can be expressed as

$$\alpha_{\mu(M,N\to\infty)} = \left|C_\mu\right|^2 = \left[\frac{sin\ (\pi(\mathrm{M}-\mu))}{\pi(M-\mu)}\right]^2 = sinc^2(M-\mu) \tag{3.8}$$

Where $sinc(x) = \sin(\pi x)/(\pi x)$. When $M = 0$, the energy in first order diffraction is zero. When the phase depth changes in the range $0 < M < 1$, the energy splits on the first order varies. When $M = 1$, the energy is entirely in the first order. This is the fundamental situation that was utilized to encode amplitude information in phase modulation using computer-generated hologram. As shown in the Figure 3.7, the amplitude of first order diffraction of the blazed phase gratings has a direct positive correlation with the maximum greylevel used on the hologram.

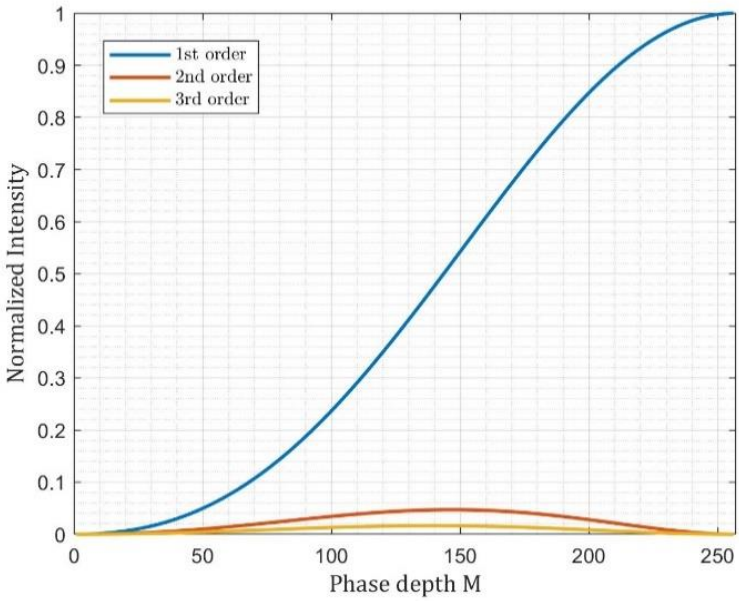

Figure 3.7 The simulation of intensity of different diffraction orders ($\mu = 1,2,3$) versus the phase depth M of a continuous phase grating ($N \to \infty$).

We can observe that the intensity of the first order increases when the phase depth is increased from 0 to 2π. When M=1, the corresponding greylevel of the SLM is 255 and the corresponding greylevel of the SLM is 0 when M=0. Therefore, the two SLMs can utilize this

property to independently control the intensity of two components when they are both modulated. Since the amplitude ratio of two beam vector basis is controlled, we can generate arbitrary linear polarization state of the final optical vector beam.

3.2.3 Look-up table of first-order diffraction intensity modulation

To acquire the target polarization angle of output beam, we need to precisely control the amplitude ratio of two polarization components. This means that we must precisely control the amplitude of both polarization components using the phase-only modulation. The amplitude information is encoded in the phase-only CGH by applying different phase depth on hologram, and then, the amplitude information is expressed into the light intensity of holographic image after the diffraction.

Firstly, we load a blazed diffraction grating hologram on LCOS SLM to experimentally analyse relationship between the intensity of the first-order diffraction light and the phase depth. Thus, the amplitude modulation capability of the first-order diffraction light based on phase depth can be found. Figure 3.8 shows the experimental setup. In experiments, the blazed gratings with same period but different phase depths are used to collect their first-order intensity across the available phase depth range of 2π. The simulated results used for reference is a blazed grating (step number N=32) generated by using Matlab. A single-pixel photo-detector (PDA100) is used to record the first-order diffraction intensity.

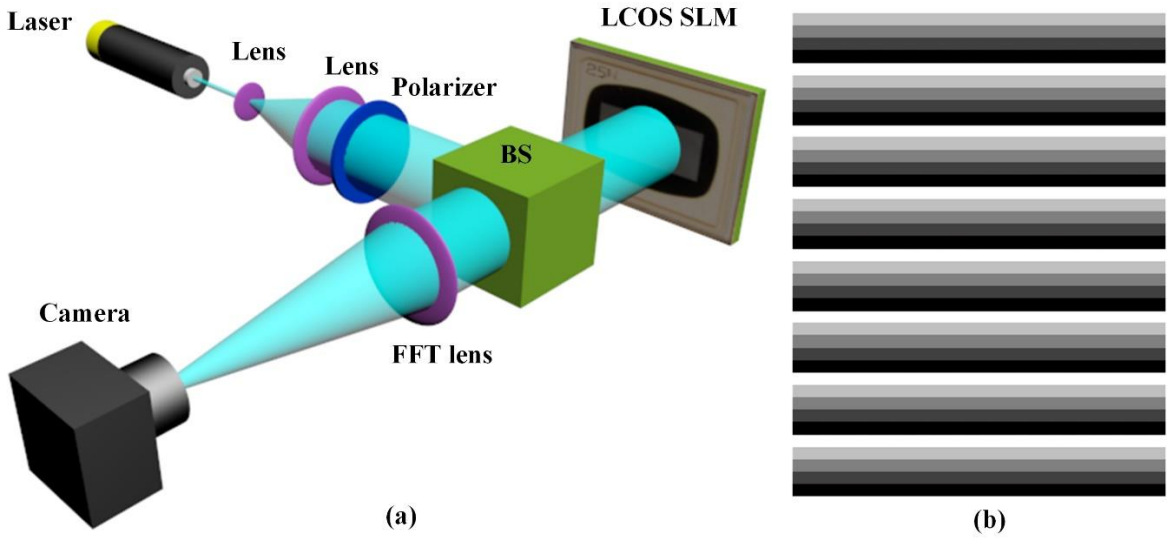

Figure 3.8 The scheme of optical setup for finding the first-order diffraction intensity look-up table (a). A blazed grating displayed on LCOS SLM (b).

As shown in Figure 3.9. the relationship between the first-order intensity and phase depth used in the grating is found. The maximum grey level controls the depth value and the maximum grey level of 255 corresponds to the phase modulation depth of 2π (M=1). The difference between experimental result and theoretical result is mainly caused by the imperfection of LCOS devices. The theoretical first-order intensity is calculated under perfect phase modulation, however, in practical experiments, the non-flatness liquid crystal layer across the cell and the gap between each pixel electrode can cause the loss the diffraction efficiency. We can observe the change of the depth can directly control the amplitude value of the first order. This further means that we can freely and dynamically control the linear polarization angle using holograms with different phase depth. For example, the desire optical vector beam is a holographic dot array with a linear polarization angle at 30° (0° is vertical axis). To achieve this target polarization state, we can set the grey level at 210 in the SLM1 (horizontal amplitude) and maximum grey level 255 in SLM2 (vertical amplitude) to provide accurate amplitude ratio of two basis beams.

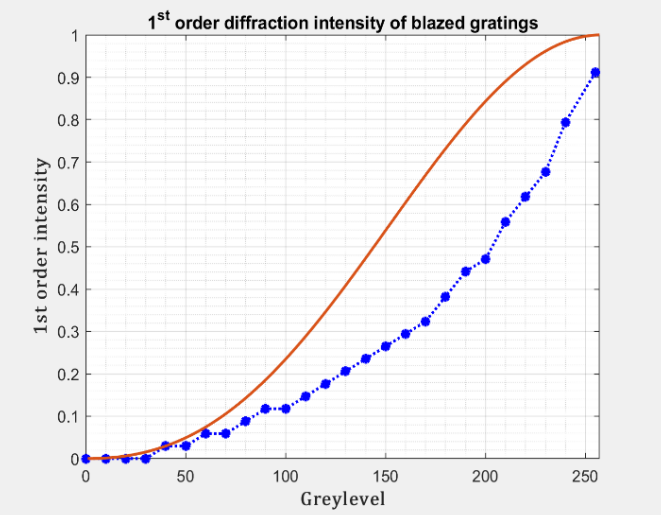

Figure 3.9 the intensity of the first diffraction order at the different grey levels, the grey level controls the phase depth used in modulation. The red line is the theoretical result and the blue line is the experimental result.

Secondly, we load a CGH of a target image on LCOS SLM to experimentally analyse the phase-depth-dependent first-order diffraction intensity of a target image that is used in experiments. In the practical experiments, holograms of arbitrary target images is used instead of a blazed grating. By doing this, a look-up for the phase depth and their corresponding first-order diffraction intensity of the LCOS SLM used in the research can be found. Since the performance of LCOS SLM in practical can be affected by many factors (liquid crystal cell uniformity, liquid crystal alignment, pixel pitch size etc.), a precise look-up of the first-order light intensity and the greylevel used on a LCOS SLM device is critical for the accurate polarization control of output beam.

3.3 Experiments

3.3.1 Experimental setup

To verify the feasibility of the proposed method, I experimentally demonstrate the capability of generating a vector beam with the encoded holographic information. Figure 3.10 shows the

experimental setup of the proof-of-concept system. First, a coherent laser beam is collimated and expanded by two lenses (Lens1 and Lens2). Then, a linear polarizer (LP) changes the expanded beam into a horizontal linearly polarized beam. Next, a beam splitter (BS) is used to split the horizontal polarization beam into two sub-beams, forming the input of the two base vectors. The two horizontally polarized beams are then encoded with the holographic information that is presented on the two LCOS SLMs. The holograms here are calculated based on the target image pattern. After that, a half wave-plate (HWP) is applied to rotate one of modulated horizontal polarization beam into a vertically polarized beam. Finally, a beam combiner is employed to superpose the two base vectors into a designed linear vector beam. The holographic pattern is imaged via relay optics and captured by a CMOS sensor.

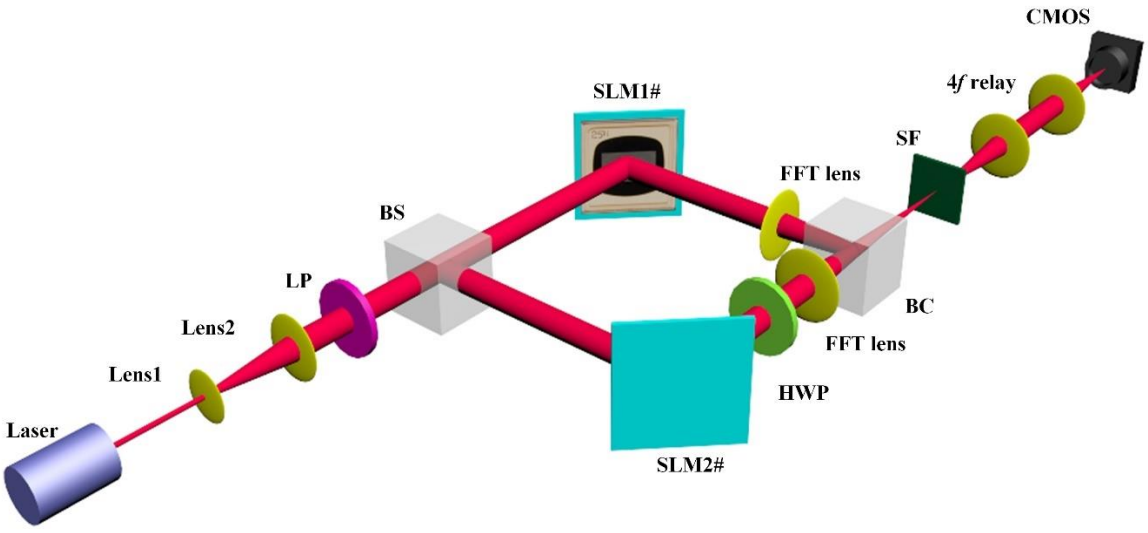

Figure 3.10 the schematic of the experimental setup, where LP is a linear polarizer, HWP is a half wave-plate, BS is a beam splitter, BC is a beam combiner, SF is a spatial filter.

The laser used in the experiment is a 0.3mW diode module with a wavelength of 633nm. The two LCOS SLM devices have a resolution of 1920×1080 with a pixel pitch of 5.3μm and a grey level scale of 0-255. A linear polarizer (LPVISC050) with a diameter of 12.5mm is used to create the input light with a linear polarization angle at 0° for the system. A polymer zero-order half-wave plate (WPH05ME) with a diameter of 0.5 inches is used to rotate the polarization angles of two separate light components. Two beam splitters (BS004) are used,

which are the non-polarizing beamsplitter cube with an energy split ratio of 50:50. A beam splitter is used to splitting the input linearly polarized beam into two with the same intensity. Another non-polarizing beam splitter is used to combine two orthogonally polarization beams into one beam with a final linear polarization state. The beam combiner may be replaced by other polarizing optical components, such as a Wollaston prism and Calcite beam displacer, to realize the recombining of two light beams. The lens (LB1374) is an N-BK7 Bi-convex lens with a diameter of 50mm and a focal length of 150mm. The CMOS sensor has a pixel size of 5.3 μm and a resolution of 4928×3624.

3.3.2 The superposition process of two separate vector beams

The final stage of phase and polarization modulation method is to combine two modulated holographic vector beams into a single vector beam. Since the horizontal and vertical components of the output holographic vector beam directly comes from two basis vector beams, the accuracy of beam combination will determine the quality of output light field.

The combination of two light beams with vertical and horizontal polarization has been studied due to the huge demands in optical fibre applications. Therefore, commercial fibre-based polarization beam combiner has been well developed. In this device, two beams are coupled into optical fibre and then combined inside a polarizing beam displacer (e.g., calcite prism). However, this method of combining light is not suitable for the generation of data writing light field. There is a major reason: coupling the holographic light field into a fibre. When we couple a light beam into a fibre, normally an objective lens is used to focus light into the area of fibre core. The focusing of light beam is a simple step. However, this step cannot be applied on holographic vector beam. Due to the principle of the Fourier hologram, the image of diffraction locates in infinite distance away from the hologram. Thus, in holographic imaging process, a converging lens is used to reconstruct the image at its focal plane. This means that when we try to couple two basis holographic beams into fibres, the

lens used for coupling can also image the whole holographic pattern. Therefore, the fibre-based polarization combiner cannot be utilized in the proposed phase and polarization method.

Considering the properties of holographic light field, a method that allows the combination of light beams with holographic pattern information is proposed. This method is based on the superposition of two coherent laser beams. As shown in Figure 3.11, in this method, two polarized collimated beams are aligned and then spatially superposed into a single beam with combined polarization state and amplitude by using a beamsplitter. The superposition of two beams in free space does not require any focusing, therefore, the holographic information in light field can be preserved in the combining process.

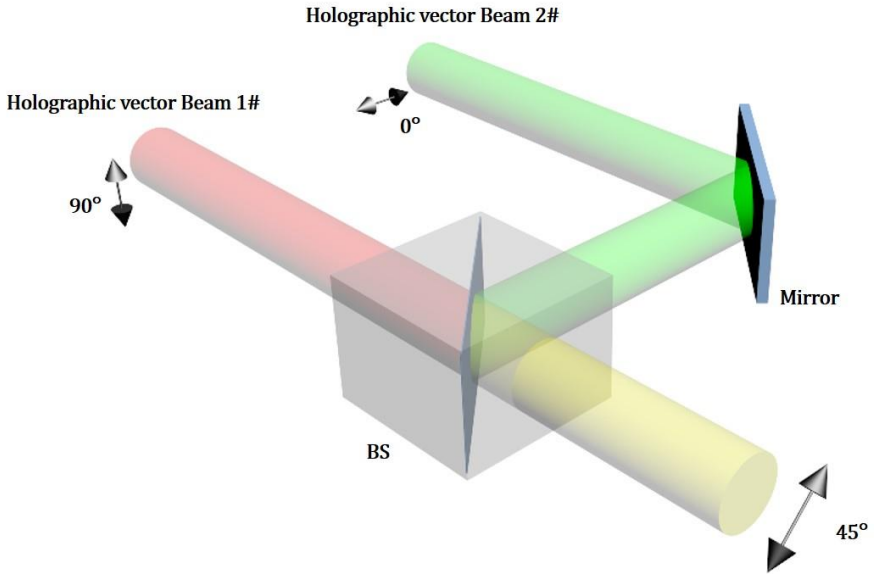

Figure 3.11 The schematic of method using spatial superposition of two holographic beams with orthogonal polarization state. The combined beams will have 45° polarization angle when the amplitude ratio of two input beams is 1:1.

When this method is applied in practical optical setup, the alignment of two input vector beams is critical for the combining process. First, to ensure the two beams are parallel, the input direction of two beams need to be normal to the surface of cubic beamsplitter. This is achieved by adjusting the angles of LCOS SLMs surface, mirror and beamsplitter. Then, the

two parallel input beams will be spatially overlapped at the interface inside beamsplitter by adjusting the position of mirror in Figure 3.12.

To check the quality of beam combining, an analyzer at 45° is placed in front of the CMOS to examine the polarization state of output beam. When two beams with same amplitude and a phase shift at 2nπ or nπ, the polarization angle of superposition beam will be 45° or - 45°. Therefore, a dark or bright beam pattern after analyzer directly can indicate the final polarization state. Here, the experimental results of two main steps of beam combining process will be shown and discussed.

First, In the parallelization and combining of two beams, the two orthogonal vector beams show the similar behaviour of light interference. When two beams have alignment error, as can been in Figure 3.12, there is a distance between two beams on the interface of beamsplitter. This means that the phase difference of two beam at different position on image plane will not remain 0 or 2π due to the difference of their optical path length. This is like when two coherent laser beams generated from two slits and forms phase difference pattern on the image plane, the location constructive (light) and destructive (dark) interference pattern corresponds to the phase difference distribution.

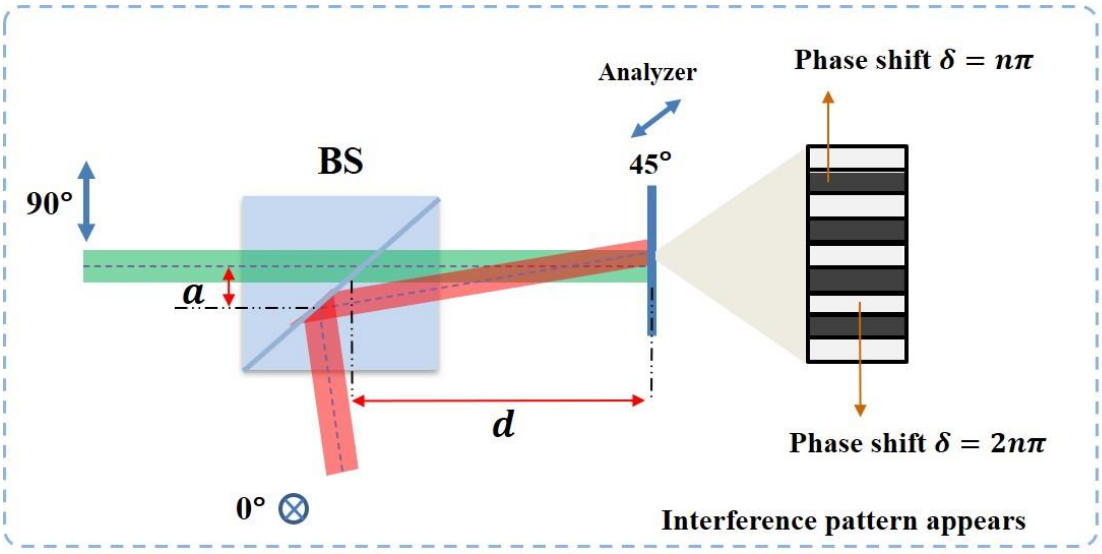

Figure 3.12 When two basis vector beams have the alignment error, two orthogonal vector beams can have a small angle at the image reconstruction plane. Due to the high coherence of two beams, they can spatially interfere. Therefore, the interference fringes can be observed under analyzer.

According to the interference of two light beams with same polarization, the phase difference of two beams at the centre of dark and light stripes are $2n\pi$ or $n\pi$. Maintaining same spatial phase difference distribution of interference of light, when two beams have orthogonal polarization, the polarization state at same place will became 45° or - 45°. Therefore, as shown in Figure 3.13, when two input beams are not spatially parallel, the dark and light pattern can be observed by using an analyzer at 45°.

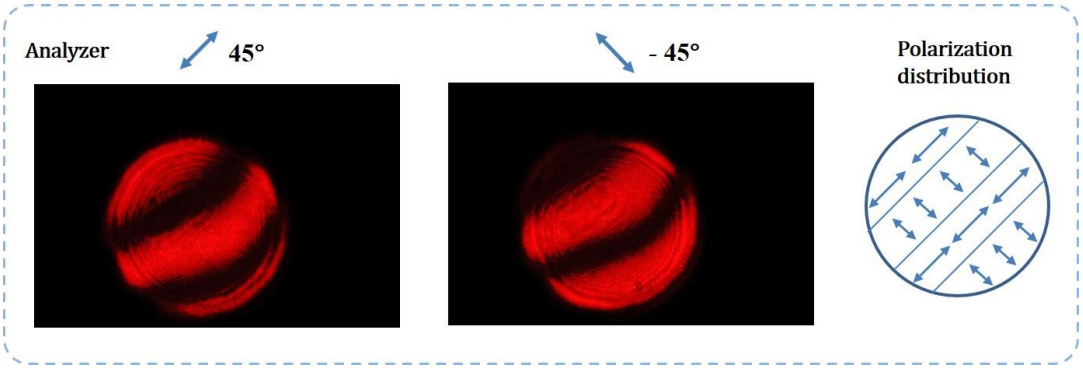

Figure 3.13 Interference patterns of two orthogonal vector beams with same shape are observed when analyser is placed at 45°.

A further experiment shows that the interference pattern only appears at superposition area of two vector beams with different beam shapes. The experimental results are shown in the Figure 3.14. This experiment proofs that the superposition of two vector beams can be find in the overlapping area of two spatially aligned orthogonal vectoral beams.

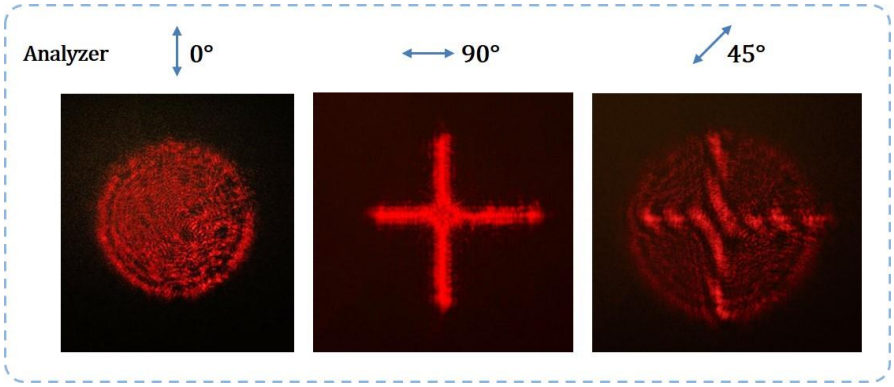

Figure 3.14 The superposition of two orthogonal vector beams with different shapes (circle and cross) is observed under different polarization analyser angle (blue double-end arrow). Interference patterns are observed when analyser is placed at 45°.

Moreover, Figure 3.15 shows that with the increase of the two beam's parallelization, the width of dark and bright stripes increased and the number of stripes in the overlap of two beams became less. The width W of stripes can be defined as:

$$W = \frac{d\lambda}{a} \tag{3.9}$$

where λ is the wavelength of light, a indicates the length of gap between two beams on the interface inside beamsplitter and d is the distance between image plane and the superposition point of two beams. When the distance a is close to zero, the width of stripes will increase to infinite. This means that the polarization state in the overlapped area will become uniform.

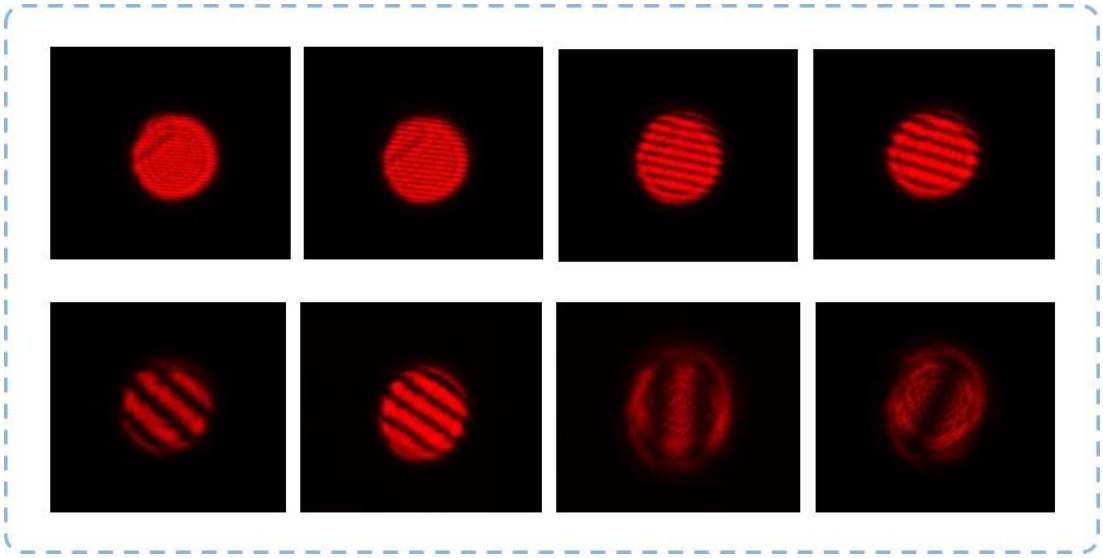

Figure 3.15 The experimental results of unparallel two vector beams with same shape combining in frees space. The width of stripes pattern varies with the degree of parallelization of two beams.

When beam alignment is well performed but two beams are not completely overlapped, the overlapping area of two vector beams will have a uniform polarization state. This means that no interference pattern can be observed or after analyzer. Thus, we can use the disappearing of interference patterns as a sign of complete alignment. Figure 3.16 shows the beams superposition results after high accuracy alignment. In the experiment, two basis vector beams are aligned into parallel for 15 meters to ensure high beam combining quality. The images are taken under analyzer that is placed at 45° and -45°. We can see that the overlapped area of two beams does not have any interference patterns. This means that the light field in the overlapped area has a single linear polarization state.

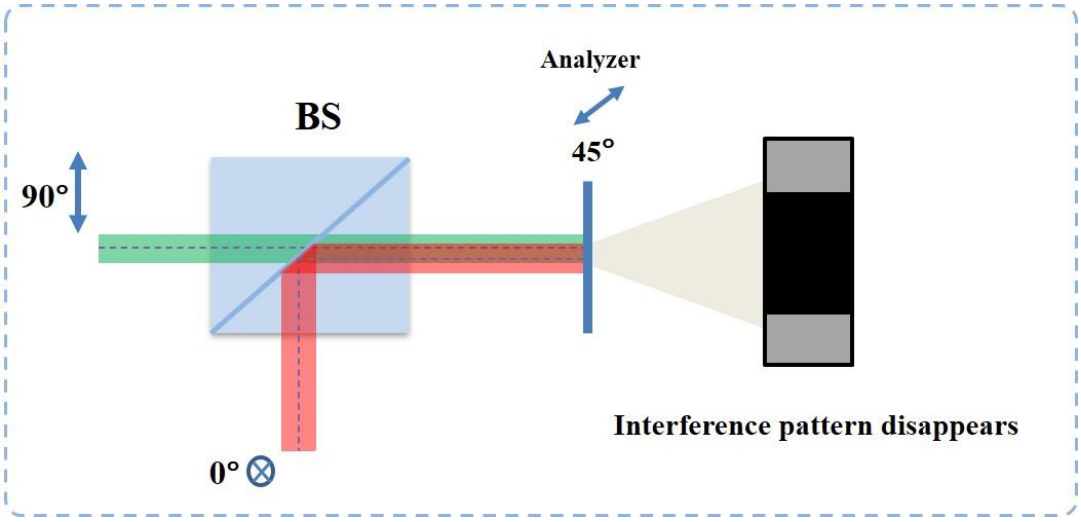

Figure 3.16 The two orthogonal vector beams are completely parallel after high accuracy aligning process and the interference pattern disappears due to the combination of two beams.

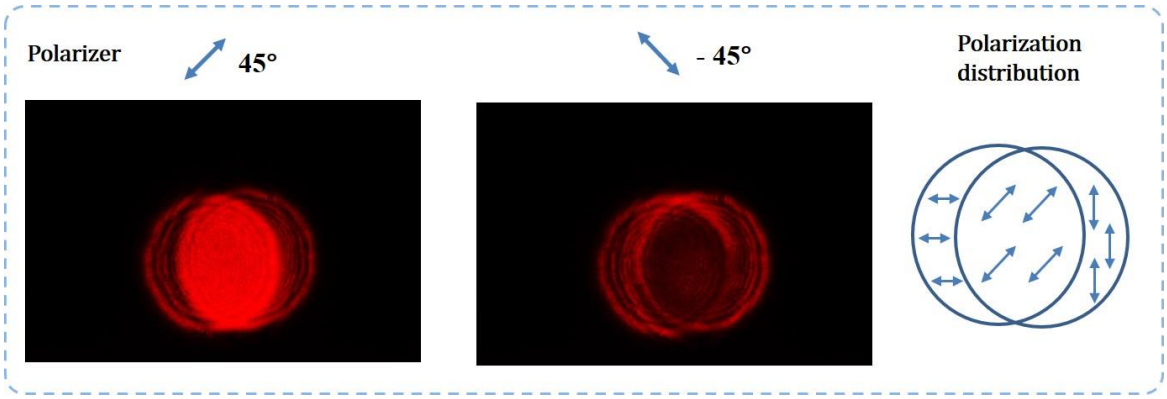

Figure 3.17 The two orthogonal vector beams are very highly aligned. The superposition area of two beams has a single polarization state.

As shown in Figure 3.17, when two orthogonal vector beams are successfully combined into one single vector beam, the amplitude and polarization angle of the output beam will be determined by two factors respectively: the absolute amplitude of two input beams and their amplitude ratio.

In the experiment, two input vector beams have the same amplitude, and the overlapped area after beam combining have polarization angle at 45°. As shown in Figure 3.18, when the analyzer is set at 45°, the intensity of superposition area is about $2\sqrt{2}$ times compared with the intensity of input beams (not overlapped part). This result is a further proof that the superposition of two vector beams in overlapped area is achieved. Then, by completely overlapping the two vector beams, the final superposition process of two vector can be finished.

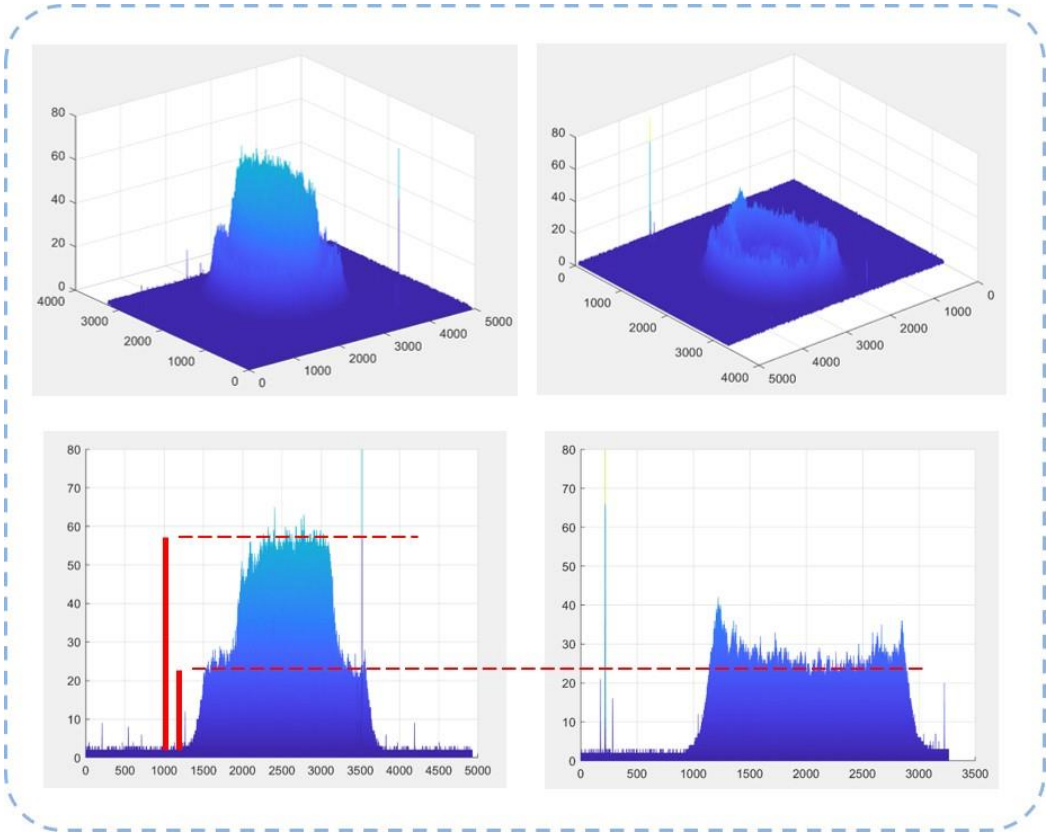

Figure 3.18 The 3D plots of the intensity of images in Figure 3.17 showed that the comparison of the overlapped area and area of input beams under analyzer at 45°.

In summary, this experimental result indicated that two vector beams can be directly combined into one single beam in free space using a beam combiner. And a precise alignment calibration in the order of wavelength is necessary. This means that two vector beams with

independent amplitude information and the same holographic information can be combined into one single light field. Therefore, the polarization angle of output light field can be actively modulated without loss of holographic information. This ensures the feasibility of phase and polarization method required for data writing light field generation.

3.3.3 Experimental results of holographic vectorial image

In this section, the effectiveness of the phase and polarization modulation method is experimentally verified. To generate data writing field, we need a data pattern image with a certain polarization state as the output light field. Therefore, the holographic information on both LCOS SLM needs to be identical, and the pre-calculated amplitude information needs to be applied to CGH. The two different amplitude information is encoded by using two phase depth values on LCOS SLMs according to the look-up table created in 3.1.3. Figure 3.19 shows the results at the different polarization states. When specific phase depths on both two LCOS SLMs are determined, the target polarization state of output holographic light field is formed.

First, a pair of phase depth combination on the two LCOS SLMs is applied to generate a target image with target polarization angle at 30°. The target image we used in experiment is a double hexagon pattern. As can be seen from Figure 3.19, the brightest image and the light cancellation are observed when the analyzer's polarization angle is at 30° and -60°, respectively. We also found that the average image intensity when analyzer is at 30° has a clear trigonometric relation with the average image intensity recorded when analyzer is at 0° and 90°. This means the final linear polarization state is the superposition of two basis vector components. Therefore, we show the successful control of the target image and the target polarization state using the proposed method.

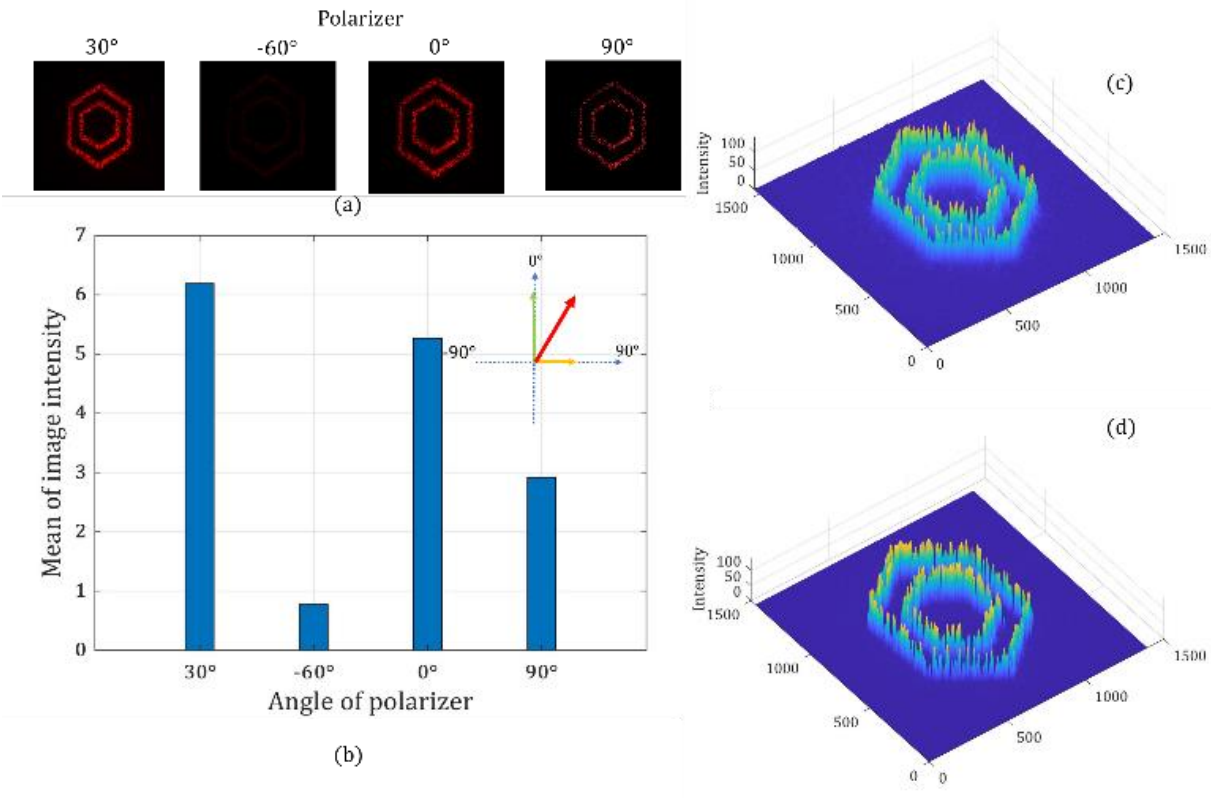

Figure 3.19 The Holographic patterns with a linear polarization state of 30°: recorded holographic images when the analyser is set at the different angles (a); The average intensity of four holographic images (b). the three-dimensional intensity distribution at 30° (c); the three-dimensional intensity distribution at 0° (d).

Moreover, we can use another pair of phase depth combination on the two LCOS SLMs to generate the image with linear polarization angle at 45°. Similarly, we can see that the brightest image is observed when the analyser's polarization angle is at target polarization angle 45°, while the light cancellation is recorded at -45°. Figure 3.20 shows different intensity of target images when the analyser is placed at different angles. We still can find that the average image intensity when analyser is at 45° has a clear trigonometric relation with the average image intensity recorded when analyser is at 0° and 90°.

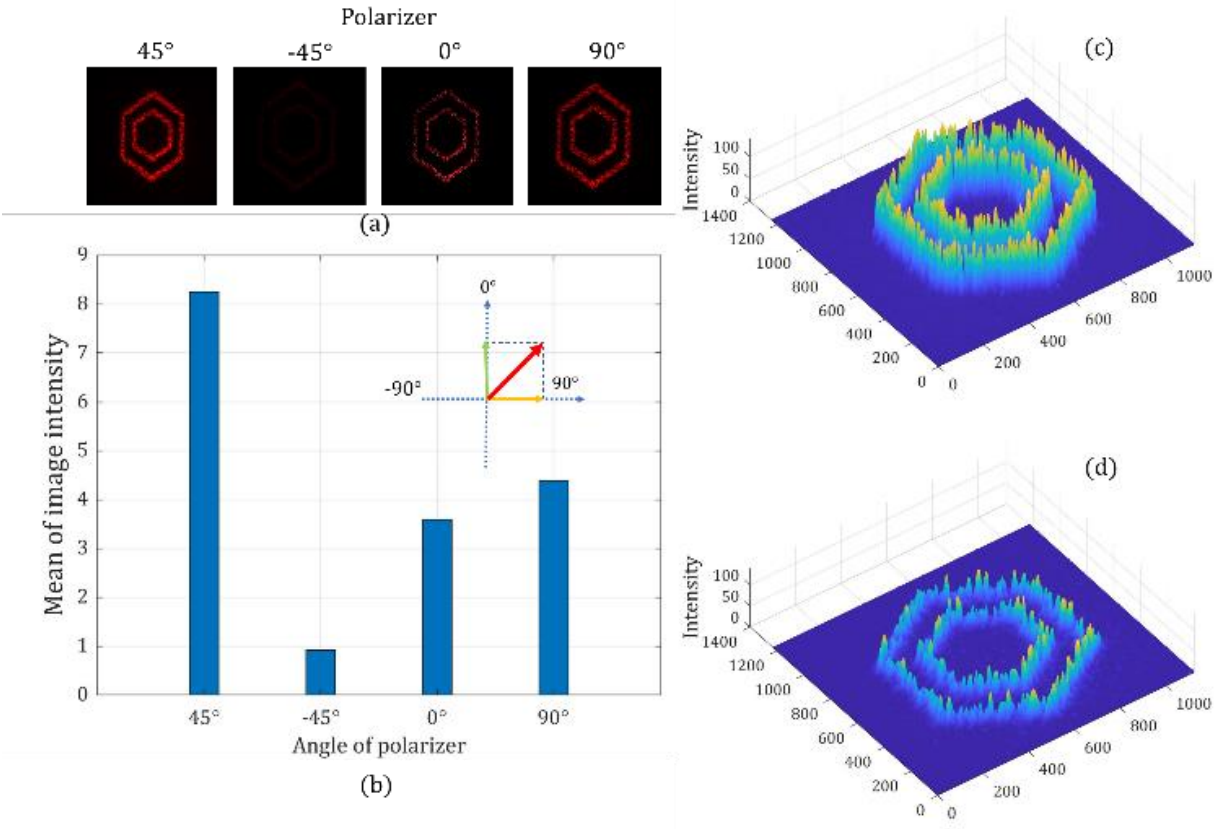

Figure 3.20 Holographic images with a linear polarization state of 45°: holographic image when the analyzer is set at the different angles (a); the average intensity of four holographic images (b); the three-dimensional intensity distribution at 45° (c); the three-dimensional intensity distribution at 0° (d).

At last, we generate the same pattern with its linear polarization angle at 60° to further prove the our effectiveness of our method. The brightest image and the darkest image are observed at designed polarization angle and its crossed angle in Figure 3.21. We still can find that the average image intensity when analyzer is at 60° has a clear trigonometric relation with the average image intensity recorded when analyzer is at 0° and 90°. From Figures.3.19-3.21, these results have confirmed that each holographic pattern has an expected polarization state.

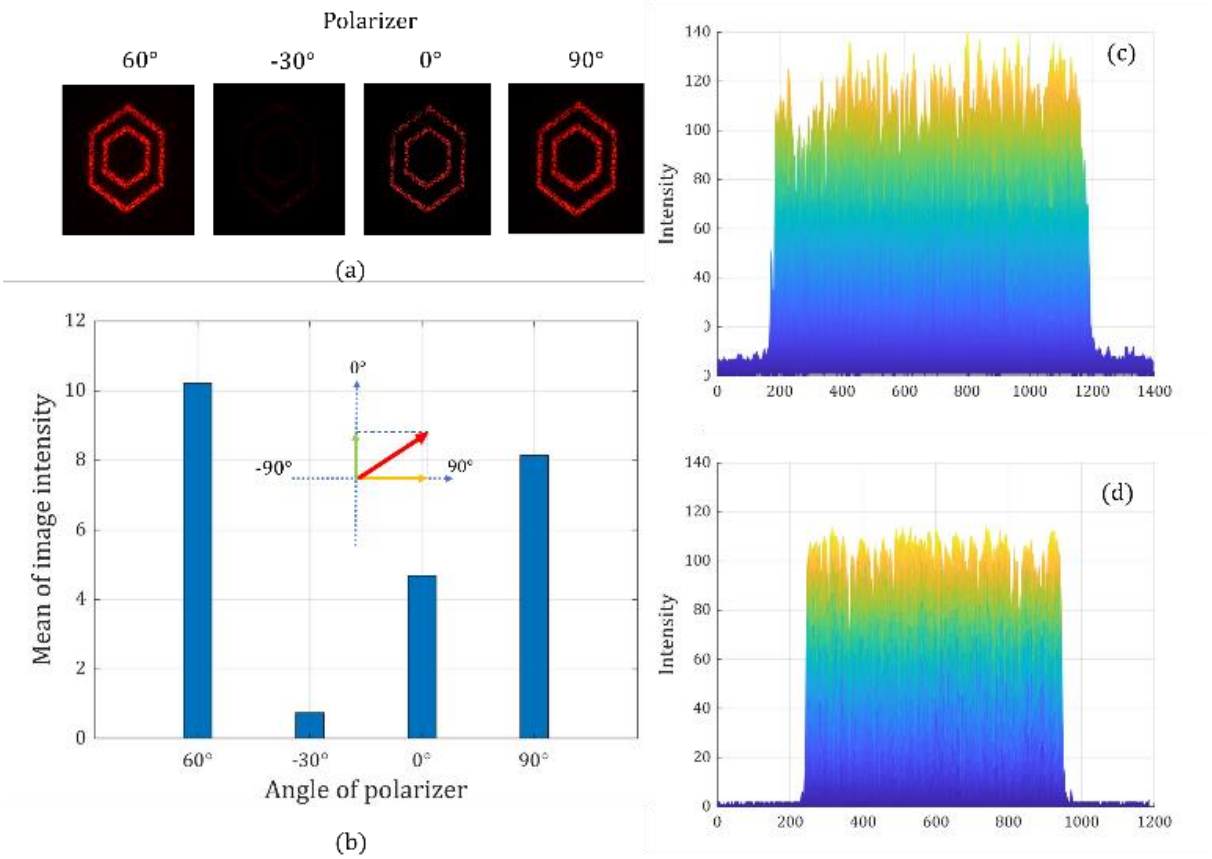

Figure 3.21 Holographic images with a linear polarization state of 60°: holographic image when the analyzer is set at the different angles (a);); the average intensity of four holographic images (b); the three-dimensional intensity distribution at 60° (c); the three-dimensional intensity distribution at 90° (d).

These results show that the proposed phase and polarization method can simultaneously achieve phase modulation (holographic image pattern) and polarization modulation (the angle of polarization state). Moreover, in this method, both phase and polarization modulation are dynamically controlled by CGH on LCOS SLM devices. No external complex or active optical elements is required. This advantage can play an important role in the application of data writing beam generation.

3.4 Discussion

After verifying the effectiveness of the proposed method of phase and polarization modulation, here is the comparison and discussion of the proposed method and existing method for the application of optical data storage in glass.

Firstly, I will summarize the demand of the generation of writing beams for optical data storage in glass. As introduced in the chapter 1, the polarization angle of voxel is one of parameter used data bits encoding. Thus, a data page in the glass block consists of voxels with different polarization angles, and the voxels with a same polarization angle can have an arbitrary location distribution according to the data encoding. Therefore, the writing beam of voxels needs to able to produce random multi-beam pattern, at the same time, the multi-beams light field needs to have the target linear polarization state. As shown in Figure 3.22, when one data page has four different polarization states of voxels (0°,45°,90°,135°), four exposures of four different writing beams (different target image and target polarization state) is needed to finish the data page.

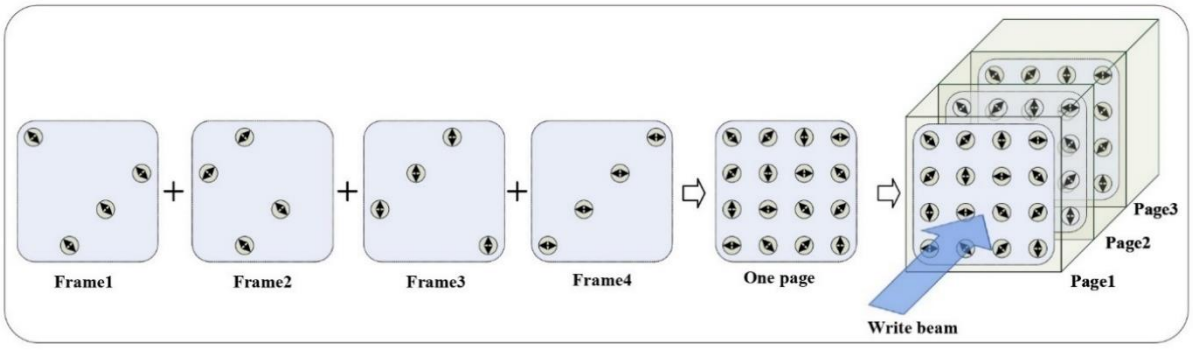

Figure 3.22 The schematic of the writing process of a data page in optical data storage in glass.

Now, we can see that the phase modulation and the polarization modulation of light are required at the same time for the generation of data writing beam. Table 3.1 is the comparison

of the proposed method and the current method in the aspects of modulation scheme and application performance.

Table 3.1 **The comparison of two methods: existing method and the proposed method**

Methods	Phase modulation	Polarization modulation	Multi-polarization states writing	Delay	Extensibility
LCOS+HWP	CGH	HWP	Glass sample movement	Limited by mechanical stage movements	Fabricate new HWP matrix
Two beams combination	CGH	Two vector beams combination	Glass motion free	SLM refresh rate (60~100Hz)	Dynamically load new CGH

1. Phase modulation

As for the current methods [30-40], the target multi-beam pattern for voxel writing is generated by the holographic imaging using phase-only LCOS SLMs. In the proposed method, the target image of data pattern is also provided by computer-generated hologram using LCOS devices. Both methods utilize phase-only modulation to encode the target image information.

2. Polarization modulation

To modulate the polarization state of light, the half-wave plate is used to rotate the original linear polarization state into the target state in the existing methods. For linearly polarized light, the effect of the half-wave plate (HWP) is to rotate the polarization vector through an angle that is two times the angle between the incident polarization vector and half-wave plate's optic axis (usually fast axis). Thus, to acquire one target polarization angle, the optic axis of HWP needs to be at a specific angle.

Another improved method using HWP is to fabricate a HWP matrix. This method is the one chosen to compare with the proposed method. The HWP matrix is a combination of four

HWP with different optic axis that can provide target polarization angle 0°,45°,90° and 135°. In this method, the rotation of a single HWP is replaced by moving the glass sample underneath the HWP matrix film. However, the principle of polarization modulation is still based on the use of HWP.

In the proposed method, in the phase-only modulation by computer-generated hologram, not only has the target data image information been encoded onto the input beam, and the amplitude information also has been encoded. Two input beams with orthogonal polarization states are parallelly modulated by two LCOS SLMs. After the reconstruction of two independent holographic images with pre-determined intensity, the two light fields are spatially combined into one final output. The control of the angle of linear polarization is achieved by the direct combing of two basis beams with pre-determined amplitude ratio.

3. Multiple polarization states writing

In the writing process of a data page in glass, more than one target polarization angle is required, and one of current method utilizes a rotatable HWP. The rotatable HWP provides the target polarization state by rotating to the correct position. It needs to synchronize a motor-driven HWP rotator to the LCOS SLM and the femtosecond laser. Thus, the complexity of the writing beam generating system is largely increased. Moreover, the mechanical delay of the HWP rotator will accumulate in each time of polarization change resulting in large reduction of the data writing speed.

The improved method using HWP matrix can avoid HWP rotation. However, it still requires the synchronization of the CGH refresh on LCOS SLMs and the glass substrate movement. When the current polarization of writing beam needs to be changed into a new one, the glass substrate will be moved to the correct position under the HWP matrix so that the polarization state of writing beams can be altered into the target one.

In the proposed method, because it uses the spatial combining of two basis beams to form any target polarization state, there will be no need for any external polarization modulator (HWP matrix system). This means that the complexity and difficulty in synchronization are largely reduced. The proposed method also does not require any glass substrate movement in the writing of each data page at certain depth. The switching of different writing beam's polarization state is achieved by loading new CGHs on LCOS SLMs.

4. Delay

The current method using HWP rotator has large delays because the rotation takes a relative long time. To provide any possible polarization angle from a fixed incident polarization state, the required maximum rotation range between a switching can be 87.5° (resolution of voxel polarization forming is 5° [22]).

The current method using HWP matrix has less delay compared with rotator. However, it still requires many times of glass sample movement for the writing of one data page. Due to the use of motor-driven platform, the mechanical delay caused by acceleration and deceleration processes take up a major part in the current writing process time duration.

The proposed method can provide motion-free writing of each data page. Because the only active optical elements used in this method for polarization control are phase-only LCOS SLMs, the switching time between two polarization states in writing is only determined by the refresh rate of CGHs on LCOS devices (60Hz ~ 100Hz for nematic LCOS devices).

5. Extensibility in available polarization state

The current method using HWP matrix can only have a limited number of available polarization states for data writing. This is because the number of HWPs with different fast axis on one HWP matrix is fixed after fabrication. When more polarization states are required

in data writing, the only solution is to fabricate new HWP matrix with more sub sections. Apart from the workload and difficulty in fabrication, the new HWP matrix will have larger area due to the increase of HWPs. Larger area means longer range of glass substrate movement in data writing, causing the further increase of delay.

The proposed method can simultaneously control the holographic target image and its polarization state by two parallel phase-only modulations. After the alignment in the two-beam combining process is finished, the optical setup will become a static component in the whole system. Any change in the writing beams can be dynamically accomplished by altering the CGHs on LCOS SLMs.

3.5 Conclusion

A phase and polarization modulation method based on LCOS SLMs capable of the simultaneous implementation of dynamically generating holographic patterns and arbitrary linear polarization states is proposed, the effectiveness of the method is experimental verified. In the proposed method, we can independently use phase-only modulation to encode the holographic target image information and amplitude information onto two input beams. After obtaining the two modulated light beams with target pattern and target amplitude ratio, the spatial superposition of two beams can provide one output light field with the target polarization state. Therefore, the polarization control in the proposed is achieved by the manipulation the amplitude ratio between vertically and horizontally polarized beams and combination of these two basis beams.

The superposition of two beams in the proposed method requires a precise alignment process to ensure high accuracy and quality output image and polarization. The spatial overlap of two beams needs to be in the order of wavelength.

Although there are methods that can generate similar number of polarization states, they require an external polarization modulator after data pattern generation. To alter the holographic target image and the target polarization state of data writing beams, we only need to load new CGHs on LCOS SLMs. Therefore, the proposed method can greatly increase the data writing speed and make this data storage technology more feasible for future cloud.

Chapter 4

Phase and polarization modulation using single-beam coding

4.1 Overview

In this chapter, a method capable of simultaneous phase and polarization modulation using single-beam coding is proposed and the effectiveness of this method is experimentally verified. This new method shows significant difference and improvement compared with method in chapter 3.

In the previous chapter, the phase and polarization modulation method based on the combination of two basis holographic vector beams has been introduced. The phase and amplitude of two basis components of input beam are independently modulated and then spatially combined into one single output beam. Due to the use of double beams, in beam combining process, high accuracy alignment of two input beams is required. This physical alignment process can be affected by devices assembly and positioning error of optical elements in system. To avoid two beams combining has become the motivation of developing

a new method. As shown in Figure 4.1, instead of using two beams, the proposed method in this chapter only uses a single beam as input beam. The phase modulation of two LCOS SLMs is used to encode holographic image information and amplitude information to both X and Y light components, instead of two independent beams. The polarization angle of input beam is set at 45°, by using the polarization sensitivity of LCOS SLM, the phase of X and Y components of light can be independently modulated. The formation of target holographic image and polarization angle of the output beam is only achieved when far field diffraction of light is focused into a focal plane. Therefore, in whole information encoding process, no physical combination of beam in free space is required. The principle of this method is introduced and explained in section 4.2. The experimental results and discussion are in section 4.3 and 4.4, respectively.

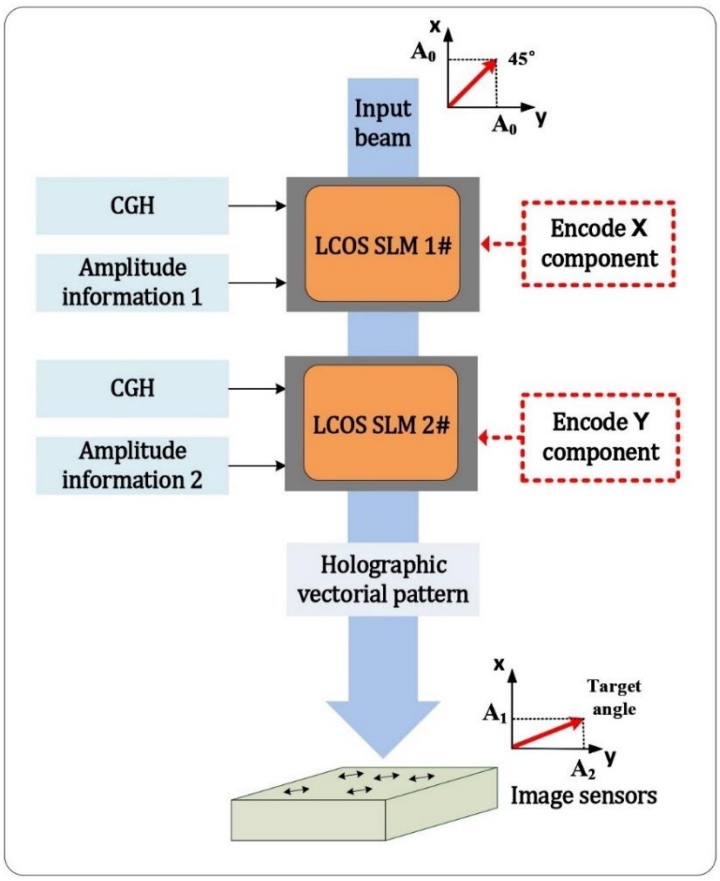

Figure 4.1 The schematic of proposed method using single beam coding.

4.2 The proposed method

4.2.1 The polarization sensitivity of phase-only LCOS SLMs

Due to the operating principle of phase-only LCOS SLM devices, they are sensitive to the polarization state of the input light [102,103]. When LCOS SLM devices are designed to perform phase-only modulation, to maximize the phase modulation efficiency, the polarization state of input light must be parallel to the alignment direction of liquid crystal molecules. This is mainly because liquid crystal modules in the most current LCOS SLM configurations can only provide the change of effective refractive index of light in one plane [79,104,105,106,107]. Therefore, the direction of the liquid crystal alignment is also considered as the operating direction of a phase-only LCOS device.

When the polarization of input light is set parallel to the working direction of LCOS SLM, the phase value from each pixel will be encoded on the input light field. However, when the polarization of input light is set to angle θ to the alignment of LCOS SLM and the working direction is at X axis, the output light field from a single pixel after phase modulation can be defined using Jones matrix as

$$E = \begin{bmatrix} (A_0 cos\theta)e^{i\varphi_x} \\ A_0 sin\theta \end{bmatrix} \tag{4.1}$$

where A_0 is the amplitude of input light and $e^{i\varphi_x}$ is the phase value encoded by LCOS SLM. Due to the polarization sensitivity of phase-only LCOS, only the X component of incident light field is encoded with phase value. When we think of the whole active area instead of one pixel on LCOS SLM, the $e^{i\varphi_x}$ now means the CGH and it carries the holographic image information. Therefore, by altering the polarization angle of input beam, we can only encode information on a CGH to one of two orthogonal light components without affecting the other one. This provides us with an opportunity to independently modulate the X and Y components of one single light beam by using two LCOS SLMs with working direction at X

and Y axis. Therefore, the polarization sensitivity of phase-only LCOS SLM can be utilized to realize the proposed phase and polarization modulation method.

4.2.2 The principle of the proposed method

By using the polarization sensitivity of LCOS-based phase-only modulation, the proposed method uses two LCOS SLMs to independently encode the holographic image and amplitude information onto the X and Y components of a single input beam. After the Fourier transform of the information-encoded beam, both holographic image information and amplitude information will be expressed via diffraction. Therefore, the image pattern and polarization state of output beam will be determined by CGH on two LCOS SLM like in chapter 3. This means that a holographic image with a target polarization angle can be generated.

As shown in the Figure 4.1 in overview section, the linearly polarized input beam is set at a pre-determined angle to the first LCOS SLM with working direction at X axis (the horizontal direction). Here, we can use β to express the pre-determined angle and the amplitude of input light is normalized as 1. Then, the Jones vector of the input light can be expressed as

$$E = \begin{bmatrix} cos\beta \\ sin\beta \end{bmatrix} \tag{4.2}$$

where the $cos\beta$ and $sin\beta$ means the amplitude of two orthogonal vector beam components E_x and E_y, respectively.

Then, the input light beam is incident on the first LCOS SLM for the first modulation. In this modulation process, we used the proposed method in chapter 3. We use a CGH with a phase depth information to successfully encode both holographic image and amplitude information into the horizontal vector beam component (E_y). As the working direction of first LCOS SLM is horizontal, the loaded CGH can only modulate the horizontal component (E_y) of input vector beam. The vertical component (E_x) will not be affected.

Here, we use $G(x)$ to indicate the holographic image information for X direction light component. The $G(x)$ can be expressed as phase value on CGH by $G(x) = e^{i\varphi_x}$. And the amplitude information A_x is encoded via phase depth of the CGH. Then, the Jones vector of optical vector beam after modulation on the first LCOS SLM can be expressed as

$$E = \begin{bmatrix} A_x(cos\beta)e^{i\varphi_x} \\ sin\beta \end{bmatrix} \tag{4.3}$$

Due to the polarization sensitivity of phase-only LCOS, the Y direction light component remains unchanged and there is no phase information (holographic image and phase depth) encoded on Y component. The phase information on X direction light component is encoded by using Fourier CGH. This means that the light field with target holographic image and amplitude are imaged at infinite distance via diffraction of light. Therefore, the X direction light component would not form diffraction pattern and become a separate beam when Fourier lens is not used after modulation. This is a critical feature of the proposed method because this design ensures the vector beam remaining as a single beam. Also, it allows the independent phase-information encoding on X and Y direction light components.

To encode the phase information on the Y direction light component, the working direction of second LCOS SLM is set at horizontal direction. When the working direction of LCOS is aligned with light component of Y direction, the second CGH can be utilized to encode the phase information on the Y direction light component without affecting the X direction light component. Figure 4.2 shows the double phase-only modulation method. This method ensures the phase information on X direction component after first modulation can be preserved. Here, we use $G(y)$ to indicate the holographic image information for Y direction light component. The $G(y)$ can be expressed as phase value on the second CGH by $G(x) = e^{i\varphi_y}$. And the amplitude information A_y is encoded via phase depth of the CGH. Then, the Jones vector of optical vector beam after the second modulation can be expressed as

$$E = \begin{bmatrix} A_x(cos\beta)e^{i\varphi_x} \\ A_y(sin\beta)e^{i\varphi_y} \end{bmatrix} \tag{4.4}$$

When we use the same target image to calculate CGHs on both LCOS SLMs, then, $G(x) = G(y)$ and $e^{i\varphi_x} = e^{i\varphi_y} = e^{i\varphi_{x,y}}$. Thus, Eq4.4 now can be rewritten as

$$E = \begin{bmatrix} A_x(cos\beta)e^{i\varphi_{x,y}} \\ A_y(sin\beta)e^{i\varphi_{x,y}} \end{bmatrix} \tag{4.5}$$

Since the holographic image information on X and Y light components are set the same, that elements can be taken out of the Jones vector and the Eq4.5 can be further rewritten as

$$E = \begin{bmatrix} A_x(cos\beta) \\ A_y(sin\beta) \end{bmatrix} \cdot e^{i\varphi_{x,y}} \tag{4.6}$$

To further simplify the output vector beam, the polarization angle of input beam can be set at β=45°, thus, sin(β) = cos(β) = 1. And Eq4.6 can be expressed as

$$E = \begin{bmatrix} A_x \\ A_y \end{bmatrix} \cdot e^{i\varphi_{x,y}} \tag{4.7}$$

Now, we can see that the Jones vector of output beam has only three elements A_x , A_y and $e^{i\varphi_{x,y}}$. The phase information $e^{i\varphi_{x,y}}$ contains the holographic image and the image can be reconstructed by performing a Fourier transform to the light field. In practical, the image can be reconstructed on the focal plane of the Fourier lens. The amplitude information A_x and A_y is directly controlled by phase depth. Therefore, by manipulating the ratio of A_x and A_y , the polarization state of output vector beam can be effectively modulated. The X and Y direction light components at a pixel on LCOS have been encoded same phase value, therefore, the phase shift between two light components remain the same as the input beam. Because the input beam has linear polarization at 45°, the output vector will remain linear polarization state and its angle is determined by A_x and A_y.

Moreover, the three information terms A_x , A_y and $e^{i\varphi_{x,y}}$ are all encoded by CGH on LCOS SLMs in the proposed method, therefore, the dynamic modulation of phase and polarization of output beam can be achieved by changing CGH. The output vector beam would have the target image pattern and a desired linearly polarized state.

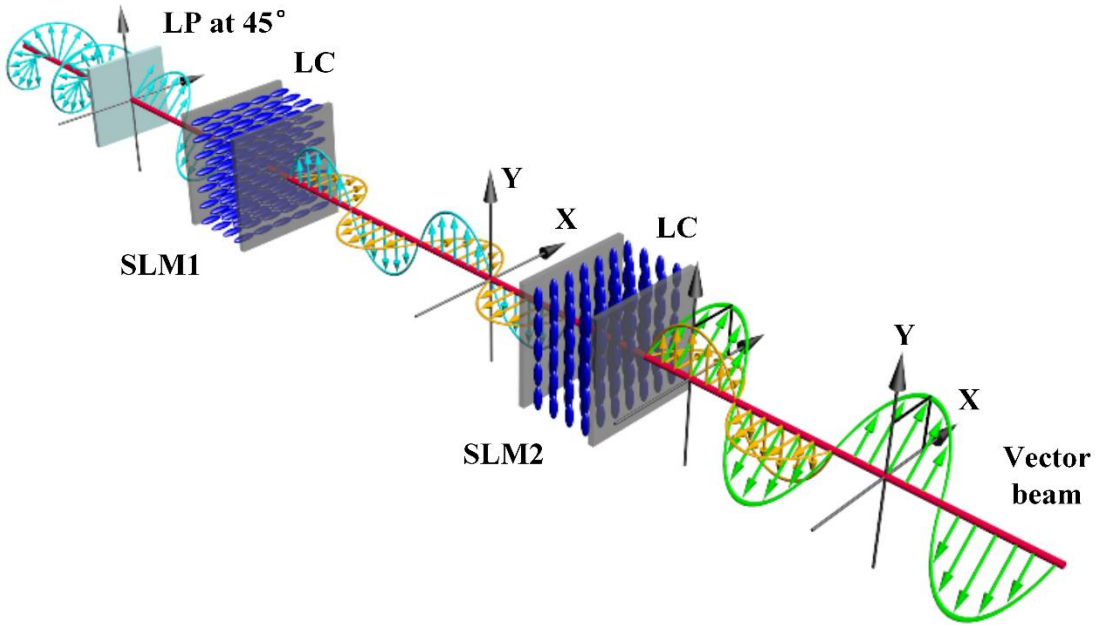

Figure 4.2 The principle of the phase and polarization modulation method using single-beam sequential coding. LC is liquid crystals, LP is a linear polarizer having an angle of 45° between the input vector and the LC molecules.

In Figure 4.2, two LCOS SLMs with orthogonal working direction are utilized sequentially code the holographic image and amplitude information to the X and Y direction light components. The polarization state of the input beam is first changed into 45° with respect to the LCOS SLM's working direction, because this can simplify the calculation of required phase depth of two CGHs in later process.

As can be seen in Figure 4.2, the first modulation process on LCOS SLM1 encode the image and amplitude information on vertical light component and horizontal light component

remain unchanged. The blue colour wave represents the input beam. After first modulation, the modulated vertical light component changed to yellow but horizontal one remains blue. The second modulation on LCOS SLM2 encodes the information on horizontal light component. At last, the output vector beam with target image and final polarization state is in green.

4.3 Experiments

To verify the feasibility of the proposed method, we experimentally demonstrate the capability of generating a vector beam using the time-delay holographic encoding of two basis components. This section demonstrates the experimental setup and final polarization and holographic patterns generation.

4.3.1 Experimental setup

The experimental setup of the proof-of-concept system is shown in Figure 4.3. We use two lenses (Lens1 and Lens2) to generate a collimated beam and expand the beam size to cover the whole active area of LCOS SLMs. This can maximize the intensity of input light for later modulation. Then, a linear polarizer (LP) is used to changes the input beam into a linearly polarized state. The LP polarization axis is placed at an angle of 45°. The linearly polarized input beam passes through a beam splitter (BS) and then incidents on the LCOS SLM. The Fourier CGHs are calculated using Gerchberg-Saxton (GS) algorithm on Matlab. They are used to encode the holographic pattern and intensity information on the horizontal polarization component of the optical vector beam. After the modulation process on the first LCOS SLM, the reflected beam passes through the BS again and its propagation direction is rotated by 90° for the second modulation. The second hologram is presented to encodes the vertical light component. To remove the zero-order noise caused by the pixelated structure of LCOS devices in holographic image reconstruction, the improved GS algorithm integrated a

computed holographic lens into the Fourier hologram. The zero-order beam can be effectively removed from the information plane. A spatial filter is utilized to block the deflected the zero-order beam of diffraction. The final target image is reconstructed on the focal plane of a Fourier Transform (FT) lens, then, the images captured by a CMOS sensor after a 4f optical relay.

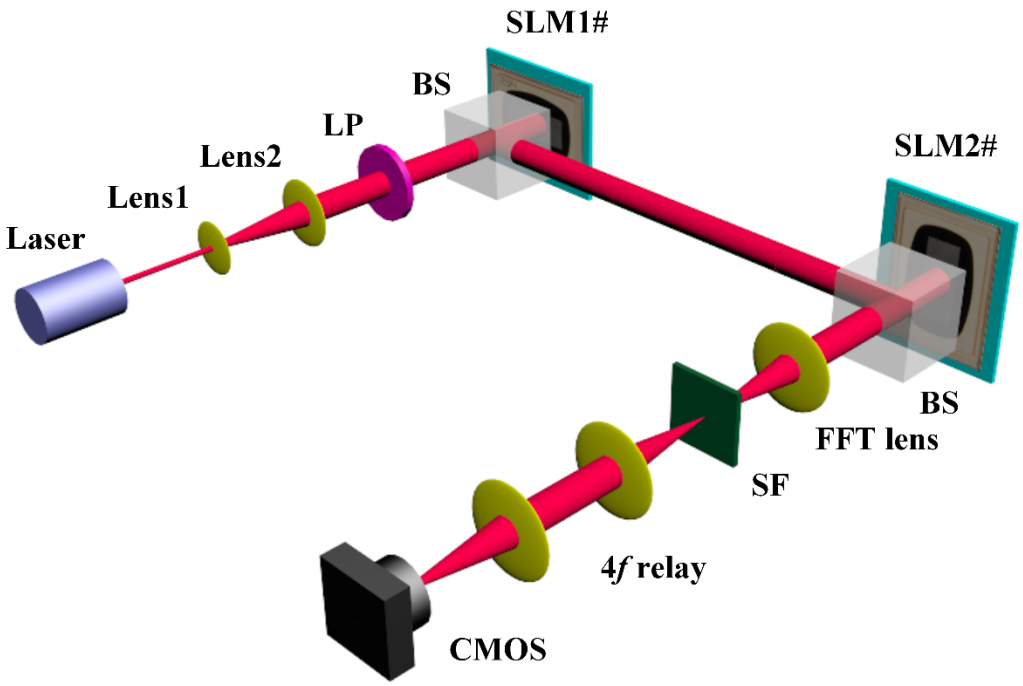

Figure 4.3 The schematic of the experimental concept-proof setup (a), where LP is a linear polarizer, HWP is a half wave-plate, BS is a beam splitter, SF is a spatial filter.

In the proof-of-concept experiment setup, the illumination source used is a collimated coherent laser, which is a 5mW diode module with a wavelength of 633nm. The two reflective-mode LCOS SLMs for coding the optical vector beam have a resolution of 1920×1080 and a pixel pitch of 5.3μm. The phase bits resolution of the LCOS SLM is 8 bits; thus, the greylevel scale of phase modulation is 0-255. The two LCOS SLMs used in experiments are fabricated in Center for Photonic Devices and Sensors, CPDS, in University of Cambridge. It used in-house developed die-level assembly techniques to ensure high quality and performance of phase modulation.

To create an input vector beam with a linear polarization angle at 45°, a linear polarizer (LPVISC050, Thorlabs Inc.) with a diameter of 12.5mm is utilized. Two beam splitters (BS004) used in experiments are non-polarizing beamsplitter cube with an energy split ratio of 50:50. The BS may be replaced by other optical components, such as a Wollaston prism and Calcite beam displacer, to manage the input and output beam of the two LCOS SLMs. Holographic images are reconstructed in replay field using a FFT lens (LB1374, Thorlabs Inc.), which is an N-BK7 Bi-convex lens with a diameter of 50mm and a focal length of 150mm. As for holographic images recording, we used a CMOS sensor with a pixel size of 5.3 μm and a resolution of 4928×3624 to capture the target images.

4.3.2 Independent coding of two polarization components

In the verification of the effectiveness of the proposed method, the capability of the encoding target image information on two light components using phase-only LCOS SLM is demonstrated. First, we can use two different target images information to code the two light components. This experiment can effectively show that the two vector components of input beam can be independently coded.

In this experiment, the hologram calculation method includes two steps: (1) a Gerchberg-Saxton (GS) algorithm is used to generate a phase-only CGH of target image (2) a holographic lens is calculated and applied on the CGH to remove the zero-order noise.

Because the focus here is to perform target image information encoding, we use the maximum phase depth (greylevel = 255) on both CGHs in light modulation to acquire highest image quality. Recalling the Eq4.4 in previous section, the Jones vector of light field after modulation on both X and Y direction light components is

$$E = \begin{bmatrix} A_x(cos\beta)e^{i\varphi_x} \\ A_y(sin\beta)e^{i\varphi_y} \end{bmatrix} \tag{4.8}$$

where $e^{i\varphi_x}$ and $e^{i\varphi_y}$ are phase holograms of the target images $G(x)$ and $G(y)$, respectively. The polarization state of input beam is at 45° and maximum phase depth is used on two CGHs, therefore, the encoded optical vector beam now can be expressed as

$$E = \begin{bmatrix} 1 \cdot e^{i\varphi_x} \\ 1 \cdot e^{i\varphi_y} \end{bmatrix} \tag{4. 9}$$

The GS algorithm of phase holograms is based on inverse Fourier transform; therefore, the target images can be reconstructed by Fourier transform. In practice, the far field diffraction is a Fourier transform process of light field. To acquire the target images in a finite distance, a converging lens is used to perform a Fourier transform through light focusing. The target images can be reconstructed on the focal plane of lens. When the phase holograms encoded on the X and Y direction components are different, the diffraction of both light components will be consequentially different. This means that the X and Y direction light components will become two separate beams after diffraction process as shown in Figure 4.4.

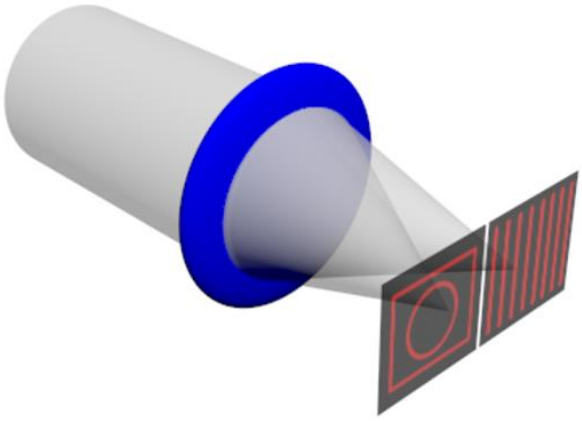

Figure 4.4 The vertical and horizontal polarization components encoded with different target image information will separate into two beams after holographic image reconstruction. The lens (blue circle) is used to perform the images reconstruction on the focal plane.

Then, the total light field can be expressed as

$$E = \begin{bmatrix} 1 \\ 0 \end{bmatrix} \cdot e^{i\varphi_x} + \begin{bmatrix} 0 \\ 1 \end{bmatrix} \cdot e^{i\varphi_y} \tag{4. 10}$$

Because the independence of two diffraction process, the output vector beam will become two beams: a vertically and a horizontally polarized beam. And the two vector beams have their own target images.

In experiment, a Lego pattern and a grating pattern are used as two target images for X and Y direction light components. We place a polarization analyzer in front of the CMOS sensor to examine the polarization state of output vectorial beam. Figure 4.5 shows the reconstructed holographic patterns when the analyzer is placed at the different angle (blue double-end arrows in Figure 4.5).

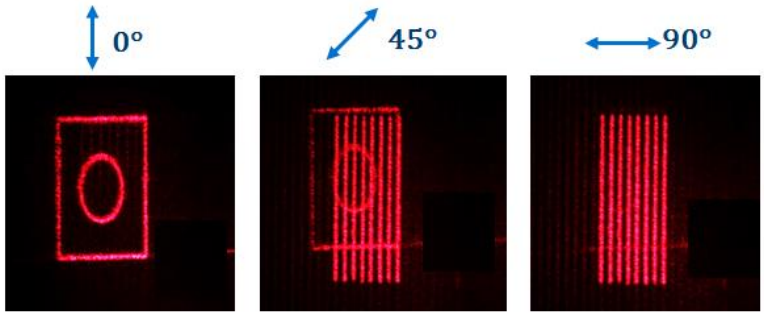

Figure 4.5 The experimental results when encoding the optical vector beam using two different holographic patterns: the analyzer is placed at 0° (a); the analyzer is placed at 45° (b); the analyzer is placed at 90° (c).

As can been seen from the reconstructed images on the focal plane of lens, the Lego pattern has vertical polarization state, while the grating has horizontal polarization state. This experiment shows that the X and Y direction components of input beam can be independently encoded with target image information.

These result also indicate that this setup can provide us with a potential polarization selective tool. First, two target images information is independently coded on vertical and horizontal light components in this experimental setup. And the amplitude information on two CGHs is

set the same. Then, the linearly polarized input light will be separated into two orthogonal beams with two different images. For example, we can use image 1 for vertical light component and image 2 for horizontal light component. By measuring the intensity of both reconstructed images, the amplitude of two orthogonal polarization components of input beam can be found. This means that the original linear polarization angle can be therefore calculated.

This polarization selective property of this setup can be used to ensure that the input polarization angle is in 45° to the working direction of both LCOS SLMs. The alignment direction of liquid crystal molecules is determined by the rubbing direction in fabrication. The alignment direction is normally completely parallel with the long side of the LCOS device's backplane. Therefore, the calibration of input beam polarization angle is needed, and this can be done by using the method stated here. Rotating the linear polarizer of input beam, when both reconstructed target images have same intensity, it means that the angle between LCOS working direction and input polarization angle is at 45°.

4.3.3 Experimental results

In this section, the experimental results of the effectiveness of phase and polarization modulation method is provided. The output vector beam with target image information and target polarization state is expressed through Fourier transform lens focusing. Recalling the Jones vector in Eq4.6, when the two vector beam components are encoded with same target image information, the output vector can be expressed as

$$E = \begin{bmatrix} A_x \\ A_y \end{bmatrix} \cdot e^{i\varphi_{x,y}} \tag{4. 11}$$

where ratio of A_x and A_y will determine the angle of final polarization and $e^{i\varphi_{x,y}}$ contains the target image information. As we know from Chapter 3 that the amplitude of X and Y light components can be controlled by using phase depth modulation. And a look-up-table of 1st

order diffraction amplitude versus the greylevel of CGH is found. Therefore, we can use specific greylevel combination of two LCOS SLMs to acquire the target amplitude ratio of two orthogonal light components. Then, as shown in Fig 4.6, 4.7, the target polarization angle can be achieved.

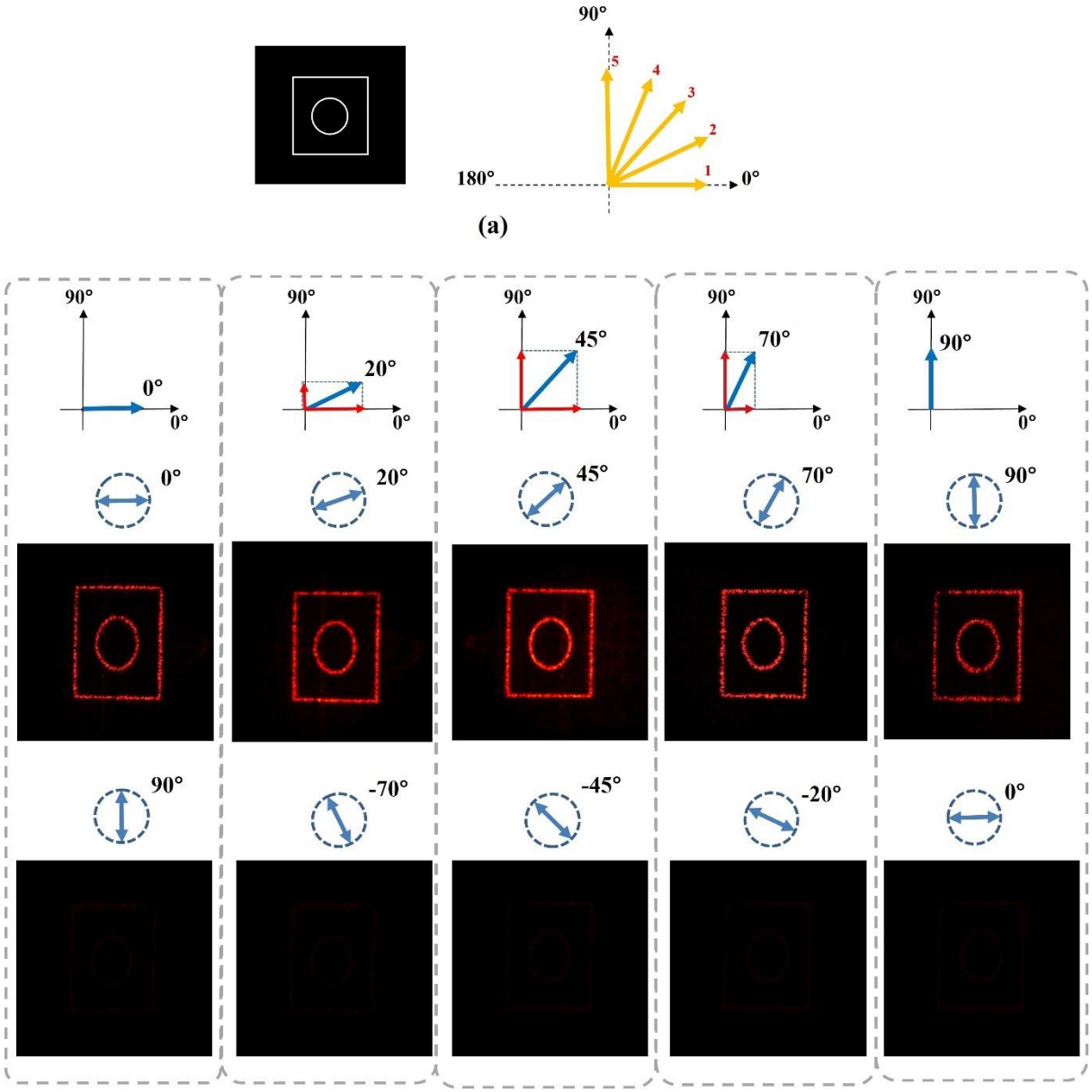

Figure 4.6 The target holographic image (circle and square) and five target polarization states 0°,20°,45°70°,90°. (b) The output holographic image with target linear polarization states under pair of orthogonal analysers.

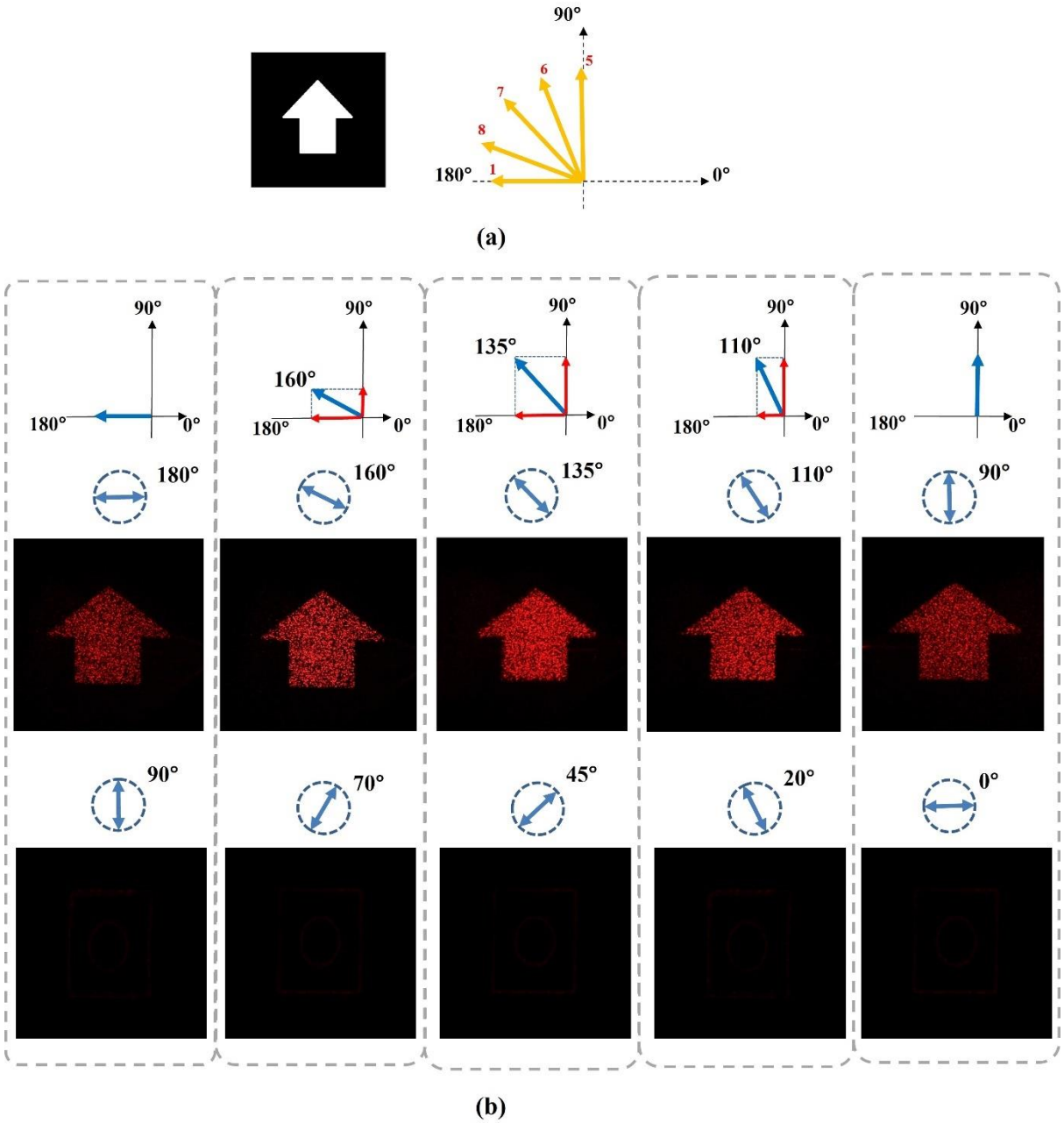

Figure 4.7 The target holographic image (circle and square) and five target polarization states 0°,20°,45°70°,90°. (b) The output holographic image with target linear polarization states under pair of orthogonal analysers.

The proposed method has a capability of dynamically providing more available linear polarization states, allowing the increase of the data bits carried by one voxel. When we consider the number of data bits that one voxel can carry, we can start from the number of available coding states (the combination of polarization states and retardance levels) for a voxel. In Fig 4.8, the example of each voxel carrying 3 bits of data has been shown.

The coding states can be expressed by 2K+L, where K is the bit number of encoding total polarization state number, L the occupied bit number of encoding total intensity state number. For example, when a femtosecond laser writing light field can provide eight different linear polarization angles: 0°, 22.5°, 45°, 67.5°, 90°, 112.5°, 135°, 157.5°. This means that polarization state encoding is expressed by a 3 digits binary code (i.e., K=3). If two different level retardance of voxel can be generated, the retardance encoding is expressed by a single digit binary code (i.e., L=1). So, the total available coding-states by combining the retardance and polarization states are 2^4=16 for the data storage.

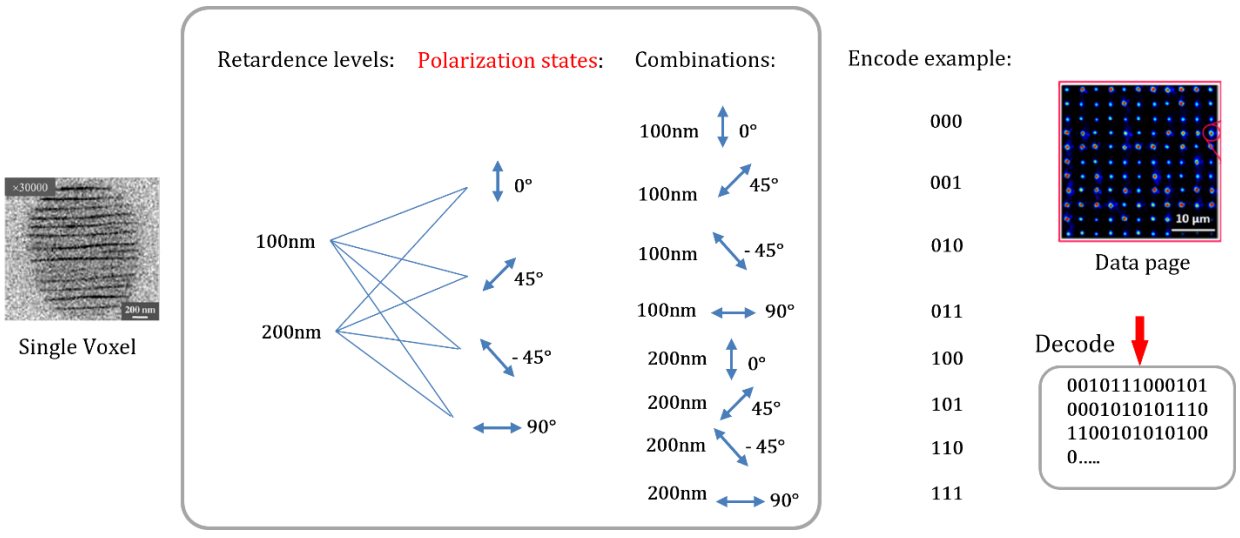

Figure 4.8 The example of data bits encoding and decoding as binary code onto the single voxel.

4.4 Discussion

As shown in Figures 4.6-4.7, the proposed method is capable of the dynamical generation of arbitrary holographic target images with desired linear polarization state. Like the proposed method in chapter 3, the data writing beams generated by the new method also can effectively write all voxels with the same polarization direction on a data page at the same time. It can largely reduce the movements of a glass sample in the writing process task of each data page. This means a significant decrease of the mechanical delay caused by the glass sample platform movement.

As shown in experimental results, the proposed method in chapter 3 and the newly proposed methods can both achieve the simultaneous phase and polarization modulation using phase-only CGHs. However, these two methods have some fundamental differences. The comparison of the two proposed methods in the research in the aspects of the principles and the practical use is provided in Table 4.1.

Table 4.1 **The comparison of two methods: Two-beam combination and Single beam sequential coding**

Methods	**Input beam numbers**	**Input beam polarization state**	**Object of modulation**	**Light modulation type on LCOS SLM**	**Formation of output vector beam**
Two beams combination	2	↔ 0° ↔ 0°	Two independent beams	Phase-only	Direct beam combining
Single beam sequential coding	1	⤢ 45°	Two orthogonal components of beam	Phase-only	Require far-filed diffraction

In Table 4.1, the detailed explanations of comparison results are demonstrated as following:

1. Object of modulation

As for the object of phase-only modulation on LCOS SLMs, two proposed methods have a fundamental difference. In the method of chapter 3, because the two-beams superposition is used to perform the polarization modulation, the two independent input beams are the object of modulation, and their modulation are independent and parallel. However, in the proposed method in this chapter, the object of phase-only modulation is two orthogonal polarization components of a single input beam. Because of the polarization sensitivity of phase modulation on LCOS SLMs, the two polarization components of beam can be independently modulated. In the experimental setup, two separate phase-only modulation processes has a sequential relationship due to the sequential optical path configuration. We can still see this method as a parallel modulation scheme because two components of light travelling simultaneously in the speed of light.

2. Input beam polarization state

In the method of two-beam parallel coding and combining, the polarization states of the two input beams are both set to be parallel to the working direction of LCOS SLMs. For the simplicity of the LCOS devices setup in the optical system, both LCOS SLMs are set horizontal working direction, thus, two input beams have horizontal linear polarization state at 0°. However, in the proposed method of single beam sequential coding, the polarization states of the input beam need to set at 45° to the working direction (0°) of LCOS SLMs. This is because the 45° linear polarization state can provide the same initial amplitude of two polarization components so that the amplitude information encoding can be simplified. The initial amplitude of two input polarization components will become their maximum output amplitude after modulation, therefore, the equal amplitude setting of both light components also provides the maximum range of available output polarization state.

3. Phase modulation

The phase modulation part of both methods is the same. The CGHs contain the information of holographic target image and amplitude. The phase-only modulation can provide arbitrary target image, and the phase depth of CGHs can be used to effectively control the amplitude of output diffraction light.

4. Formation of output vector beam and Polarization modulation

The formation process of output vector beam of these two proposed methods is fundamentally different. In the method of two-beam combining, the light fields of two holographic target image with determined amplitude and orthogonal polarization state (vertical and horizontal) is generated before the beam combining process. The target image reconstruction of two parallelly phase-modulated beams is firstly completed using lens, and then two light fields are spatially superposed to provide the final holographic image and target polarization state. As for polarization modulation, it is achieved by superposition of two orthogonally polarized beams, and the angle of linear polarization state is controlled by the amplitude ratio of two beams.

However, in the proposed method in this chapter, instead of modulating and combining two basis beams, the single beam's two polarization components are independently modulated. The use of characteristic of polarization sensitivity of phase-only LCOS SLMs makes modulating the light components possible. The CGHs encode the information of target image and amplitude on both light components, at this moment, the light field with two modulated polarization components is still in the far field diffraction situation. This mean that the modulated beam is still a parallel beam without image reconstruction, and its diffracted image is at infinite distance from the hologram plane. Therefore, to acquire the output reconstructed target light field from computer-generated holograms, the converging lens is used to move the far field diffraction pattern to the lens' focal plane. As for polarization modulation, the amplitude ratio of light components has already been determined, therefore, the polarization

modulation in the newly proposed method is within the formation of output vector beams. Table 4.2 shows the summary of the comparison between two methods in terms of data storage application.

Table 4.2 **The comparison of two methods in data storage application**

Methods	Phase modulation	Polarization modulation	Polarization angle control	Multi-polarization states	Alignment of two basis vectors	Sensitivity of LCOS non-flatness
Two beams combination	CGH	Two vector-beams combinations	Amplitude ratio of two beams	Glass sample motion free	Precise physical alignment	Medium
Single beam coding	CGH	Sequential coding of two components	Amplitude ratio of two light components	Glass sample motion free	None	High

In Table 4.2, two important comparison results are detailed explained as following:

1. **Alignment requirement**

In the method of two orthogonally-polarized beams combining, a very high precise physical alignment of two independent beams is required for the superposition. Because both holographic target images from two beams have been reconstructed before the combination, to ensure formation of the target polarization of output image, the position shift between two beams needs to be minimized to the wavelength level. This alignment requirement can lead to large optical path calibration workload. Moreover, due to the difficulty in pixel-level alignment of two beams, the resolution of beam dots image is also limited by the spatial superposition accuracy.

In the proposed method based on single beam coding, the status of single beam is not altered in the phase modulation and propagation. After two independent phase modulations on both

vertical and horizontal light components, the beam has already been encoded with holographic target image information and information of amplitude on two components without any change of light propagation status. Therefore, due to the principle of this method, no physical alignment of light is required. More importantly, the resolution of holographic imaging is now only limited by LCOS SLMs, and the high accuracy polarization control is also achieved.

2. Sensitivity of LCOS non-flatness

In the phase-only modulation on LCOS SLMs, the phase retardance provided by the liquid crystal molecules on each pixel is mainly determined by voltage applied. However, due to the non-flatness of liquid crystal cell, the actual phase retardance on each pixel is not equal in value in CGHs. This is the main source of phase modulation accuracy loss for LCOS devices. Therefore, to obtain high phase modulation accuracy, a phase correction map is calculated and applied according to the thickness variation across the whole active area.

In a normal non-flatness phase compensation method, the phase correction is designed for when the linear polarization state of input light is parallel with the liquid crystal molecules' long axis. In other words, it is designed for the phase-only modulation. It only compensates the phase delay caused by thickness variation on one polarization direction.

In the method of two-beam combining, the two input beams are linearly polarized and parallel to the direction of liquid crystal molecules alignment on both LCOS SLMs. After the phase compensation for cell's non-flatness, the high phase modulation accuracy of two modulations in this method can be ensured.

However, In the proposed method, the input light has 45° to the LCOS SLM's working direction (X polarization direction). Therefore, the polarization component that is parallel to the liquid crystal's long axis (with extraordinary refractive index) will experience the phase retardence introduced by CGH, and the normal phase correction for non-flatness on this direction will be effective. For the polarization component that is perpendicular to the liquid crystal's short axis (with ordinary refractive index), it will not experience a phase change

when CGH is loaded. However, the thickness variation across the cell causes phase delay on the Y polarization direction because of the existence of ordinary refractive index. And this phase error will affect the second phase modulation for Y polarization components. Thus, the normal phase correction method for non-flatness is not effective for 45° input. For the proposed method, ideally, both X and Y polarization requires a phase compensation in the proposed method.

4.5 Conclusion

The newly proposed method of phase and polarization modulation based on single beam coding is introduced and experimentally verified. In this method, the two orthogonal polarization components of input beam are independently modulated. The information of holographic target image and amplitude are simultaneously encoded by using CGHs. The amplitude modulation is achieved by controlling the first-order diffraction efficiency. Due to the status of single beam is not affected by the modulation, the formation of output light field is achieved by using a converging lens to reconstruct the image on its focal plane. Therefore, comparing with the method in chapter 3, the proposed method can provide pixel-level alignment accuracy without any external alignment calibration. The imaging resolution is no longer limited by the beam combining, and it can reach maximum imaging resolution of the LCOS SLMs.

The use of LCOS SLMs in this method is not common phase-only modulation mode. This method needs 45° linearly polarized input light, thus, to obtain very high output vector beams, it requires phase correction for cell's non-flatness on both X and Y input polarization components. Because of a single beam is utilized in the proposed method, the sequential information coding can largely simplify the optical system configuration. Therefore, the proposed method can be a potential compact and plug-in technology in the writing beam generation of optical data storage in glass.

Chapter 5

Compact system of phase and polarization modulation

5.1 Overview

In the previous chapter, a phase and polarization modulation method of light based on independent coding of two orthogonal light components is introduced. Two LCOS SLMs devices are required in the proof-of-concept system for the sequential information encoding on two light components. In this chapter, a new method based on a single LCOS SLM is proposed. And based on the simplicity and flexibility of new method, a compact system is developed and fabricated.

The proposed method adopts the same idea of independent coding two orthogonal light components in chapter 4. This means that the target image and amplitude information are firstly independently encoded on horizontal and vertical light components. Then, the target image reconstruction and output polarization formation are simultaneously completed by using the focusing lens to perform Fourier transform. However, to use single LCOS SLM in

the method, a new modulation scheme of two polarization components is needed due to the single working direction of liquid crystal molecules.

In this method, a rotation scheme of the polarization plane of two light components is proposed. The active area of LCOS SLM is divided into two sections to load two CGHs. As shown in Figure 5.1, the X direction component of 45° polarized input beam is firstly coded by CGH1. Then, the rotation of both polarization components makes the Y component available for coding by CGH2. After two coding processes, the output target image with target polarization can be obtained. The principle of the method is introduced in detail in section 5.2. The compact system design based on this modulation method is proposed in section 5.3. The engineering details of the prototype device are shown. And the effectiveness of the compact system is also experimentally verified.

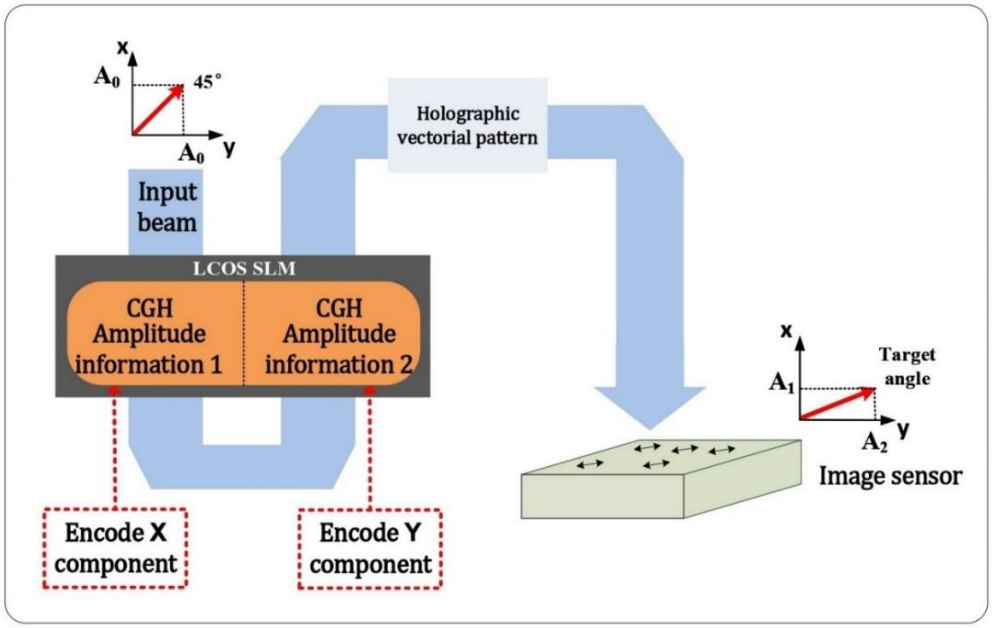

Figure 5.1 The schematic of proposed compact system of phase and polarization modulation method using a single LCOS SLM.

5.2 The proposed method

5.2.1 Half-wave plate

In this proposed method, the half-wave plate plays an important role. A half-wave plate can be used to manipulate the polarization state of a light wave passing through it. The half-wave plate is a birefringent crystal with a designed orientation and thickness. In the plane of a half-wave plate, there are two perpendicular optic axes: the ordinary axis with refractive index n_o and the extraordinary axis with refractive index n_e . When a light wave normally incident on the plate, the polarization component on the ordinary axis passes through the plate with a speed $v_o = \frac{c}{n_o}$, while the polarization component on the extraordinary axis passes through the plate with a speed $v_e = \frac{c}{n_e}$. This results in a phase shift between the two polarization components when they exit the crystal. When $n_e < n_o$, for example in calcite, the extraordinary axis is referred to as the fast axis and the ordinary axis is referred to as the slow axis. The half-wave plate can introduce a fixed π phase shift between the two perpendicular polarization components of input light wave, therefore altering its polarization direction.

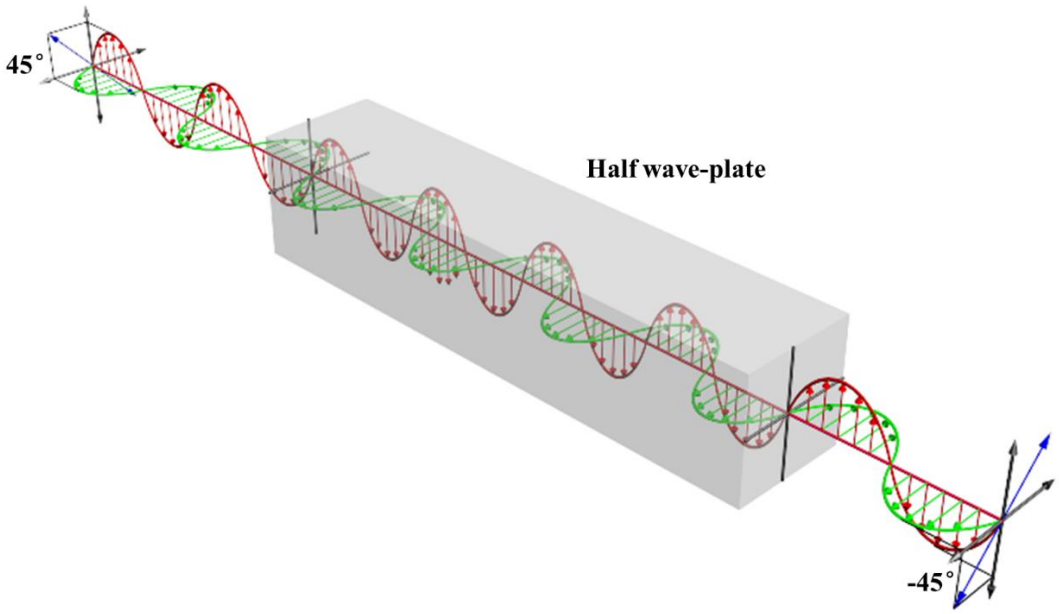

Figure 5.2 The principle of the proposed phase and polarization modulation method using single LCOS SLM. The yellow light wave is the modulated polarization component, while the blue one means the unaffected one after modulation by LCOS SLM.

As shown in Figure 5.2, when the incident light has a linear polarization, the angle of polarization direction of the input light can be shifted by the half-wave plate. And the change of polarization direction is determined by relative angle between the input light wave and optic axis of the half-wave plate. For example, when the linear polarization direction of the input light wave is vertical and the fast axis of the half-wave plate is at 45°, the polarization direction of output beam can change into horizontal. This behaviour of half-wave plate can be utilized in the proposed method. To encode target image information and amplitude information on the two orthogonal polarization components of input light wave, the polarization direction of input light is set at 45°. Due to the use of single LCOS SLM device in the proposed method, the working direction of liquid crystal will be single: either horizontal or vertical. Therefore, the rotation of two linear polarization components based on half-wave plate is the key to the success of information coding using one LCOS SLM.

5.2.2 The principle of the method

As introduced in the chapter 4, by using the polarization sensitivity of LCOS-based phase-only modulation, the independent encoding of the holographic image and amplitude information onto the X and Y components of a single input beam has been achieved. Before the Fourier transform of the information-encoded beam, both target image information and amplitude information will not be expressed. And both will be stored in the form of a phase distribution, and the phase distribution is directly controlled by the CGHs on LCOS SLM.

As shown in the Figure 5.3, the linearly polarized input beam is set at 45° to the LCOS SLM with working direction at Y axis (the horizontal direction). Then, the normalized Jones vector of the input light can be expressed as

$$E = \begin{bmatrix} 1 \\ 1 \end{bmatrix} \tag{5.1}$$

where the amplitude of two orthogonal vector components E_x and E_y are the same.

Then, the input light beam is incident on the first half of the active area of LCOS SLM for first modulation. In this modulation process, as shown in the schematic diagram in overview section, we use CGH1 with a certain phase depth information to successfully encode both target image information and amplitude information into the horizontal vector beam component (E_x). As the working direction of the LCOS SLM is horizontal, the loaded CGH1 can only modulate the horizontal component (E_x) of input vector beam. The vertical component (E_y) will not be affected.

Here, we use $G(x)$ to indicate the target image information for X direction light component. The $G(x)$ can be expressed as phase distribution on CGH1 by $G(x) = e^{i\varphi_x}$. And the amplitude information A_x is encoded via phase depth of the CGH1. Then, the Jones vector of optical vector beam after the first modulation can be expressed as

$$E = \begin{bmatrix} A_x \cdot e^{i\varphi_x} \\ 1 \end{bmatrix} \tag{5.2}$$

Due to the polarization sensitivity of phase-only LCOS, the Y direction component (the light wave in blue) remains unchanged and there is no phase information (target image and phase depth) has been encoded on it. After the phase-only modulation of X direction component (the light wave in yellow) of the input light wave, the target image will be reconstructed through the diffraction of light at infinite distance. This is due to the use of Fourier CGH. To reconstruct the target image, a converging lens is utilized to perform a Fourier transform so that the diffraction can occur on the focal plane of lens. This means that the X direction component of input light will maintain the superposition state with Y direction component

after the first modulation process when there is no lens applied. This is the key to polarization component rotation of the proposed method.

Physically, the light wave at X direction after phase-only modulation on LCOS SLM has become the diffracted light beam, while the light wave at Y direction has not been affected. Due to the property of far field diffraction in Fourier hologram, the image and amplitude information of light field at X direction are stored in the form of phase. This means that except the phase value of X direction components of each pixel on light beam area, the other property of the light waves at X direction will remain unchanged. Now, we can consider the X direction light component as a diffracted beam with diffraction angle 0° to its original propagating direction and state. Therefore, the X direction component of light maintains the superpositional state with Y direction component, meanwhile, they are separated into two beams in the viewpoint of wave optics. In physical optics, they are still two orthogonal polarization components of one single beam but with different phase value.

Because we can treat the X and Y direction of light components as two independent light waves, the half-wave plate can be introduced to independently and simultaneously rotation the direction of these two polarization components. Now, we can separately write the Jones vector of X and Y X and Y direction of polarization components as

$$E_x = \begin{bmatrix} A_x \cdot e^{i\varphi_x} \\ 0 \end{bmatrix} \qquad E_y = \begin{bmatrix} 0 \\ 1 \end{bmatrix} \tag{5.3}$$

Because of the use of single LCOS SLM, as shown in Figure 5.3, only the horizontal polarization components can be modulated. Therefore, the Y direction components (the light wave in blue) needs to be rotated into a horizontal polarization component before the second modulation. And CGH2 would be loaded on the second half of the active area of LCOS SLM to code the rotated Y direction polarization component. Moreover, to prevent the phase

information on X direction polarization components (the light in yellow) will not be affected in the second modulation process, we must rotate it into vertical direction in advance. Hence, the half-wave plate with fast axis at 45° is placed in front of the second half LCOS SLM. By doing this, the target rotation of two polarization components can be simultaneously achieved before the second phase modulation. The Jones matrix of a half-wave plate with fast axis at 45° can be expressed as

$$HWP_{45} = \begin{bmatrix} 0 & 1 \\ 1 & 0 \end{bmatrix} \tag{5.4}$$

Then, the Jones vector of X and Y direction polarization components after travelling through the half-wave plate can be written as

$$E_{x'} = HWP_{45} \cdot E_x = \begin{bmatrix} 0 & 1 \\ 1 & 0 \end{bmatrix} \cdot \begin{bmatrix} A_x \cdot e^{i\varphi_x} \\ 0 \end{bmatrix} = \begin{bmatrix} 0 \\ A_x \cdot e^{i\varphi_x} \end{bmatrix} \tag{5.5}$$

$$E_{y'} = HWP_{45} \cdot E_y = \begin{bmatrix} 0 & 1 \\ 1 & 0 \end{bmatrix} \cdot \begin{bmatrix} 0 \\ 1 \end{bmatrix} = \begin{bmatrix} 1 \\ 0 \end{bmatrix} \tag{5.6}$$

Now, we can see that the previous two polarization components have exchanged their polarization direction after half-wave plate. The $E_{x'}$ is now at vertical direction, while the $E_{y'}$ is changed into horizontal direction and ready for information encoding. It is important to notice that the rotation of polarization direction of two light components using half-wave plate will not change their physical superposition relationship.

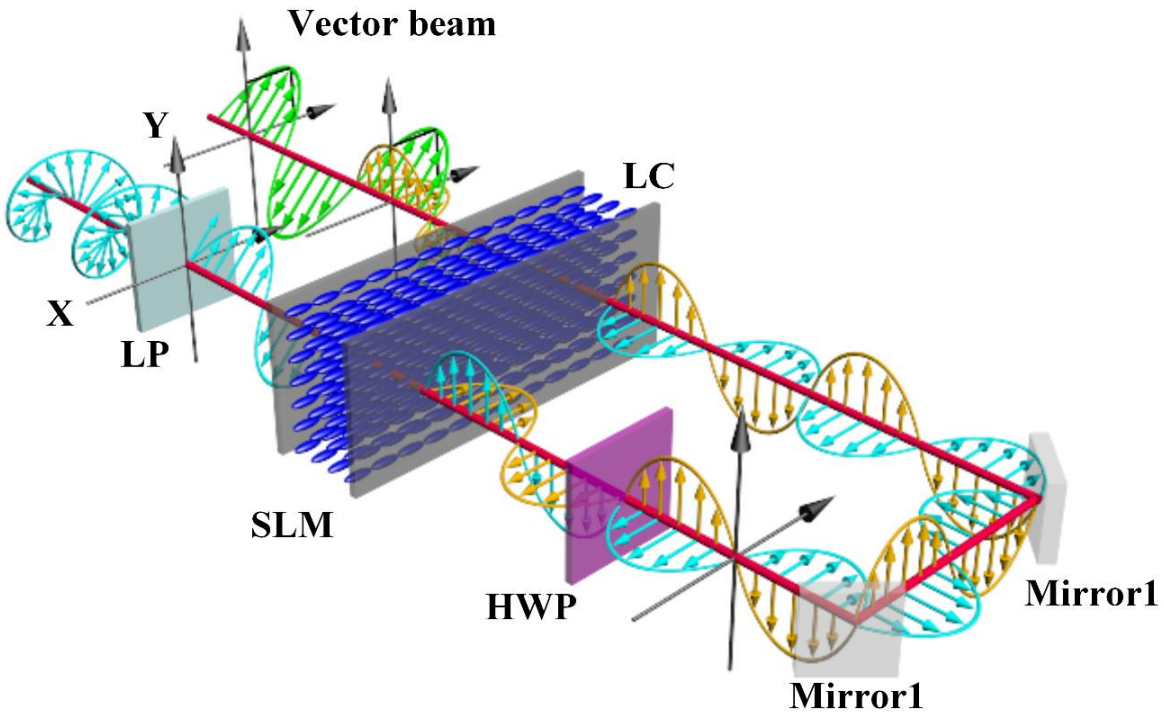

Figure 5.3 The principle of the proposed phase and polarization modulation method using single LCOS SLM. The yellow light wave is the modulated polarization component, while the blue one means the unaffected one after modulation by LCOS SLM.

Then, we use $G(y)$ to indicate the target image information for $E_{y'}$. $G(y) = e^{i\varphi_y}$. And the amplitude information A_y is encoded via phase depth of the CGH2. So, the $E_{y''}$ after second phase modulation can be expressed as

$$E_{y''} = \begin{bmatrix} A_y \cdot e^{i\varphi_y} \\ 0 \end{bmatrix} \tag{5.7}$$

Here, we can see that both two orthogonal polarization components have been encoded with the target image information and amplitude information. Like the situation in the first modulation for E_x , the modulated light component here has also become a far field diffracted light. This means that it remains the superpositional state with $E_{x'}$ .Therefore, the superposition of two polarization components is not affected by the two separate phase

modulations and polarization components rotation. Therefore, the final output light field can be expressed as the direct superposition of two light components

$$E_{out} = E_{x'} + E_{y''} = \begin{bmatrix} 0 \\ A_x \cdot e^{i\varphi_x} \end{bmatrix} + \begin{bmatrix} A_y \cdot e^{i\varphi_y} \\ 0 \end{bmatrix} = \begin{bmatrix} A_y \cdot e^{i\varphi_y} \\ A_x \cdot e^{i\varphi_x} \end{bmatrix} \tag{5.8}$$

To simultaneously manipulating the polarization state of output light with a certain target image, we set the target information on both CGH1 and CGH2 the same

$$G(y) = e^{i\varphi_y} = \ G(x) = e^{i\varphi_x} = e^{i\varphi} \tag{5.9}$$

Then, the Jones vector of output light will be rewritten as

$$E_{out} = \begin{bmatrix} A_y \\ A_x \end{bmatrix} \cdot e^{i\varphi} \tag{5.10}$$

Now, the phase (target image $e^{i\varphi}$) and polarization (amplitude ratio of A_x and A_y) modulation of light has been achieved in the proposed method. The control of amplitude information is the same as the method in chapter 3 and 4.

5.3 Experiments

Due to the use of a single LCOS SLM in the proposed method, it provides us with an opportunity to develop a compact system for phase and polarization modulation. In this section, the design and fabrication of compact system is introduced, and the effectiveness of the proposed method is experimentally verified. In the compact system, the only active optical device is the LCOS SLM, while other optical elements like half-wave plate and polarizer are all passive. This means that the compact system has potential to become a plug-in technology for generating data writing light field in optical data storage.

5.3.1 Experimental prototype

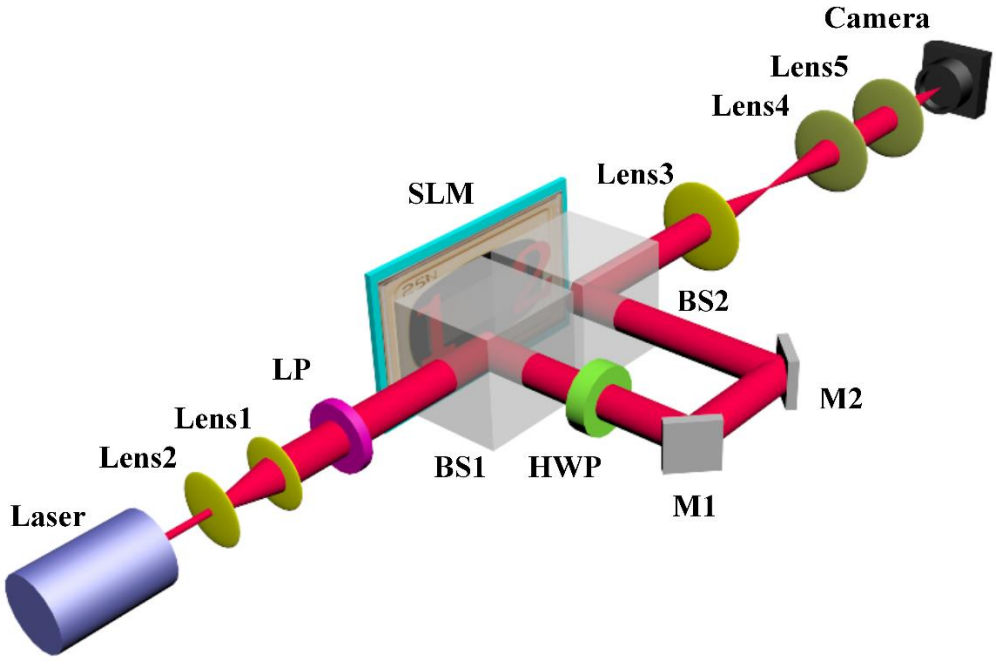

Figure 5.4 The schematic of the 3D optical configuration of proposed polarization modulation system where a linear polarizer (LP), mirrors (M1 and M2), a half-wave plate (HWP), beam splitters (BS1 and BS2), and a polarization beam combiner (PBC) are used. (b) the principle of the proposed polarization modulation method where the Jones matrix indicates the polarization state of light components and $e^{i\varphi}$ represents the information introduced by the hologram of data pattern.

Figure 5.4 shows the schematic of the proposed compact system of phase and polarization modulation using single LCOS SLM. The expanded and collimated laser beam passing through a linear polarizer is used as light source. The fast axis of the linear polarizer is set at 45° to the working direction (0°) of LCOS device. Then, the linearly polarized beam, passing through a non-polarizing beam splitter (NPBS), will illuminate the left-half of active area of the SLM. The hologram uploaded on the SLM performs modulation to the horizontally polarized light, while the vertically polarized light is not affected and then reflected to the HWP. By passing through the HWP, the horizontally polarized light component is now rotated into a vertically polarized light component and then be perpendicular to the working direction of LCOS device.

Accordingly, the previously vertically polarized light component is then rotated into a horizontally polarized light component that is ready for modulation. Two mirrors here are used to redirect the light to the right-half of SLM for the second modulation. The second modulation will only affect the light component that is not modulated at the first modulation. After two independent modulations on each of orthogonal light components, both horizontal and vertical components of the output light field now carry same diffraction image. Then, the two beams with orthogonal polarization states (0° and 90°) will be combined into a final polarization state.

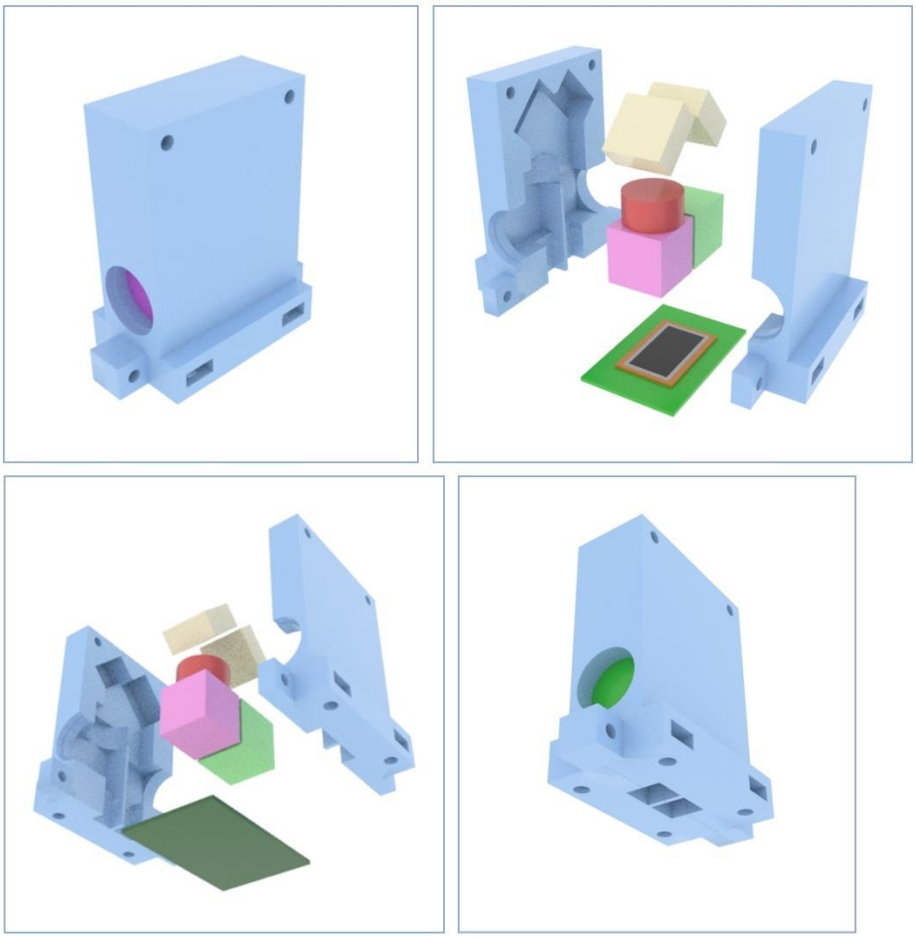

Figure 5.5 The practical 3D structure of the compact system from design software 3Dmax.The optical elements and LCOS SLM are also shown in the system. The pink and green cubes represent the two non-polarizing beam splitters. The red cylinder is the half-wave plate, and the two cream cuboids are the mirrors.

Based on the proposed principle, we design an integrated optical system to implement the polarization modulation. Figure 5.5 shows the proof-of-concept compact system. The LCOS SLM is fabricated by in-house developed die-level assembly techniques. The resolution of the LCOS device used in the experiment is 1920×1080. Two beam splitters (BS004) are used, which are the non-polarizing beam splitter cube with energy split ratio at 50:50. Two mirrors (BBSQ05-E02) with 0.5-inch ×0.5-inch is a broadband dielectric mirror with a working wavelength of 400-750 nm. A polymer zero-order half-wave plate (WPH05ME) with a

diameter of 0.5 inches is used to rotate the polarization angles of two separated light components. A linear polarizer (LPVISC050) with a diameter of 12.5 mm is used to create the input light with linear polarization at 45° for the system.

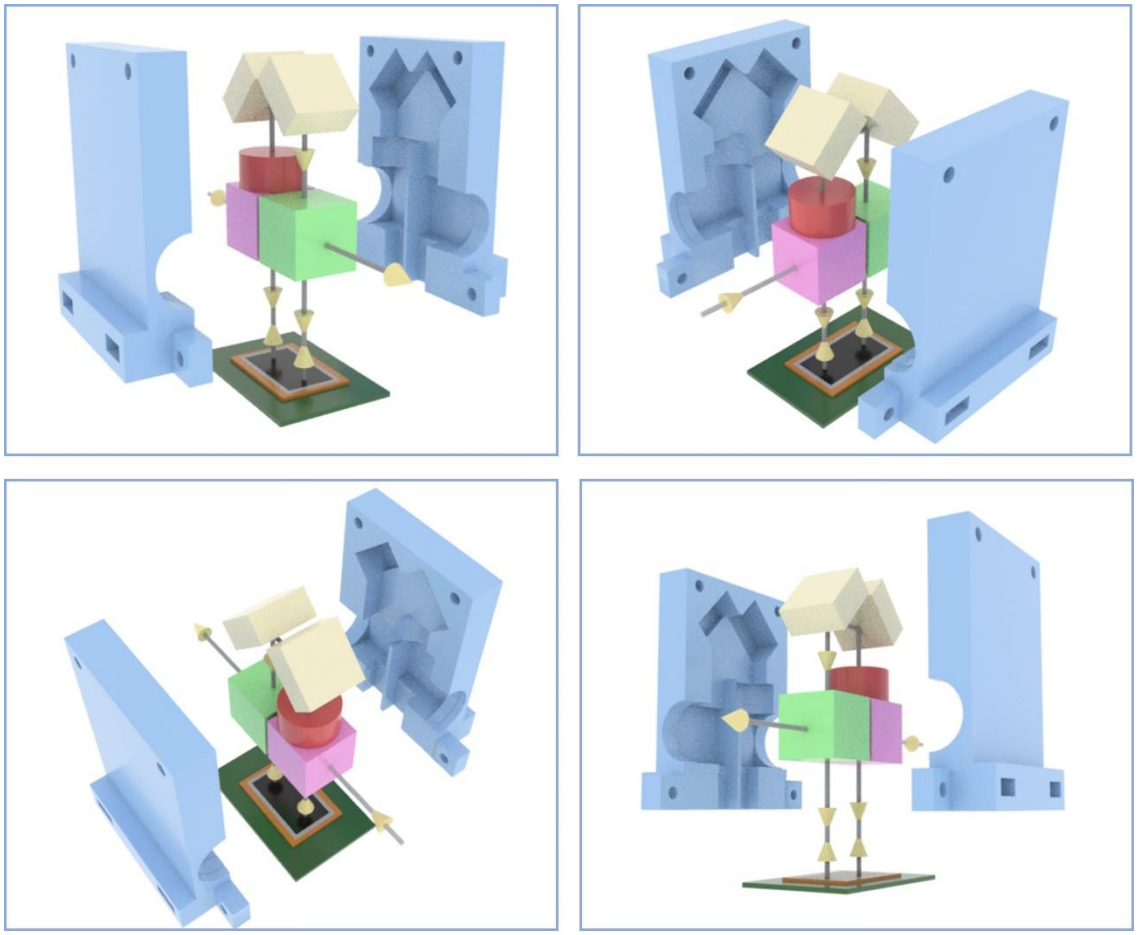

Figure 5.6 The optical path schematic of the compact system.

Figure 5.6 shows the optical path of the compact system. The input and output beams are parallel and in the same direction in the design to increase the employing flexibility of the system in a larger optical system. The input beam enters the system from the from the pink beam splitter, and the output beam exist from the green beam splitter. Because the LCOS SLM is in reflective mode, the incident beam is designed to be normal to the LCOS surface and be bounced back to the coming direction. The LCOS SLM is split into two independent

halves by loading two independently calculated CGHs. To avoid the input beam transmissive propagation through the beam splitter, an extra beam blocking film will be placed between two beam splitters.

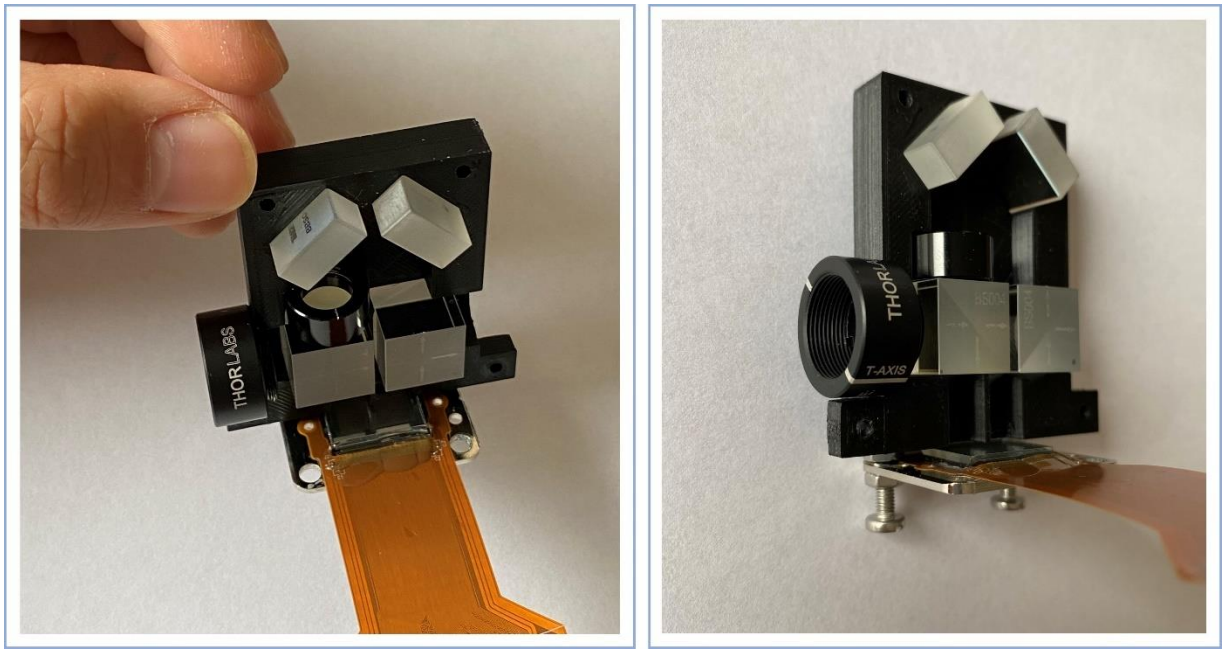

Figure 5.7 The prototype of the proposed compact system. All optical elements and LCOS SLM has been assembled, and the half of structure is removed to show the inside of the optical system.

Figure 5.7 is the prototype of the compact system when half of the frame is not assembled so that the optical elements in the system can be displayed. The structure of the compact system is designed using software 3Dmax and be fabricated by high precision 3D print (Ultimaker S5). The fabrication error is around 0.1mm after each making. To ensure high precision assembly of every optical element, the final version of compact system has been selected from five experimental versions. Figures 5.8 and 5.9 are the mechanical blueprints of the compact system's frame for high precision 3D print.

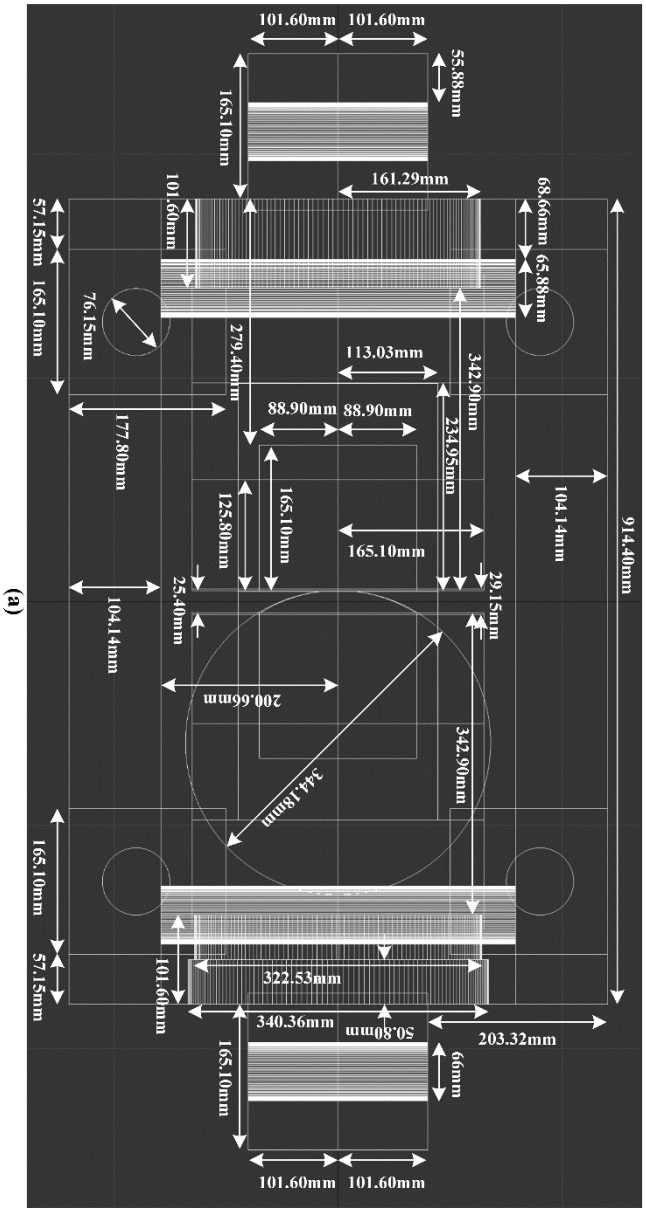

Figure 5.8 The mechanical size of the system structure: top view.

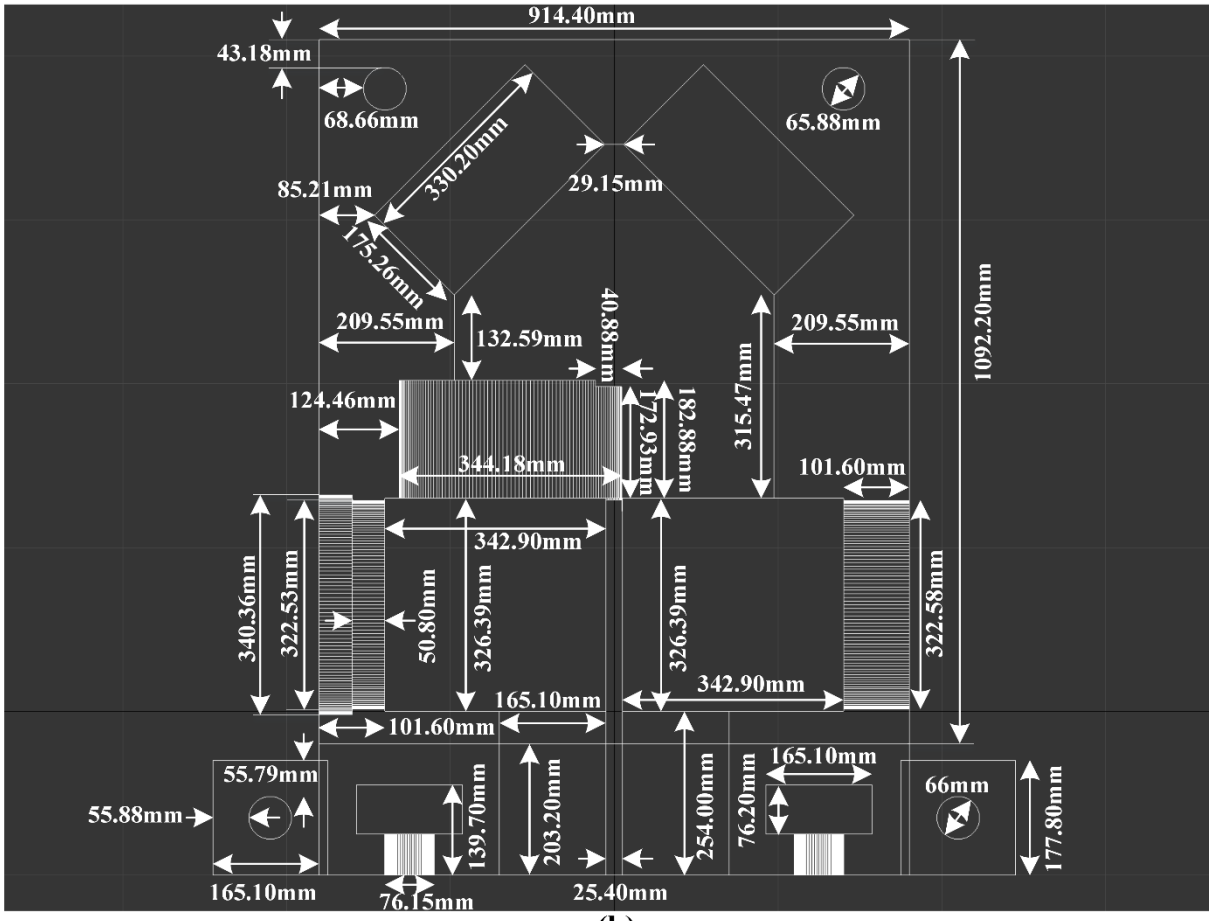

(b)

Figure 5.9 The mechanical size of the system structure: front view.

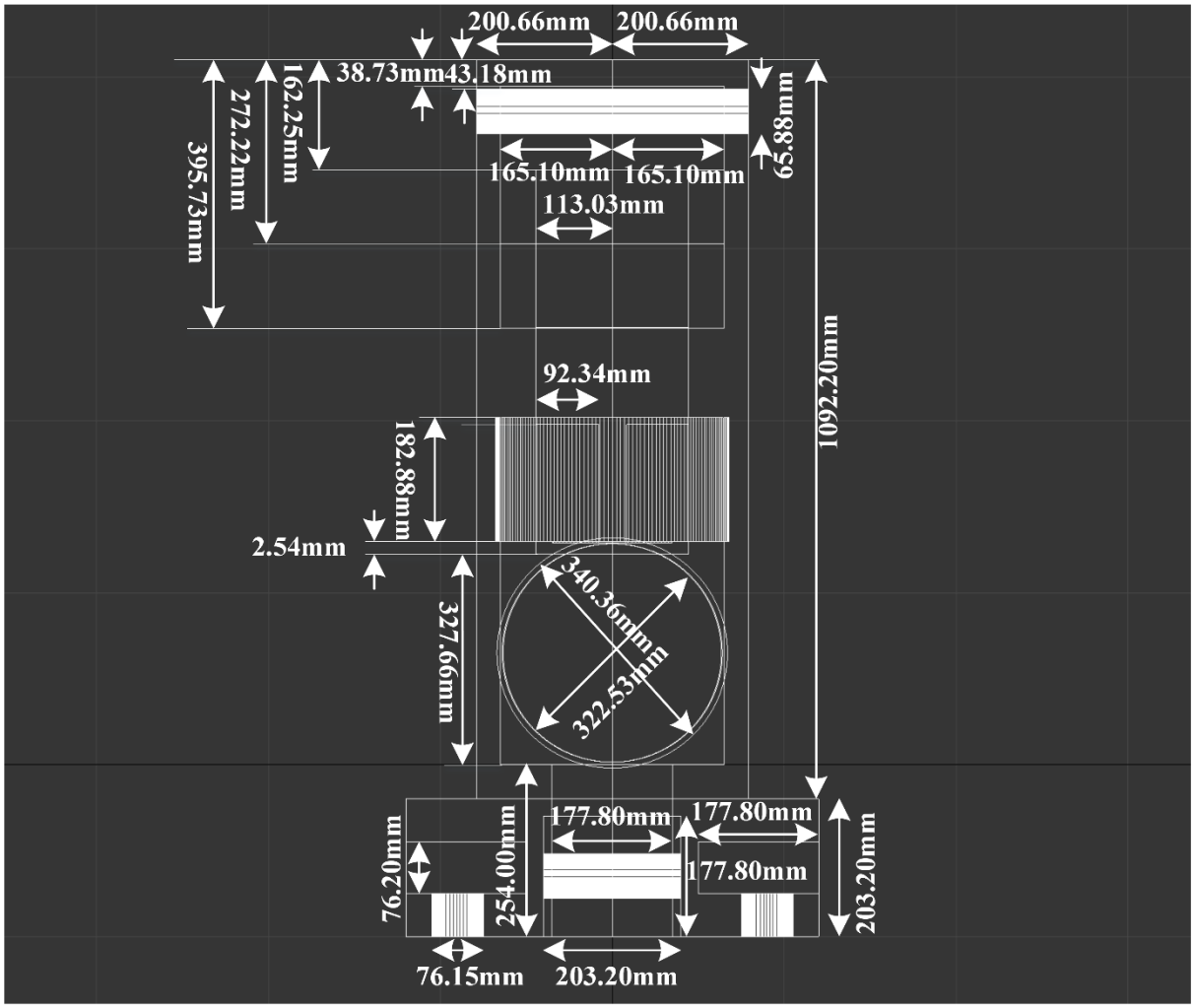

(c)

Figure 5.10 The mechanical size of the system structure: left view.

Moreover, the optical path alignment has been tested before and after the assembly of the LCOS SLM so that the two incidences on LCOS surface has been calibrated to be perpendicular. The angle input linear polarizer has been also calibrated to ensure that the input polarization has 45° to the working direction of LCOS SLM. Also, the angle of half-wave plate is calibrated to ensure that two polarization components has been both rotated 90° after passing through the wave plate.

5.3.2 Experimental results of holographic vectorial image

In this part, the experiment results of phase and polarization modulation using compact system has been shown. Due to the use of single LCOS, two CGHs with the same target image information and different amplitude information (according to the target polarization) has been independently calculated and put spliced to form one joint CGH. Each of sub-CGHs takes half of the active area of LCOS SLM.

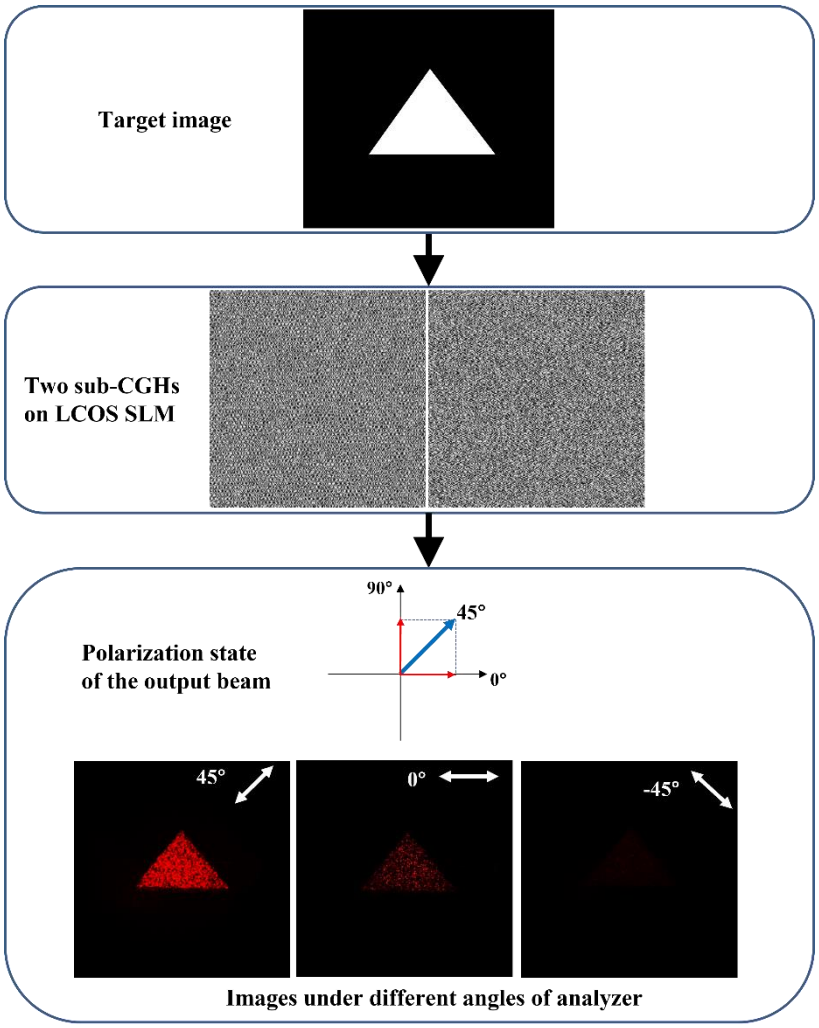

Figure 5.11 The images of output light field with target image (solid triangle) and target polarization state (45°).

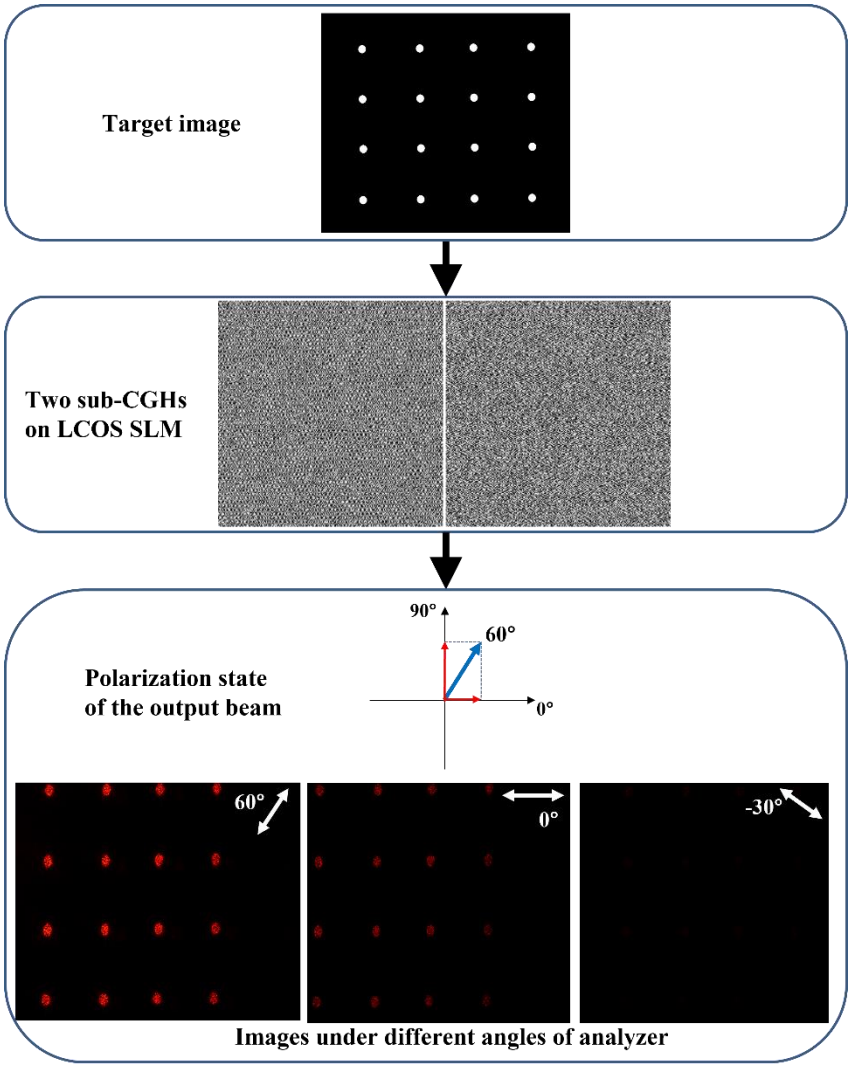

Figure 5.12 The images of output light field with target image (4x4 dot array) and target polarization state (60°).

Here, two experiment results are shown in Fig 5.11 and Fig 5.12. This means that the compact system can achieve the same performance in simultaneous phase and polarization modulation as the method of single beam coding. To provide high quality experimental results, the adjustment in optical elements position in the compact system is required. To acquire high accuracy polarization modulation, the calibration of half-wave plate angle to the LCOS SLM working direction is also needed.

5.4 Comparison of single beam coding and compact system

The phase and polarization modulation method proposed in the compact system is based on the principle of single beam coding method firstly introduced in last chapter. Thus, these two methods have similarity in many aspects. The major difference between two methods comes from the new design of polarization components rotation in compact system. Table 5.1 listed the similarity and difference of the two methods.

Table 5.1 **The comparison of single beam coding method and compact system in data storage application**

Methods	Phase modulation	Polarization modulation	Multi-polarization states writing	Delay	Output polarization states and image
Single beam coding	CGH	Sequential coding of two components	Glass motion free	SLM refresh rate (60~100Hz)	Customizable
Compact system	CGH	Sequential coding of two components	Glass motion free	SLM refresh rate (60~100Hz)	Customizable

The principle of phase and polarization modulation in both compact system and single beam coding are the same. In both methods, the object of phase-only modulation on LCOS SLMs is the two orthogonal polarization components of one single input beam. The holographic target image information and polarization components amplitude information are simultaneously encoded by computer-generated holograms. The target image information is calculated by GS algorithm, and the polarization components amplitude information is controlled by using different phase depth of holograms to manipulate the first-order diffraction efficiency. Therefore, like the single beam coding method, the proposed compact system can also provide the glass-motion-free data writing in optical data storage in glass. Moreover, the output target image and target polarization can be reconfigurable and dynamically altered at the speed of refresh rate of LCOS SLMs.

The fundamental difference between the compact system and the method single beam coding is at the use of two polarization components. In the method of single beam coding, two orthogonal polarization components are independently and sequentially modulated by two orthogonally placed LCOS SLMs. The working direction of two LCOS SLMs is aligned to their corresponding polarization component, respectively. This is because the directions of two polarization components of input beam are left unchanged in this method. However, in the compact system, only one LCOS SLM is used so that there is only one working direction (either horizontal or vertical) for information encoding. Therefore, in the compact system, the independent rotation of two polarization components' direction is introduced to adapt the single liquid crystal molecule direction. This optical rotation can effectively exchange the direction of two polarization components for sequential information encoding, and the rotation do not affect the coded holographic target image information and amplitude information on polarization components. Table 5.2 exhibits the further difference between two methods in terms of the utilization of LCOS SLM.

Table 5.2 **The further comparison of single beam coding method and compact system**

Methods	**Input beam size**	**SLM utilization for polarization modulation**	**Polarization components calibration**	**Polarization control resolution**
Single beam coding	SLM size	Two SLMs	Direction of two SLMs	15 degrees
Compact system	Half SLM size	Single SLM	Direction of single SLM	8 degrees

Due to the use of single LCOS SLM in compact system, the cost of the writing beam generation system is largely reduced. This is because the LCOS SLM devices (liquid crystal cell and driving system) take up the most hardware cost apart from femtosecond laser system in data writing. More importantly, the compact system method can also greatly simplify polarization direction calibration. Because the input light needs to be 45° to the working

direction of LCOS SLM, a precise polarization direction calibration is required. When only one LCOS SLM and one input beam are used, the direction calibration only needs to be conducted between one input beam and one LCOS SLM. However, in the previous method of single beam coding, when two LCOS SLMs and one input beam are used, the input beam needs to be at 45° for both LCOS devices at the same time. Therefore, the calibration process becomes more complicated in this situation. In the compact system, the maximum input beam size can be half of the active area of LCOS SLM due to the use of single LCOS device, thus, the total light intensity for phase and polarization modulation is reduced comparing with the single beam coding method.

The proposed compact system can provide higher resolution of polarization control comparing with single beam coding. This difference is also caused by the number of LCOS panels used in the system. In the method of single beam coding that uses two separate LCOS devices, the spatial positioning of two LCOS panels, especially the tilting angle between two LCOS surface, can result in error in the second phase modulation when we see the first panel as reference of flatness. However, when only one panel of LCOS is used, the spatial positioning issue became less. The two pairs of tilting and rotating angles of two independent panels have become one pair. The normal incident for two phase modulations in the compact system can be calibrate by using the reflective mirrors. As for the application of optical data storage, the resolution of the voxel's polarization angle reading is 4.7° [16], therefore, the current polarization control performed by the compact system can provide sufficient resolution (about 8°) for the use of data writing beam generation.

5.5 Zero-order elimination using holographic lens

When a Fourier CGH is displayed on a LCOS SLM, the incident light on the hologram will be modulated. Becuase the diffraction image would be formed in an infinite distance; the modulated light will need to pass through a converging lens so that the holographic image

can be obtained. In terms of laser writing, when we use CGH to generate the writing beam in voxel creating, the objective lens not only perform laser focusing but also plays the role of a Fourier lens. Therefore, the zero-order light component occurs in our voxel writing light field. Due to the limitation in LCOS devices fabrication, physical gaps between each pixel electrode exist. Thus, the liquid crystal molecules located in the gap area will not be controlled by the applied electric field. This means that the light that incident on the pixel gap will not be effectively modulated and will become a fixed light component arriving at the focal point of Fourier lens. This high energy zero-order light component will locate in the holographic image plane as shown in Figure 5.13 (a). In voxel writing process, the zero-order beam will be focused into the glass block causing damage and strong light scattering, which will significantly affect the quality of voxels.

Therefore, a method to efficiently remove the zero-order noises from the holographic image using a computer-generated holographic lens is proposed. Becasue the zero-order beam is the unaffected light component after modulation, this holographic lens will only change the image from hologram. Therefore, we can separate the focal planes of zero-order component and holographic image and steer the holographic image with designed angle to the optical axial. The proposed holographic lens can provide two types of zero-order elimination: on-axis and off-axis (Figure 5.13 (b) and (c)). The on-axis type can shift the zero-order focus from the holographic image in the optical axis direction. The off-axis design can allow the holographic image to deviate from the optical axis direction. With the use of a spatial filter, the zero-order-free holographic image can be obtained in its focal plane.

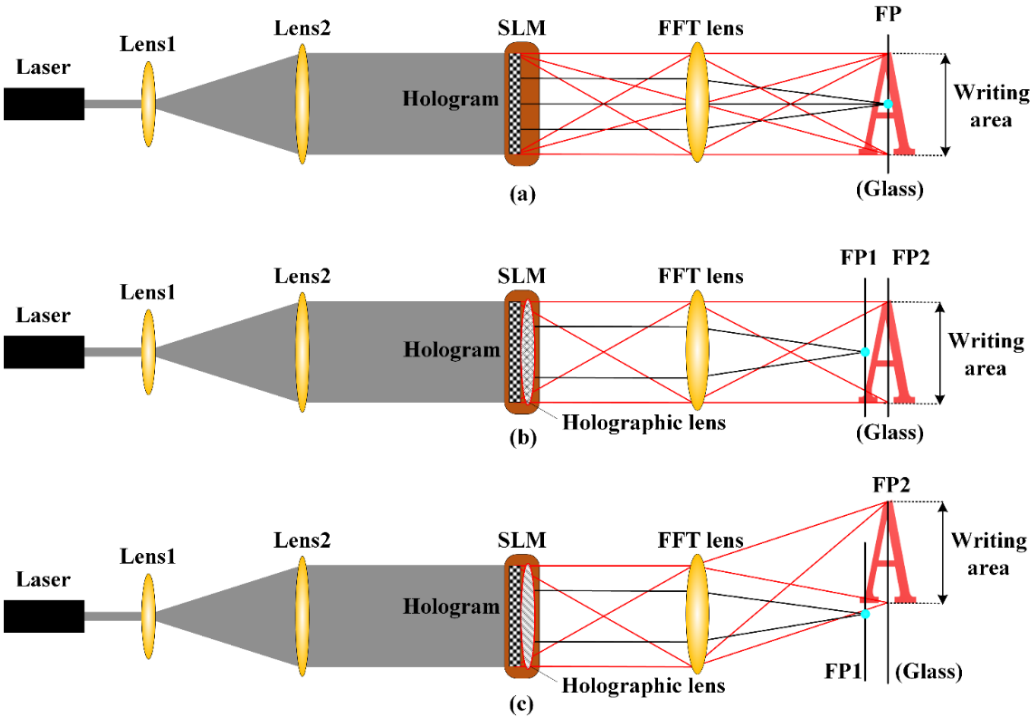

Figure 5.13 The normal holographic imaging with zero-order beam at its focal plane. (b), (c) The schematic of two types zero-order beam elimination using computer-generated holographic lens.

5.5.1 The principle of zero-order noise removal

In this work, the proposed holographic lens is a calculated holographic zone plate. The holographic zone plate can provide desired spatial focal position for arbitrary light wavelength and can be adaptively calculated for LCOS SLMs with different pixel number and size. When a zone plate is designed interferometrically, it will locate source points that constructively interfere at its focus [108,109]. This is accomplished by achieving a required phase difference at $2n\pi$ (n=1,2,3…) between a marginal and an axial ray [108,109]. The phase difference and optical path difference (OPD) have the relationship of $=2\pi$ OPD/λ, therefore, when the phase difference is set as 2π, the optical path differences can be written as

$$\sqrt{x^2 + y^2 + f^2} = \lambda \tag{5.11}$$

where x and y are the position coordinate on the LCOS SLM, and f is the designed focal length of the zone plate. λ is the wavelength of input light. As shown in Figure 5.14, when the input light is a plane wave, the optical path differences distribution on the zone plate plane will determine the phase value of different points on the holographic zone plate. Every pixel on zone plate will experience the phase shift corresponding to its own OPD when a focal length f is determined. Thus, to achieve all pixels having a fixed 2π phase shift at the focal point for constructively interfering, a specific phase value for light field at each pixel according to its spatial position is required. Therefore, the phase map δ_H of holographic lens with focal point at (x_0,y_0,f) can be written as

$$\delta_H = 2\pi \cdot (normalized \frac{\sqrt{(x-x_0)^2+(y-y_0)^2+f^2}}{\lambda}) \tag{5.12}$$

where x_0 and y_0 determine the position of focus on the focal plane.

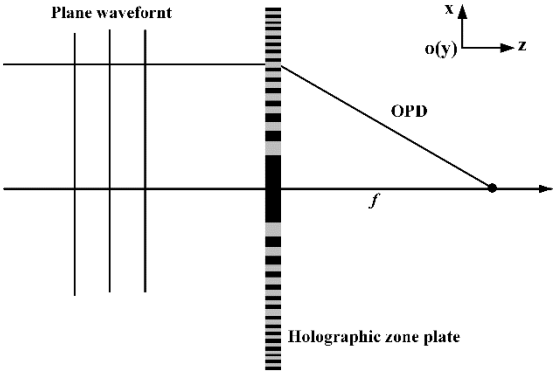

Figure 5.8 The principle of interferometric holographic zone plate calculation using optical path differences (OPD).

This holographic lens can be easily integrated into our target hologram as shown in Figure 5.15 (a). Figure 5.15 (b) shows an example when the off-axis parameters of the holographic lens are set the different values. We can observe this lens can steer the holographic image to deviate the principal optical axis located by the zero-order, which is helpful to remove the zero-order noise disturbance in the laser writing.

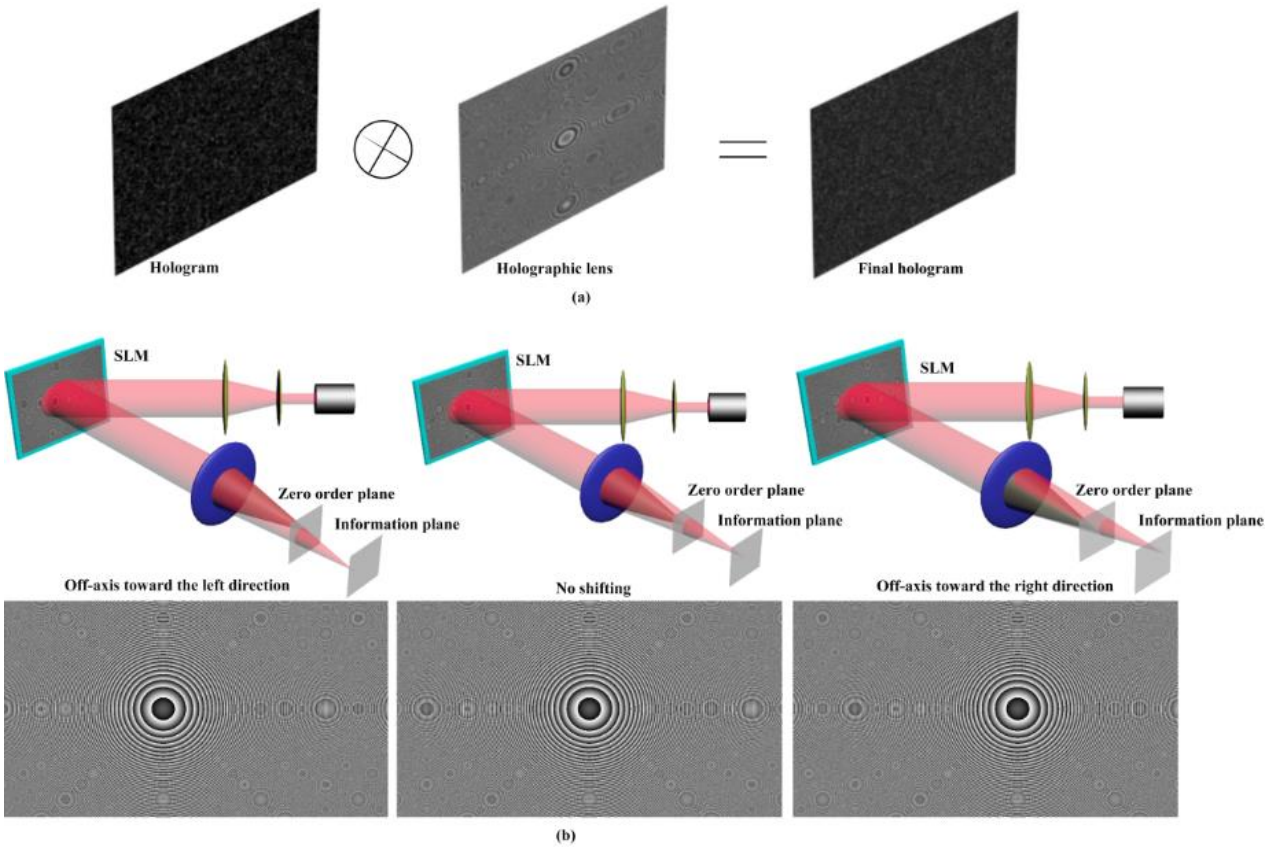

Figure 5.9 The principle of the hologram using a computed holographic lens, (b) the on-axis holographic lens and two examples of off-axis holographic lens providing left and right shift of image.

5.5.2 Experimental results

We used Zemax software to perform the simulation of the holographic lens. In the simulation model, we use a standard surface to simulate a hologram; a Fresnel lens is used to simulate a Fourier lens to control the light propagation. The green rays are the light of the zero-order beam, while blue rays indicate the light of the holographic image. The simulation results are shown in Figure 5.16. When the holographic lens is not applied on the target hologram, the zero-order beam and the holographic image are converged on the same plane (Figure 5.16 (a)). When a hologram lens without any off-axis shifting is in use, the zero-order and the

target image are converged on the different plane by controlling the focal length of the hologram lens (Figure 5.16 (b)). Accordingly, we can set the off-axis value of the hologram lens to make the zero-order and the holographic image travel along different axes (Figure 5.16 (c)-(d)). This simulation results showed that a hologram lens can effectively eliminate the zero-order beam on target image plane.

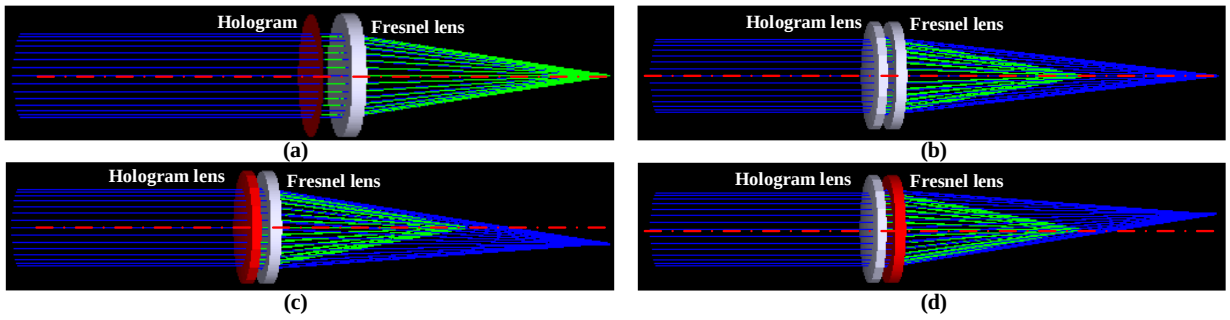

Figure 5.10 Simulation results using Zemax: (a) no hologram lens, (b) using hologram lens without the shifting, (c) shifting with 10mm, and (d) shifting with -10mm.

To verify the feasibility of our approach, we used our proof-of-concept setup (Figure 5.4) to perform the experiments of the displaying holographic images. An image of letters is used to be calculated by our CGH algorithm to generate a hologram and then be attached to a pre-calculated holographic lens. We used a CMOS camera to observe the holographic images. Figure 5.11 and Figure 5.12 show the experimental results of holographic images captured by our experimental camera.

When the image plane of the camera is set to the zero-order planes, we observed that the holographic image is in a defocused state while the zero-order beam is in focus (Figure 5.11 (a)). When the image plane of the camera is set to the holographic image planes, we observed that the holographic image is clear while the zero-order noise is in a defocused state (Figure 5.12 (b)). This means that the holographic lens successfully separates the zero-order beam away from the holographic image plane. Furthermore, the complete zero-order beam removal

can be simply done by blocking. Therefore, we place a spatial blocker at the zero-order planes to block the zero-order light when it has smallest beam size. This can minimize the loss of light information. This processing can be helpful to the laser writing beam generation without the influence of zero-order. Besides, this holographic lens based zero-order beam elimination method can be useful holographic display application, for example, the current Coarse Integral Hologram display systems [110-113].

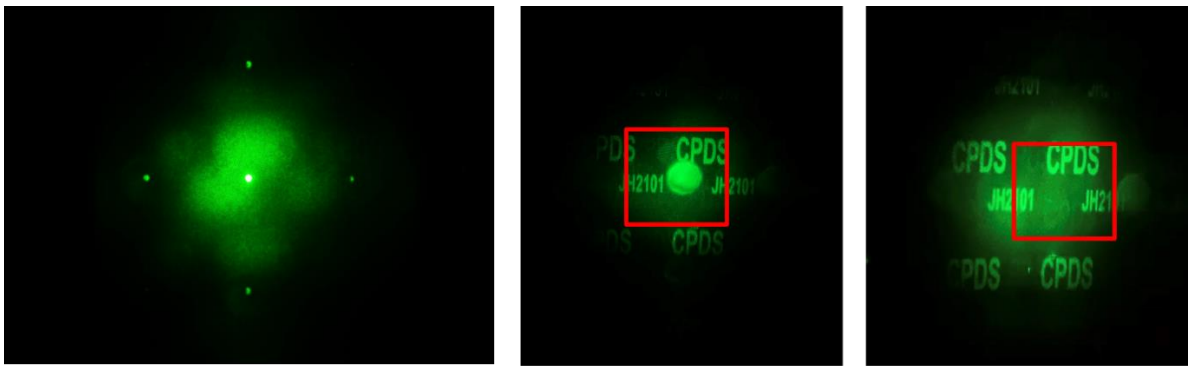

Figure 5.11 Experimental results of holographic image generation using holographic lens: (a) the image plane is located on the zero-order plane, (b) the image plane is located on the holographic image plane, and (c) the zero-order is removed using a spatial filter.

Moreover, we applied the off-axis value to the computed holographic lens in experiments. We used a dot pattern as the target image. Different holographic lenses with different off-axis values are attached to the same hologram. Consequently, multiple photos taken from the image plane are presented in Figure 5.12. By placing the CMOS plane at the zero-order focal plane after Fourier lens, we can observe the same results of a clear zero-order and defocused image (Figure 5.12 (a)). When dot pattern is sharp in images, the defocused zero-order spot can be observed. When the off-axis shift value of dot pattern is increased, we can see that the relative location of zero-order spot to the dot pattern is shifted to the right.

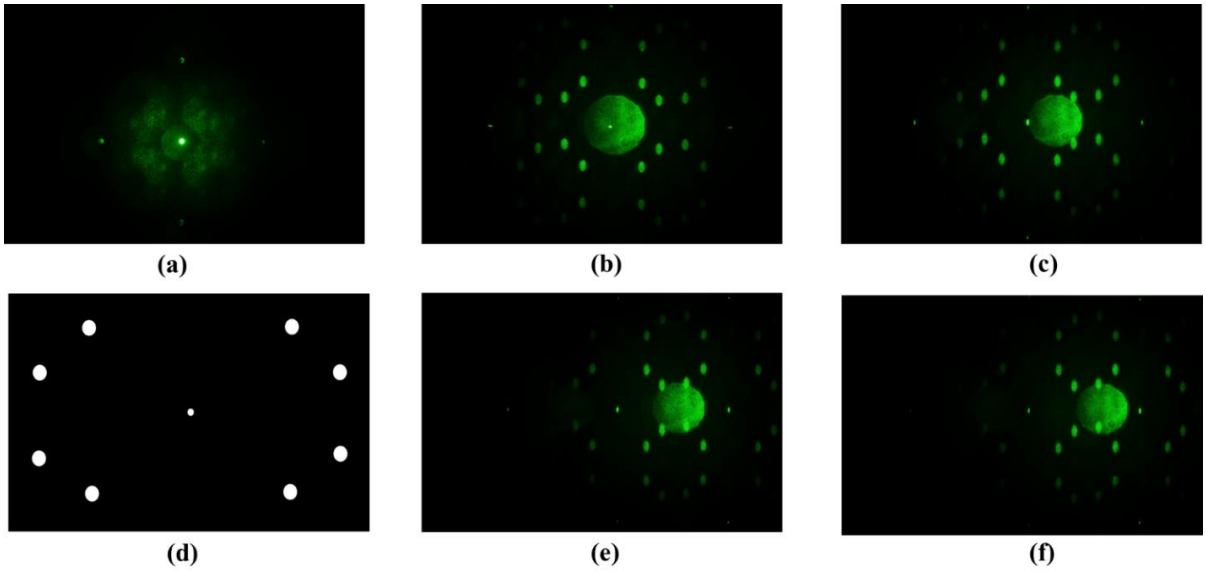

Figure 5.12 Generation results using the holographic lens with different off-axis value (a) at the zero-order plane and (b)-(e) the image plane; the defocused zero-order is set to the different position.

5.6 Conclusion

In this chapter, the compact system for simultaneous phase and polarization modulation has been proposed. To verify the effectiveness of the method, the compact system has been physically designed and fabricated by using high-precision 3D printing. The compact system of phase and polarization modulation can independently control the diffraction pattern of horizontal and vertical polarization light component. When we utilize this system to generate the desired polarization information for data writing in optical data storage using glass, the polarization state of output light field can be dynamically controlled by only changing the CGH on LCOS SLM without any external device.

To further improve the feasibility and flexibility of the compact system, the focus has been moved to the zero-order noise caused by the pixelated structure of LCOS devices. The zero-order noise can become a serious issue in optical data storage due to its very high intensity.

Therefore, to eliminate the zero-order noise from the target image, a method using a computed holographic lens adding to the target hologram with information has been proposed. Because of the use of CGHs on the LCOS device, the holographic lens that be superposed on the hologram will only affect diffractive light field, and it will not affect reflective light from the pixel array gap. Thus, the proposed method can split the focal plane of target image and zero-order beam.

Chapter 6

Conclusion and Future works

6.1 Conclusion

The purpose of this PhD research has been to build an innovative phase and polarization modulation approach that can provide simultaneous control of target holographic image and target linear polarization states that fulfils the requirements of 5D optical storages in Glass. The overview of this thesis work is summarized in Figure 6.1.

During the period achieving the goal, this research conducted a wide overview covering not just optical storages in general, but also phase and polarization modulation approaches. This overview work had been going on even before this thesis was written, to ensure that as much

related knowledge as possible was covered. Chapter 2 was written to provide an overview of our phase-only LCOS SLM technology, which is the core component in the experiment of Chapter 3 to 4. This aims not just to collate the overview works which have been done, but also help thesis readers to have a better understanding of the polarization modulation field. It is worth mentioning that the detailed overview for polarization modulation approaches was separated into three parts: polarization modulation using two parallel beams (Chapter 3), the polarization modulation using single beams (Chapter 4) and folded polarization modulation structure (Chapter 5).

Chapter 3 shows a polarization modulation approach based on the two optical vectors (two input beams) combining was developed, where their two base vectors are manipulated by two orthogonally polarization beams modulated by computer-generated holograms (CGHs) presented on two Liquid Crystal on Silicon Spatial light modulators (LCOS SLMs). The output linear vector beams created by the superposition of the two base beams. The output vector angle is controlled by combining two base vectors with independent depth of the phase-only CGHs, while the output holographic image is encoded by using the CGHs on both vector channels. In the Chapter 4, a method in this chapter only uses single beam as input beam to achieve target modulation is proposed. Like in chapter 3, the phase-only modulation performed by two LCOS SLMs are used to encode holographic image information and amplitude information, while the object of modulation are two orthogonal light components, instead of two independent beams. By using the polarization sensitivity of LCOS SLM, two components of a single beam can be independently modulated. Because the status of single beam is not affected by the modulation, the formation of output light field is simply achieved by using a converging lens to reconstruct the image on its focal plane. Furthermore, in the Chapter 5, a compact dynamic polarization-modulation system using LCOS-SLM is designed and developed. The new method uses two cascade-connected CGHs that presented on single LCOS-SLM in conjunction with a half-wave plate to create the modulation of multiple linear polarization states and simultaneously allowing the implementation of the holographic image generation. Moreover, to further improve the feasibility and flexibility of the compact system,

we also developed a zero-order suppression method based on a computed holographic lens capable of on-axis and off-axis controlling for the compact system to improve the quality of data writing light field.

The results confirmed that the proposed method is capable of dynamical generation of arbitrary holographic target image with desired polarization state. This makes it possible to write all voxels with the same polarization direction on a data page at the same time. For example, when there are 8 different polarization angles of voxels on a data page in glass, only 8 writing cycles are needed to finish the whole data page writing instead of sequentially writing all voxels. This makes it possible to have fewer movements of a glass sample in a data writing process task. It provides a valuable mean to significantly decrease the mechanical delay that is caused by the glass sample platform movement. The mechanical delay takes up a major part in time duration of current sequential writing method. Therefore, we can say that this method can largely increase the data writing speed and make this data storage technology more feasible for future cloud.

This successful development also suggests several avenues for potential future research.

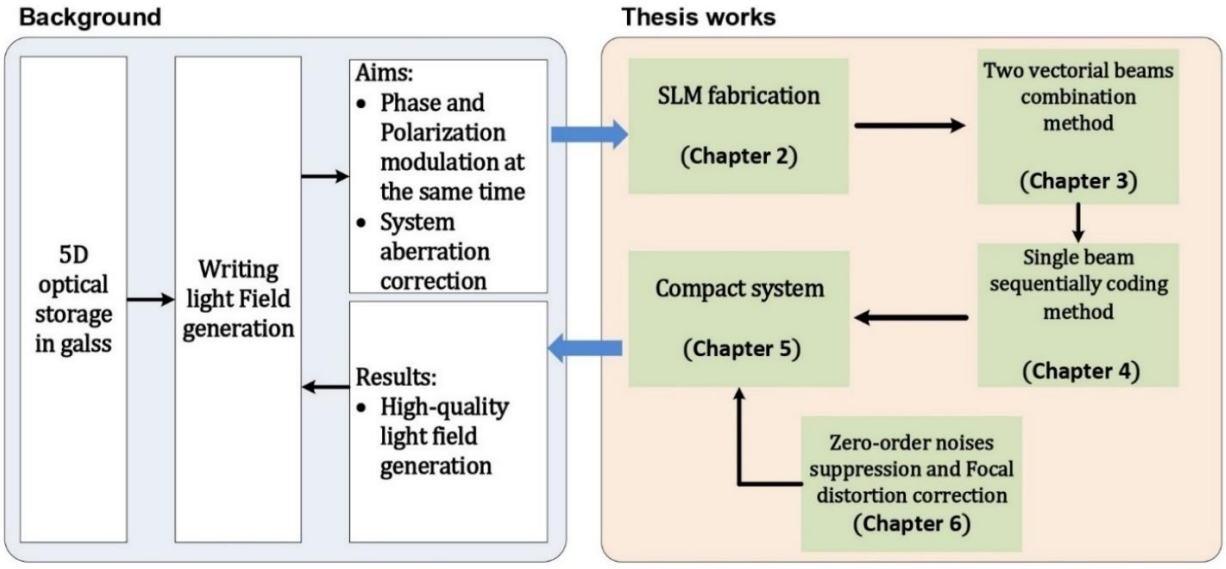

Figure 6.1 Summary of this work involving five Chapters.

6.2 Future works

Future works can be separated into three main parts: the SLM, the computational system, and the optical system.

6.2.1 High-quality spatial Light Modulators

The high-quality polarization beam generation heavily depends on the SLM performance. To develop a high quality SLM, there are possible research direction for the high-quality polarization beam generation in 5D optical storage in Glass. First, the phase response (i.e., phase flicker) of the LCOS device needs to be stable in the systems operating on holographic polarization modulation systems. Holography relies on accurate representation of the phase information at any given time to reconstruct the intended light field. In other words, the phase information cannot be averaged with a root mean square (RMS) value. Therefore, the phase flicker of the LCOS device needs to be suppressed to an acceptable level. Second, current SLM-based polarization modulation systems used for the field of 5D optical storage in Glass mainly adopts a 8-bit mode. A 10-bit or higher will be significantly resolution phase level that is helpful to the polarization modulation system.

6.2.2 High-quality generation of hologram

In the current polarization modulation system, a computational holographic lens is used to calculate hologram to remove the zero order noises. To further improve this algorithm performance, a potential approach is to perform an iterative loop calculation involving the actual SLM for each layer calculation. Different from the other holographic systems, the hologram-based polarization modulation is not observed by human visual system. The more iterative loop number would contribute to the holographic image quality, but the

computational overhead will be increased. Two helpful methods can be considered. Firstly, the system should adopt the dedicated field-programmable gate array (FPGA) which allows for a customized circuit to further optimize performance. The second is to design an integration system which can integrate multiple computer units, such as FPGA chips or GPUs, which could make computational power scalable for holography calculations. With these three improvements, calculation speeds might possibly be improved to the level of 10 G pixel/sec. By utilizing the ultrafast generation platform, the imaging quality can be significantly improved for the high-quality polarization beam generation.

6.2.3 Optical Configuration with minimal optical aberrations

The optical aberrations of the polarization modulation system also influence the quality of the beam generation. To obtain the minimal optical aberrations, an efficient approach is to design an integration system capable of polarization combination in a chip planar structure. Also important is the system calibration because this system requires the strict assembly accuracy. A potential approach is to design a self-collimated calibration to calibrate the whole system. Overall, many engineering challenges remain and structural research is needed to further improve the performance of the current prototype. These improvements will include the SLM technology, the hologram generation algorithm, and the optics configuration.

6.2.4 Optical storage system design

A clear factor that influences the designing of a storage system based on this technology is: Cloud-first. As the designing is for the cloud use priority, there are no factors or physical constraints from application outside cloud (such as mobile devices, homes, or offices). And Cloud storage systems need to find the balance between performance and low cost, because these storage infrastructures will need to store multiple zettabytes of data in the future.

Storage system using glass can make the balance between low cost, low access latency and high workloads efficiency. Besides, considering the two of fundamental limitations of storage systems (Entanglement and split workloads) mentioned above, how much change a storage system using glass can make will be discussed.

References

[1] IDC. (2017). Data age 2025. https://www.seagate.com/our-story/data-age-2025/.

[2] Gu, M., Li, X., & Cao, Y. (2014). Optical storage arrays: a perspective for future big data storage. Light: Science & Applications, 3(5), e177-e177.

[3]Gan, F., & Wang, Y. (2015). Data Storage at the Nanoscale: Advances and Applications, 740. Taylor &Francis Group, LLC.

[4]Zhang, J., Čerkauskaitė, A., Drevinskas, R., Patel, A., Beresna, M., & Kazansky, P. G. (2016, March). Eternal 5D data storage by ultrafast laser writing in glass. In Laser-based Micro-and Nanoprocessing X (Vol. 9736, p. 97360U). International Society for Optics and Photonics.

[5]Anderson, P., Black, R., Cerkauskaite, A., Chatzieleftheriou, A., Clegg, J., Dainty, C., ... & Yang, M. (2018). Glass: A new media for a new era?. In 10th {USENIX} Workshop on Hot Topics in Storage and File Systems (HotStorage 18).

[6] Pinheiro, E., Weber, W. D., & Barroso, L. A. (2007). Failure trends in a large disk drive population. In Proceedings of the 5th USENIX Conference on File and Storage Technologies (2007), FAST '07, USENIX Association.

[7] Schroeder, B., & Gibson, G. A. (2006). Disk Failures in the Real World: What Does an MTTF of 1,000,000 Hours Mean to You?(CMU-PDL-06-111). In Proceedings of the 5th USENIX Conference on File and Storage Technologies (Berkeley, CA, USA, 2007), FAST '07, USENIX Association.

[8]Wood, R., Williams, M., Kavcic, A., & Miles, J. (2009). The feasibility of magnetic recording at 10 terabits per square inch on conventional media. IEEE Transactions on Magnetics, 45(2), 917-923.

[9] SEAGATE. Hamr technology. https://www.seagate.com/www-content/ti-dm/tech-insights/en- us/docs/TP707-1-1712US_HAMR.pdf, 2017.

[10] DIGITAL, W. Western digital unveils next-generation technology to preserve and access the next decade of big data. https://www.wdc.com/about-wd/newsroom/press- room/2017-10-11-western-digital-unveils-next- generation-technology-to-preserve-and-access-the-next-decade-of-big-data.html, 2017.

[11] Zhu, J. G., & Wang, Y. (2010). Microwave assisted magnetic recording utilizing perpendicular spin torque oscillator with switchable perpendicular electrodes. IEEE Transactions on Magnetics, 46(3), 751-757.

[12] Zhu, J. G., Zhu, X., & Tang, Y. (2007). Microwave assisted magnetic recording. IEEE Transactions on Magnetics, 44(1), 125-131.

[13]Brewer, E., Ying, L., Greenfield, L., Cypher, R., & T'so, T. (2016). Disks for data centers. Tech. rep., Google, 2016.

[14]Curtis, K., Dhar, L., Hill, A., Wilson, W., & Ayres, M. (2010). Holographic data storage: from theory to practical systems. John Wiley and Sons, Wiley Publishing.

[15]Grawinkel, M., Nagel, L., Mäsker, M., Padua, F., Brinkmann, A., & Sorth, L. (2015). Analysis of the {ECMWF} Storage Landscape. In 13th {USENIX} Conference on File and Storage Technologies ({FAST} 15) (pp. 15-27).

[16]Shimotsuma, Y., Sakakura, M., Kazansky, P. G., Beresna, M., Qiu, J., Miura, K., & Hirao, K. (2010). Ultrafast manipulation of self-assembled form birefringence in glass. Advanced materials, 22(36), 4039-4043.

[17] Zhang, J., Gecevičius, M., Beresna, M., & Kazansky, P. G. (2014). Seemingly unlimited lifetime data storage in nanostructured glass. Physical review letters, 112(3), 033901.

[18] Kazansky, P., Cerkauskaite, A., Beresna, M., Drevinskas, R., Patel, A., Zhang, J., & Gecevicius, M. (2016). Eternal 5D data storage via ultrafast-laser writing in glass. SPIE Newsroom, 11.

[19]Taylor, R. S., Hnatovsky, C., Simova, E., Rajeev, P. P., Rayner, D. M., & Corkum, P. B. (2007). Femtosecond laser erasing and rewriting of self-organized planar nanocracks in fused silica glass. Optics Letters, 32(19), 2888-2890.

[20] Glezer, E. N., Milosavljevic, M., Huang, L., Finlay, R. J., Her, T. H., Callan, J. P., & Mazur, E. (1996). Three-dimensional optical storage inside transparent materials. Optics letters, 21(24), 2023-2025.

[21] Richter, S., Miese, C., Döring, S., Zimmermann, F., Withford, M. J., Tünnermann, A., & Nolte, S. (2013). Laser induced nanogratings beyond fused silica-periodic nanostructures in borosilicate glasses and ULE™. Optical Materials Express, 3(8), 1161-1166.

[22] Yang, W., Kazansky, P. G., & Svirko, Y. P. (2008). Non-reciprocal ultrafast laser writing. Nature Photonics, 2(2), 99-104.

[23] Gecevičius, M., Beresna, M., Zhang, J., Yang, W., Takebe, H., & Kazansky, P. G. (2013). Extraordinary anisotropy of ultrafast laser writing in glass. Optics express, 21(4), 3959-3968.

[24] Kazansky, P. G., Shimotsuma, Y., Sakakura, M., Beresna, M., Gecevičius, M., Svirko, Y., ... & Hirao, K. (2011). Photosensitivity control of an isotropic medium through polarization of light pulses with tilted intensity front. Optics express, 19(21), 20657-20664.

[25] Karpathy, A., Toderici, G., Shetty, S., Leung, T., Sukthankar, R., & Fei-Fei, L. (2014). Large-scale video classification with convolutional neural networks. In Proceedings of the IEEE conference on Computer Vision and Pattern Recognition (pp. 1725-1732).

[26] Krizhevsky, A., Sutskever, I., & Hinton, G. E. (2012). Imagenet classification with deep convolutional neural networks. Advances in neural information processing systems, 25, 1097-1105.

[27]Shribak, M., & Oldenbourg, R. (2003). Techniques for fast and sensitive measurements of two-dimensional birefringence distributions. Applied Optics, 42(16), 3009-3017.

[28]Shimotsuma, Y., Sakakura, M., Kazansky, P. G., Beresna, M., Qiu, J., Miura, K., & Hirao, K. (2010). Ultrafast manipulation of self‐assembled form birefringence in glass. Advanced materials, 22(36), 4039-4043.

[29] J. D. Kalen , R. S. Boyce , J. D. Cawley , J. Am. Ceram. Soc. 1991 , 74 ,203 . Kalen, J. D., Boyce, R. S., & Cawley, J. D. (1991). Oxygen tracer diffusion in vitreous silica. Journal of the American Ceramic Society, 74(1), 203-209.

[30] Allegre, O. J., Jin, Y., Perrie, W., Ouyang, J., Fearon, E., Edwardson, S. P., & Dearden, G. (2013). Complete wavefront and polarization control for ultrashort-pulse laser microprocessing. Optics express, 21(18), 21198-21207.

[31]Jin, Y., Allegre, O. J., Perrie, W., Abrams, K., Ouyang, J., Fearon, E., ... & Dearden, G. (2013). Dynamic modulation of spatially structured polarization fields for real-time control of ultrafast laser-material interactions. Optics express, 21(21), 25333-25343.

[32]Allegre, O. J., Perrie, W., Edwardson, S. P., Dearden, G., & Watkins, K. G. (2012). Laser microprocessing of steel with radially and azimuthally polarized femtosecond vortex pulses. Journal of Optics, 14(8), 085601.

[33]Lam, B., Zhang, J., & Guo, C. (2017). Generation of continuously rotating polarization by combining cross-polarizations and its application in surface structuring. Optics letters, 42(15), 2870-2873.

[34]Hasegawa, S., & Hayasaki, Y. (2014). Holographic vector wave femtosecond laser processing. International Journal of Optomechatronics, 8(2), 73-88.

[35]Ono, H., Matsumoto, T., Sasaki, T., Noda, K., Takahashi, R., Nishioka, E., & Kawatsuki, N. (2012). Intensity and polarization modulation holographic recordings and vector holograms using inhomogeneous polarized beams. Japanese Journal of Applied Physics, 51(8R), 082501.

[36]Kazansky, P., Lei, Y., Wang, L., Yu, Y., Wang, H., & Sarao, B. (2020). Virtually eternal 5D data storage in quartz glass. In ASCEND 2020 (p. 4044).

[37]Kazansky, P. G., Cerkauskaite, A., Drevinskas, R., & Zhang, J. (2016, November). Eternal 5D optical data storage in glass (Conference Presentation). In Optical Data Storage 2016 (Vol. 9959, p. 99590D). International Society for Optics and Photonics.

[38]Zhang, J., Gecevičius, M., Beresna, M., & Kazansky, P. G. (2013, June). 5D data storage by ultrafast laser nanostructuring in glass. In CLEO: Science and Innovations (pp. CTh5D-9). Optical Society of America.

[39]Ohfuchi, T., Sakakura, M., Yamada, Y., Fukuda, N., Takiya, T., Shimotsuma, Y., & Miura, K. (2017). Polarization imaging camera with a waveplate array fabricated with a femtosecond laser inside silica glass. Optics express, 25(20), 23738-23754.

[40]Hill, C. A., Beckman, S., Chinone, Y., Goeckner-Wald, N., Hazumi, M., Keating, B., ... & Takakura, S. (2016, July). Design and development of an ambient-temperature continuously-rotating achromatic half-wave plate for CMB polarization modulation on the POLARBEAR-2 experiment. In Millimeter, Submillimeter, and Far-Infrared Detectors and Instrumentation for Astronomy VIII (Vol. 9914, p. 99142U). International Society for Optics and Photonics.

[41]Peña, A., & Andersen, M. F. (2018). Complete polarization and phase control with a single spatial light modulator for the generation of complex light fields. Laser Physics, 28(7), 076201.

[42]Moreno, I., Davis, J. A., Hernandez, T. M., Cottrell, D. M., & Sand, D. (2012). Complete polarization control of light from a liquid crystal spatial light modulator. Optics Express, 20(1), 364-376.

[43]Rosales-Guzmán, C., Bhebhe, N., & Forbes, A. (2017). Simultaneous generation of multiple vector beams on a single SLM. Optics express, 25(21), 25697-25706.

[44]Serrano-Trujillo, A., Palafox, L. E., & Ruiz-Cortés, V. (2017). Engineering of cylindrical vector fields with a twisted nematic spatial light modulator. Applied Optics, 56(5), 1310-1316.

[45]Zheng, X., Lizana, A., Peinado, A., Ramírez, C., Martínez, J. L., Márquez, A., ... & Campos, J. (2015). Compact lcos–slm based polarization pattern beam generator. Journal of Lightwave Technology, 33(10), 2047-2055.

[46]Otte, E., Schlickriede, C., Alpmann, C., & Denz, C. (2015, March). Complex light fields enter a new dimension: holographic modulation of polarization in addition to amplitude and phase. In Complex Light and Optical Forces IX (Vol. 9379, p. 937908). International Society for Optics and Photonics.

[47]Waller, E. H., & von Freymann, G. (2013). Independent spatial intensity, phase and polarization distributions. Optics express, 21(23), 28167-28174.

[48]Chen, Z., Zeng, T., Qian, B., & Ding, J. (2015). Complete shaping of optical vector beams. Optics express, 23(14), 17701-17710.

[49]García-Martínez, P., Marco, D., Martínez-Fuentes, J. L., del Mar Sánchez-López, M., & Moreno, I. (2020). Efficient on-axis SLM engineering of optical vector modes. Optics and Lasers in Engineering, 125, 105859.

[50]Kenny, F., Lara, D., Rodríguez-Herrera, O. G., & Dainty, C. (2012). Complete polarization and phase control for focus-shaping in high-NA microscopy. Optics express, 20(13), 14015-14029.

[51] Li, R., Peng, T., Zhou, M., Yu, X., Min, J., Yang, Y., & Yao, B. (2020). Full-polarization wavefront shaping for imaging through scattering media. Applied Optics, 59(17), 5131-5135.

[52]Fu, S., Gao, C., Wang, T., Zhai, Y., & Yin, C. (2018). Anisotropic polarization modulation for the production of arbitrary Poincaré beams. JOSA B, 35(1), 1-7.

[53]Chen, X., Liu, S., Lin, Z., Chen, Z., & Pu, J. (2018). Dual-cavity digital laser for intra-cavity mode shaping and polarization control. Optics express, 26(14), 18182-18189.

[54]Roider, C., Jesacher, A., Bernet, S., & Ritsch-Marte, M. (2014). Axial super-localisation using rotating point spread functions shaped by polarisation-dependent phase modulation. Optics express, 22(4), 4029-4037.

[55]Zhao, T., & Chi, Y. (2020). Modified Gerchberg–Saxton (GS) Algorithm and Its Application. Entropy, 22(12), 1354.

[56]Zalevsky, Z., Mendlovic, D., & Dorsch, R. G. (1996). Gerchberg–Saxton algorithm applied in the fractional Fourier or the Fresnel domain. Optics Letters, 21(12), 842-844.

[57]Sun, P., Chang, S., Liu, S., Tao, X., Wang, C., & Zheng, Z. (2018). Holographic near-eye display system based on double-convergence light Gerchberg-Saxton algorithm. Optics express, 26(8), 10140-10151.

[58]Salter, P. S., & Booth, M. J. (2019). Adaptive optics in laser processing. Light: Science & Applications, 8(1), 1-16.

[59]Tong, Y., Pivnenko, M., & Chu, D. (2020). Implementation of 10-Bit Phase Modulation for Phase-Only LCOS Devices Using Deep Learning.

[60]Tong, Y., Pivnenko, M., & Chu, D. (2019). Improvements of phase linearity and phase flicker of phase-only LCoS devices for holographic applications. Applied optics, 58(34), G248-G255.

[61]Thalhammer, G., Bowman, R. W., Love, G. D., Padgett, M. J., & Ritsch-Marte, M. (2013). Speeding up liquid crystal SLMs using overdrive with phase change reduction. Optics express, 21(2), 1779-1797.

[62]Zhang, Z., You, Z., & Chu, D. (2014). Fundamentals of phase-only liquid crystal on silicon (LCOS) devices. Light: Science & Applications, 3(10), e213-e213.

[63]Dhar, L., Curtis, K., & Fäcke, T. (2008). Coming of age. Nature photonics, 2(7), 403-405.

[64]Bahadur, B. (Ed.). (1990). Liquid Crystal-Applications And Uses (Volume 1) (Vol. 1). World scientific.

[65]Schiekel, M. F., & Fahrenschon, K. (1971). Deformation of nematic liquid crystals with vertical orientation in electrical fields. Applied Physics Letters, 19(10), 391-393.

[66]Schadt, M. (1997). Liquid crystal materials and liquid crystal displays. Annual review of materials science, 27(1), 305-379.

[67]Efron, U. (Ed.). (1994). Spatial light modulator technology: materials, devices, and applications (Vol. 47). CRC press.

[68]Blinov, L. M. (2010). Structure and properties of liquid crystals (Vol. 123). Springer Science & Business Media.

[69]Shurcliff, W.A. (1982) Polarized Light: Production and Use, Harvard University Press.

[70]Robinson, M. D., Sharp, G., & Chen, J. (2005). Polarization engineering for LCD projection (Vol. 4). John Wiley & Sons.

[71]Lazarev, G., Hermerschmidt, A., Krüger, S., & Osten, S. (2012). LCOS spatial light modulators: trends and applications. Optical Imaging and Metrology: Advanced Technologies, 1-29.

[72]Wu S. T., Yang D. K. (2006) Fundamentals of Liquid Crystal Devices. New York: John Wiley & Sons.

[73] Underwood I., (1987). An CMOS addressed liquid crystal spatial light modulator, PhD thesis, University of Edinburgh.

[74]Soref, R. A., & Rafuse, M. J. (1972). Electrically controlled birefringence of thin nematic films. Journal of Applied Physics, 43(5), 2029-2037.

[75]Labrunie, G., & Robert, J. (1973). Transient behavior of the electrically controlled birefringence in a nematic liquid crystal. Journal of Applied Physics, 44(11), 4869-4874.

[76]Bos, P. J., & Koehler/Beran, K. R. (1984). The pi-cell: a fast liquid-crystal optical-switching device. Molecular Crystals and Liquid Crystals, 113(1), 329-339.

[77] Fergason, J. (1973). Display Devices Utilizing Liquid Crystal Light Modulation. U.S. Patent No. 3,731,986. Washington, DC: U.S. Patent and Trademark Office.

[78]Khoo, I. C., & Wu, S. T. (1993). Optics and nonlinear optics of liquid crystals (Vol. 1). World Scientific Lublishing Co. Pte. Ltd, London.

[79]Zhang, Z. (2012). Phase-only nematic liquid crystal on silicon devices (Doctoral dissertation, University of Cambridge).

[80]Yang, D. K., & Wu, S. T. (2014). Fundamentals of liquid crystal devices. John Wiley & Sons.

[81]Raynes, E. P. (1975). Optically active additives in twisted nematic devices. Revue de Physique Appliquee, 10(3), 117-120.

[82]Wu S.T., Yang D. K. (2006). Reflective Liquid Crystal Display. Wiley & Sons Ltd, The Atrium, Southern Gate, Chichester, West Sussex PO19 8SQ, England.

[83]Chigrinov, V. G. (1999). Liquid crystal devices: physics and applications. Artech-House, Boston-London

[84]García-Márquez, J., López, V., González-Vega, A., & Noé, E. (2012). Flicker minimization in an LCoS spatial light modulator. Optics express, 20(8), 8431-8441.

[85]De Smet, H., Van den Steen, J., & Colson, P. M. (2002, April). Use of stitching in microdisplay fabrication. In Projection Displays VIII (Vol. 4657, pp. 23-30). International Society for Optics and Photonics.

[86]Lu, M. (2002). Nematic liquid‐crystal technology for Si wafer‐based reflective spatial light modulators. Journal of the Society for Information Display, 10(1), 37-47.

[87]Zhang, Z., Jeziorska-Chapman, A. M., Collings, N., Pivnenko, M., Moore, J., Milne, W. I., ... & Chu, D. P. (2010, February). High quality assembly of liquid crystal on silicon (LCOS) devices for phase-only holography. In Emerging Liquid Crystal Technologies V (Vol. 7618, p. 761815). International Society for Optics and Photonics.

[88]Kazlas, P. T., Johnson, K. M., & McKnight, D. J. (1998). Miniature liquid-crystal-on-silicon display assembly. Optics letters, 23(12), 972-974.

[89]Zhang, Z., Pivnenko, M., Medina-Salazar, I., You, Z., & Chu, D. (2016). Advanced die-level assembly techniques and quality analysis for phase-only liquid crystal on silicon devices. Proceedings of the Institution of Mechanical Engineers, Part B: Journal of Engineering Manufacture, 230(9), 1659-1664.

[90]Banks, L., Birch, M., Krueerke, D., Buckley, E., Cable, A., Lawrence, N., & Mash, P. (2006, June). 73.4: Real‐time Diffractive Video Projector Employing Ferroelectric LCOS SLM. In SID Symposium Digest of Technical Papers (Vol. 37, No. 1, pp. 2018-2021). Oxford, UK: Blackwell Publishing Ltd.

[91]Moore, J. R., Collings, N., Crossland, W. A., Davey, A. B., Evans, M., Jeziorska, A. M., ... & Xu, H. (2007). The silicon backplane design for an LCOS polarization-insensitive phase hologram SLM. IEEE Photonics Technology Letters, 20(1), 60-62.

[92]Yöntem, A. Ö., & Onural, L. (2011). Integral imaging using phase-only LCoS spatial light modulators as Fresnel lenslet arrays. JOSA A, 28(11), 2359-2375.

[93]Konforti, N., Marom, E., & Wu, S. T. (1988). Phase-only modulation with twisted nematic liquid-crystal spatial light modulators. Optics letters, 13(3), 251-253.

[94]Difato, F., Dal Maschio, M., Beltramo, R., Blau, A., Benfenati, F., & Fellin, T. (2011). Spatial light modulators for complex spatiotemporal illumination of neuronal networks. In Neuronal Network Analysis (pp. 61-81). Humana Press.

[95]Cofré, A., Vargas, A., Torres-Ruiz, F. A., Campos, J., Lizana, A., Sánchez-López, M. M., & Moreno, I. (2017). Dual polarization split lenses. Optics express, 25(20), 23773-23783.

[96]Davis, J. A., Chambers, J. B., Slovick, B. A., & Moreno, I. (2008). Wavelength-dependent diffraction patterns from a liquid crystal display. Applied optics, 47(24), 4375-4380.

[97]Chen, H. M. P., Yang, J. P., Yen, H. T., Hsu, Z. N., Huang, Y., & Wu, S. T. (2018). Pursuing high quality phase-only liquid crystal on silicon (LCoS) devices. Applied Sciences, 8(11), 2323.

[98]Lizana, A., Moreno, I., Márquez, A., Iemmi, C., Fernández, E., Campos, J., & Yzuel, M. J. (2008). Time fluctuations of the phase modulation in a liquid crystal on silicon display: characterization and effects in diffractive optics. Optics express, 16(21), 16711-16722.

[99]Lingel, C., Haist, T., & Osten, W. (2013). Optimizing the diffraction efficiency of SLM-based holography with respect to the fringing field effect. Applied optics, 52(28), 6877-6883.

[100]Davis, J. A., Cottrell, D. M., Campos, J., Yzuel, M. J., & Moreno, I. (1999). Encoding amplitude information onto phase-only filters. Applied optics, 38(23), 5004-5013.

[101]Erteza, I. A. (1995). Diffraction efficiency analysis for multi-level diffractive optical elements (No. SAND-95-1697). Sandia National Labs., Albuquerque, NM (United States).

[102]Wu, L., Wang, X., Xiong, C., Huang, Z., Zhuo, R., Rao, J., & Tan, Q. (2017). Polarization-independent two-dimensional beam steering using liquid crystal optical phased arrays. Chinese Optics Letters, 15(10), 101601.

[103]Li, Y., & Wu, S. T. (2011). Polarization independent adaptive microlens with a blue-phase liquid crystal. Optics express, 19(9), 8045-8050.

[104]Kujawinska, M., Porras-Aguilar, R., & Zaperty, W. (2012). LCoS spatial light modulators as active phase elements of full-field measurement systems and sensors. Metrology and Measurement Systems, 19(3), 445-458.

[105]Zhu, L., & Wang, J. (2014). Arbitrary manipulation of spatial amplitude and phase using phase-only spatial light modulators. Scientific reports, 4(1), 1-7.

[106]Zhang, Z., Jeziorska-Chapman, A. M., Collings, N., Pivnenko, M., Moore, J., Crossland, B., ... & Milne, B. (2011). High quality assembly of phase-only liquid crystal on silicon (LCOS) devices. Journal of Display Technology, 7(3), 120-126.

[107]Zhang, Z., Yang, H., Robertson, B., Redmond, M., Pivnenko, M., Collings, N., ... & Chu, D. (2012). Diffraction based phase compensation method for phase-only liquid crystal on silicon devices in operation. Applied optics, 51(17), 3837-3846.

[108]Fiala, P., Li, Y., & Dorrer, C. (2018). Investigation of focusing and correcting aberrations with binary amplitude and polarization modulation. Applied optics, 57(4), 763-771.

[109]Li, Y., de La Rochefoucauld, O., & Zeitoun, P. (2020). Simulation of Fresnel Zone Plate Imaging Performance with Number of Zones. Sensors, 20(22), 6649.

[110]Li, J., Smithwick, Q., & Chu, D. (2020). Scalable coarse integral holographic video display with integrated spatial image tiling. Optics express, 28(7), 9899-9912.

[111]Li, J., Smithwick, Q., & Chu, D. (2020, April). Full bandwidth coarse integral holographic video displays with spatial tiling for scalability. In Optics, Photonics and Digital Technologies for Imaging Applications VI (Vol. 11353, p. 113530K). International Society for Optics and Photonics.

[112]Li, J., Smithwick, Q., & Chu, D. (2018, June). Bandwidth utilization improvement methods of Coarse Integral Holographic video displays. In Digital Holography and Three-Dimensional Imaging (pp. DTh3D-6). Optical Society of America.

[113]Chen, J. S., Smithwick, Q., Li, J., & Chu, D. (2017). Auxiliary resonant scanner to increase the scanning capability of coarse integral holographic displays. Chinese Optics Letters, 15(4), 040901.

[114] Pawley, J. (Ed.). (2006). Handbook of biological confocal microscopy (Vol. 236). Springer Science & Business Media